

# **User Manual of the Multicomponent Variably- Saturated Flow and Transport Model HP1**

Description, Verification, and Examples

Version 1.0

Diederik Jacques\* and Jirka Šimůnek<sup>#</sup>

\*Waste and Disposal

SCK•CEN, Mol, Belgium

<sup>#</sup>Department of Environmental Sciences

University of California, Riverside, USA

June, 2005

SCK•CEN  
Boeretang 200  
2400 Mol  
Belgium

Waste & Disposal Department



# **User Manual of the Multicomponent Variably- Saturated Flow and Transport Model HP1**

Description, Verification, and Examples

Version 1.0

Diederik Jacques\* and Jirka Šimůnek<sup>#</sup>

\*Waste and Disposal

SCK•CEN, Mol, Belgium

<sup>#</sup>Department of Environmental Sciences

University of California, Riverside, USA

June, 2005

Status: Unclassified

ISSN 1379-2407

SCK•CEN  
Boeretang 200  
2400 Mol  
Belgium

Waste & Disposal Department

© SCK•CEN  
Belgian Nuclear Research Centre  
Boeretang 200  
2400 Mol  
Belgium

Phone +32 14 33 21 11  
Fax +32 14 31 50 21

<http://www.sckcen.be>

Contact:  
Knowledge Centre  
library@sckcen.be

**RESTRICTED**

All property rights and copyright are reserved. Any communication or reproduction of this document, and any communication or use of its content without explicit authorization is prohibited. Any infringement to this rule is illegal and entitles to claim damages from the infringer, without prejudice to any other right in case of granting a patent or registration in the field of intellectual property.

SCK•CEN, Studiecentrum voor Kernenergie/Centre d'Etude de l'Energie Nucléaire  
Stichting van Openbaar Nut – Fondation d'Utilité Publique - Foundation of Public Utility  
Registered Office: Avenue Herrmann Debroux 40 – B-1160 Brussel  
Operational Office Boeretang 200, 2400 Mol, Belgium

# TABLE OF CONTENTS

LIST OF TABLES.....	v
LIST OF FIGURES.....	vii
<b>1 Introduction .....</b>	<b>1</b>
<b>1.1 Background.....</b>	<b>1</b>
<b>1.2 Features and limitations of the coupled HPI model.....</b>	<b>3</b>
<b>1.2.1 Features .....</b>	<b>3</b>
<b>1.2.2 Limitations .....</b>	<b>3</b>
<b>2 Description of the model .....</b>	<b>5</b>
<b>2.1 Water flow in the vadose zone.....</b>	<b>5</b>
<b>2.1.1 The water flow equation .....</b>	<b>5</b>
<b>2.1.2 Initial and boundary conditions for water flow.....</b>	<b>6</b>
<b>2.2 Solute transport in the vadose zone .....</b>	<b>7</b>
<b>2.2.1 The solute transport equation .....</b>	<b>7</b>
<b>2.2.2 Initial and boundary conditions for the solute transport equation .....</b>	<b>9</b>
<b>2.3 Heat transport in the vadose zone.....</b>	<b>9</b>
<b>2.3.1 The heat transport equation.....</b>	<b>9</b>
<b>2.3.2 Initial and boundary conditions for heat transport .....</b>	<b>10</b>
<b>2.4 Geochemical reactions .....</b>	<b>10</b>
<b>2.4.1 Homogeneous aqueous reactions.....</b>	<b>11</b>
<b>2.4.2 Heterogeneous ion exchange reactions .....</b>	<b>11</b>
<b>2.4.3 Heterogeneous mineral dissolution/precipitation.....</b>	<b>12</b>
<b>2.4.4 Kinetic reactions .....</b>	<b>13</b>
<b>2.5 Multicomponent reactive transport.....</b>	<b>13</b>
<b>2.6 Coupling procedures .....</b>	<b>15</b>
<b>2.7 Model structure.....</b>	<b>18</b>
<b>2.7.1 PHREEQC .....</b>	<b>18</b>
<b>2.7.2 HYDRUS-1D.....</b>	<b>19</b>
<b>3 Description of data input .....</b>	<b>21</b>
<b>3.1 Input data.....</b>	<b>21</b>
<b>3.2 Running the model and output .....</b>	<b>23</b>
<b>4 Verification problems.....</b>	<b>25</b>
<b>4.1 Modelling the transport of a single component or decay chain .....</b>	<b>25</b>
<b>4.1.1 Physical equilibrium and nonequilibrium transport of chloride.....</b>	<b>25</b>
<b>4.1.2 Transport of a nonlinearly adsorbing solute subject to first-order decay</b>	<b>28</b>
<b>4.1.3 Transport of first-order decay chain of nonlinearly adsorbing</b>	
<b>contaminants during transient flow .....</b>	<b>35</b>

<b>4.2</b>	<b><i>Multicomponent transport during steady-state flow</i></b> .....	<b>39</b>
4.2.1	Cation exchange reactions .....	39
4.2.2	Mineral dissolution .....	42
<b>4.3</b>	<b><i>More complicated verification problems of HP1 model</i></b> .....	<b>44</b>
4.3.1	Heavy metal transport in a medium with a pH-dependent cation exchange complex (Verification Problem 8 – MCATEXCH) .....	44
4.3.2	Infiltration of a hyperalkaline solution in a clay sample (Verification Problem 9 – ALKALINE) .....	50
<b>5</b>	<b>Example</b> .....	<b>59</b>
5.1	<i>Long term transient flow and transport of major cations and heavy metals in a soil profile (HEAVMET)</i> .....	59
5.1.1	Problem definition and governing chemical reactions .....	59
5.1.2	Analysis of the simulation results .....	61
<b>6</b>	<b>Concluding Remarks</b> .....	<b>67</b>
	<b>References</b> .....	<b>71</b>
	 <b>Acknowledgements</b> .....	 <b>69</b>
	<b>References</b> .....	<b>71</b>
	<b>APPENDIX A – LISTING OF NOTATION</b> .....	<b>75</b>
	<b>APPENDIX B – RELEASED VERSIONS AND BENCHMARKING</b> .....	<b>79</b>

## **ABSTRACT**

Jacques, D., and J. Šimůnek, 2004. User manual of the Multicomponent variably-saturated transport model HP1 (Version 1.0): Description, Verification and Examples. SCK•CEN, Mol, Belgium, BLG-998, 79 p.

This report describes a new comprehensive simulation tool HP1 (HYDRUS1D-PHREEQC) that was obtained by coupling the HYDRUS-1D one-dimensional variably-saturated water flow and solute transport model with the PHREEQC geochemical code. The HP1 code incorporates modules simulating (1) transient water flow in variably-saturated media, (2) transport of multiple components, and (3) mixed equilibrium/kinetic geochemical reactions. The program numerically solves the Richards equation for variably-saturated water flow and advection-dispersion type equations for heat and solute transport. The flow equation incorporates a sink term to account for water uptake by plant roots. The heat transport equation considers transport due to conduction and convection with flowing water. The solute transport equations consider advective-dispersive transport in the liquid phase. The program can simulate a broad range of low-temperature biogeochemical reactions in water, soil and ground water systems including interactions with minerals, gases, exchangers, and sorption surfaces, based on thermodynamic equilibrium, kinetics, or mixed equilibrium-kinetic reactions. The program may be used to analyze water and solute movement in unsaturated, partially saturated, or fully saturated porous media. The flow region may be composed of nonuniform soils or sediments. Flow and transport can occur in the vertical, horizontal, or a generally inclined direction. The water flow part of the model can deal with prescribed head and flux boundaries, boundaries controlled by atmospheric conditions, as well as free drainage boundary conditions. The governing flow and transport equations were solved numerically using Galerkin-type linear finite element schemes.

To test the accuracy of the coupling procedures implemented in HP1, simulation results were compared with (i) HYDRUS-1D for transport problems of multiple components subject to sequential first-order decay, (ii) PHREEQC for steady-state flow conditions, and (iii) calculations obtained from an independent geochemical transport model (CRUNCH) for several relatively complex problems. Nine verification examples of increasing complexity are described in this report.

This report serves as both a user manual and reference document. Detailed instructions for input data preparation and interpretation of output data are given in the manuals of the original HYDRUS-1D and PHREEQC codes. The graphical user interfaces of both HYDRUS-1D and PHREEQC can be used for easy input data preparation and output display in the MS Windows environment.

## **KEYWORDS**

Biogeochemical model, variably-saturated water flow, multicomponent solute transport, vadose zone, dissolution/precipitation, cation exchange, aqueous complexation, benchmark calculations

The software has been verified against selected test cases. However, no warranty is given that the program is completely error-free. If you do encounter problems with the code, find errors, or have suggestions for improvement, please contact one of the authors at

Diederik Jacques  
Tel: +32-14-333209  
Fax: +32-14-323553  
E-mail: [djacques@sckcen.be](mailto:djacques@sckcen.be)

Jirka Šimůnek  
Tel: 1-951-827-7854  
Fax: 1-951-827-3993  
E-mail: [jiri.simunek@ucr.edu](mailto:jiri.simunek@ucr.edu)

## LIST OF TABLES

<b>Table 2.1</b> <i>Description of variables that are used in both HYDRUS-1D and PHREEQC, or newly defined in HYDRUS-1D.</i> .....	20
<b>Table 4.1</b> <i>Transport and simulation parameters for Verification Problem 3.</i> .....	30
<b>Table 4.2</b> <i>Soil hydraulic, transport, and reaction parameters for Verification Problem 5.</i> .....	36
<b>Table 4.3</b> <i>Input simulation parameters and numerical results for Verification Problem 5.</i> .....	37
<b>Table 4.4</b> <i>Initial and inflow concentrations for Verification Problem 6.</i> .....	39
<b>Table 4.5</b> <i>Soil hydraulic properties and cation exchange capacities of five soil layers.</i> .....	45
<b>Table 4.6</b> <i>pH and solution concentrations used in the simulation (<math>\mu\text{mol l}^{-1}</math>).</i> .....	45
<b>Table 4.7</b> <i>Overview of aqueous equilibrium reactions and corresponding equilibrium constants (data from phreeqc.dat database, Parkhurst and Appelo, 1999).</i> .....	45
<b>Table 4.8</b> <i>Log K parameters for multi-site exchange complex.</i> .....	46
<b>Table 4.9</b> <i>Mineralogical reactions, Log(K), molar volume, volume percent and moles present in Opalinus Clay, and secondary minerals considered.</i> .....	51
<b>Table 4.10</b> <i>Parameters for the kinetic dissolution reactions (Eq. (4.7)).</i> .....	51
<b>Table 4.11</b> <i>Overview of aqueous equilibrium reactions, and cation exchange half reactions with corresponding equilibrium constant.</i> .....	52
<b>Table 4.12</b> <i>Chemical composition of the initial pore water and the inflowing alkaline solution.</i> .....	53
<b>Table 5.1</b> <i>Soil hydraulic and other properties of six soil horizons</i> .....	59
<b>Table 5.2</b> <i>Chemical composition of the rain water (from Stolk, 2001) and in the initial soil solution.</i> .....	60



## LIST OF FIGURES

<b>Figure 2.1</b>	<i>Schematic of the modelling approach of the coupled HPI model.</i>	17
<b>Figure 4.1</b>	<i>Outflow concentrations for Verification Problem 1. Full and dashed lines are results for physical equilibrium and nonequilibrium transport, respectively, obtained with HYDRUS-1D. Dots are results obtained with HPI.</i>	26
<b>Figure 4.2</b>	<i>Outflow concentrations for Verification Problem 2. The full line was generated with HYDRUS-1D, while dots were obtained with HPI.</i>	27
<b>Figure 4.3</b>	<i>Depth profiles of Cont after 250, 500, and 750 d for different simulations defined in Table 4.1 for Verification Problem 3. Tests consider effects of grid size for PHREEQC (a), and effects of maximum time steps for HPI (b).</i>	31
<b>Figure 4.4</b>	<i>Depth profiles of Cont after 250, 500, and 750 d for different simulations defined in Table 4.1 (Verification Problem 4 with a first-order decay coefficient of <math>0.2 \text{ d}^{-1}</math>).</i>	34
<b>Figure 4.5</b>	<i>Distribution of Conta, Contb, and Contc versus depth after 250, 500, and 1000 d for different simulations as defined in Table 4.3 (Verification Problem 5).</i>	38
<b>Figure 4.6</b>	<i>Distribution of pH, dissolved Ca, Cl, Zn, and Cd concentrations, exchangeable Ca, Na, Zn, and Cd concentrations versus depth after three days of infiltration for Verification Problem 6.</i>	41
<b>Figure 4.7</b>	<i>pH, Ca, Cl, Zn, and Cd concentrations in the effluent for Verification Problem 6 (Full line: HPI, dashed line: PHREEQC).</i>	42
<b>Figure 4.8</b>	<i>Distribution of pH, Si, Al, amorphous <math>\text{SiO}_2</math>, and Gibbsite versus depth after 150 days of infiltration for Verification Problem 7 (Full line: HPI, dashed line: PHREEQC).</i>	43
<b>Figure 4.9</b>	<i>Selected results for cation and heavy metal transport with a pH-dependent cation exchange complex. (a) and (b) pH and Cd concentrations in outflow at 50 cm depth, respectively; (c) and (d) distributions of pH and Cd concentrations versus depth after 0.3, 0.5, and 0.7 y, respectively; (e) and (f) distribution of the fraction of deprotonated sites (1 - H-sites) and sites with Cd versus depth after 0.3, 0.5, and 0.7 y, respectively.</i>	48
<b>Figure 4.10</b>	<i>Effect of pH and Cl concentration on Cd concentrations of leaching water at the 50-cm depth.</i>	49
<b>Figure 4.11</b>	<i>Distribution of pH and selected elements versus depth (mol/l) after 0.3, 0.7, and 1.1 y of infiltration of a high pH solution in an Opalinus Clay core.</i>	56
<b>Figure 4.12</b>	<i>Outflow curves of selected elements (mol/l) during infiltration of a high pH-solution in an Opalinus Clay core.</i>	57
<b>Figure 5.1</b>	<i>Cumulative precipitation, evaporation and surface flux into the soil between 1972 and 1982.</i>	60
<b>Figure 5.2</b>	<i>Time series of inflow minus outflow (dashed line) and change in the total amount present in the soil profile (dots) for Cl, Na, Ca, and Cd.</i>	62

<b>Figure 5.3</b> <i>Relative mass balance errors, <math>\varepsilon_r</math>, as a function of time for Na, Ca, and Cd.</i> .....	63
<b>Figure 5.4</b> <i>Space-time plots of (a) water content, (b) amount of Cl (mmol / 1000 cm<sup>3</sup> soil), (c) pH, and (d) amount of aqueous Cd (mmol / 1000 cm<sup>3</sup> soil) in the A-horizon (0 – 7 cm depth).</i> .....	64
<b>Figure 5.5</b> <i>Time series of water content, Cl concentration (mmol / 1000 cm<sup>3</sup> soil), pH, and Cd concentration (mmol / 1000 cm<sup>3</sup> soil) in the third horizon (Bh1-horizon) at 22 cm depth.</i> .....	65

# 1 Introduction

## 1.1 Background

The migration of many naturally occurring elements and contaminants in the subsurface is affected by a multitude of complex, interactive physical, chemical, mineralogical, geological, and biological processes. Cycles of precipitation and evaporation largely determine if contaminants remain near the soil surface. Changes in the chemical composition or pH of the soil solution may impact the retention of heavy metals on organic matter or iron oxides. Dissolution and precipitation of minerals generally buffer the transport of a solution with a different pH through the soil profile. Simulation of these and related processes requires a coupled reactive transport code that integrates the physical processes of water flow and advective-dispersive solute transport with a range of biogeochemical processes.

In this report, we present a new code that resulted from the coupling of two existing codes: HYDRUS-1D (Šimůnek et al., 1998) and PHREEQC-2 (Parkhurst and Appelo, 1999). The new code should significantly expand applicability of the individual codes by preserving most of their original features and capabilities.

HYDRUS-1D simulates water, heat, and solute movement in one-dimensional variably saturated porous media for various boundary conditions, including precipitation and evaporation. A sink term accounting for water uptake by roots is also included in the model. Solutes can be exchanged between the water and gas phase and may interact linearly or nonlinearly with the solid phase assuming either equilibrium or nonequilibrium reactions between the dissolved and adsorbed solutes. The only possible interaction between the different solutes is a consecutive chain reaction in which the solutes are sequentially transformed along the chain by means of first-order reactions (which hence depend only on the concentration of the first solute) (van Genuchten, 1985). These chain reactions can be used to describe the degradation of pesticides (e.g., Wagenet and Hutson, 1987) or chlorinated volatile organic compounds (e.g., Schaerlaekens et al., 1999; Casey and Šimůnek, 2001), and consecutive decay chains involving radionuclides (e.g., Mallants et al., 2003), endocrine disrupting chemicals (Casey et al., 2003, 2004), and many other chemicals. No other interactions between different species or components are currently considered in the HYDRUS-1D model.

The only attempts to include geochemistry into HYDRUS-1D-related models were those by Šimůnek and Suarez (1994, 1996) and Suarez and Šimůnek (1997), resulting in UNSATCHEM-2D (which was based on the SWMS-2D code (Šimůnek et al., 1992), a two-dimensional precursor of HYDRUS-2D) and UNSATCHEM. These two models considered interactions only between major ions whose possible components (Ca, Mg, Na, K, SO<sub>4</sub>, Cl,

alkalinity, and CO<sub>2</sub>) and geochemical reactions (speciation, cation exchange, and precipitation/dissolution of minerals (and their kinetics)) are predefined and hence can not be changed by the user. Although these two codes can be applied to a wide range of important problems such as salinization of agricultural soils under irrigation or reclamation of sodic soils (Šimůnek and Suarez, 1997), they can not be used to simulate the transport and reactions of other chemical species, such as trace elements, radionuclides, and other chemicals.

PHREEQC-2 can simulate a large number of low-temperature geochemical reactions in water, soil and ground water systems, including interactions with minerals, gases, solid solutions, exchangers, and sorption surfaces, based on thermodynamic equilibrium, kinetics, or mixed equilibrium-kinetic reactions (e.g., Appelo et al., 2002). PHREEQC-2 also allows one to simulate one-dimensional reactive transport using a mixing cell solution approach (see Appelo and Postma, 1999, for details; e.g., Appelo et al., 1998; Postma and Appelo, 2000). This model hence can be used to simulate reactive transport during steady-state flow, including a wide variety of geochemical reactions. However, the model can not deal with solute transport during transient water flow conditions.

In recent years, the PHREEQC geochemical code has been coupled to various (groundwater) water flow and solute transport models. For example, the PHT-3D model (Prommer, 2002) couples PHREEQC-2 with MT3DMS (Zheng and Wang, 1998), the latter being an extension of the single-species transport simulator by Zheng (1990). However, this coupled program deals only with solute transport and reactions, while the groundwater flow field needs to be computed using a separated simulation model. Xu (1996) developed a coupled model TRAN-PHREEQE that links PHREEQE with a two-dimensional finite element code for flow and transport in aquifers. PHREEQE is a precursor of PHREEQC without cation exchange, surface complexation, or kinetic reactions. Another example of coupling between PHREEQC and a two-dimensional transport model for water-saturated conditions and constant temperature was presented recently by Källvenius and Ekberg (2003) in the TACK model (Transport And Chemical Kinetics). However, this model does not simulate water flow. A recent detailed review of available numerical multicomponent transport models is given by Šimůnek and Valocchi (2002), including an overview of the mathematical equations representing the major chemical reactions and governing transport processes, a brief discussion how these equations can be implemented in reaction multispecies transport models, and a description of several possible applications.

This report describes a new comprehensive simulation tool HP1 (HYDRUS1D-PHREEQC) that results from coupling the HYDRUS-1D one-dimensional variably-saturated water flow and solute transport model with the PHREEQC geochemical code. The model incorporates modules simulating (1) transient water flow in variably-saturated media, (2) transport of multiple components, and (3) mixed equilibrium/kinetic geochemical reactions. The accuracy of the coupled HP1 model was evaluated by comparing simulation results with HYDRUS-1D,

PHREEQC for steady-state flow conditions, and with calculations obtained with an independent geochemical transport model CRUNCH (Steeffel, 2002) for several more complicated problems.

## ***1.2 Features and limitations of the coupled HP1 model***

### **1.2.1 Features**

Any combination of the following features can be described with the HP1 model:

- One-dimensional transient water flow for different boundary conditions including atmospheric conditions (precipitation, evaporation, transpiration)
- Root water uptake as a sink for water
- Root growth
- One-dimensional transient convective and conductive heat transport for time-variable temperatures at the soil surface
- One-dimensional advective, dispersive and diffusive transport of multiple solutes
- Effect of temperature on transport parameters, thermodynamic constants, and rate parameters
- Different functional forms for the soil hydraulic properties, including hysteresis
- Physical non-equilibrium solute transport
- Physical and chemical spatial heterogeneity
- Equilibrium aqueous speciation reactions and kinetically controlled aqueous reactions such as radioactive decay
- Multi-site cation exchange related to type and amount of minerals present
- Equilibrium and kinetic dissolution/precipitation of primary and secondary minerals
- User-defined kinetic reactions
- Simultaneous presence of different reactions (sequential and parallel kinetic reactions, equilibrium and kinetic reactions, homogeneous and heterogeneous reactions, biogeochemical reactions)

### **1.2.2 Limitations**

Specific limitations of the PHREEQC model for various geochemical calculations are discussed in detail by Parkhurst and Appelo (1999, p. 4-6), and are not further discussed here. Of these limitations, those related to flow and transport modelling are no longer of concern here, since HYDRUS-1D is used to simulate transient water flow and solute transport.

One possible limitation involves the invoked method of coupling HYDRUS-1D and PHREEQC, i.e. a non-iterative sequential coupling method (SNIA). This method is still being discussed in the literature (e.g., Steefel and MacQuarrie, 1996, Mayer, 1999), with some authors claiming that mass balance errors may occur when this coupling procedure is used. However, by using appropriate time steps, accurate results can be obtained as we will show with examples later in this manual (see also Mayer, 1999, for some guidelines). In addition, we believe that uncertainty in the assumed processes and its parameters likely will contribute much more to uncertainty in the model simulations than possible (limited) numerical errors caused by the coupling procedure.

This manual documents Version 1.0 of the coupled HP1 model. The following features of PHREEQC are not yet operational in the current version: surface complexation, solid solutions, and redox reactions. Diffusion and advection of components in the gas phase are also not considered. We further do not account for changes in the volume of minerals and corresponding changes in porosity, hydraulic properties, and solute transport parameters.

## 2 Description of the model

The HP1 model is the result of coupling the variably-saturated water flow and solute transport model HYDRUS-1D (Šimůnek et al., 1998) with the geochemical model PHREEQC (Parkhurst and Appelo, 1999). Details about the governing equations, initial and boundary conditions, parameterization, and adopted numerical methods are given in manuals of the original HYDRUS-1D and PHREEQC models. In this chapter we give only a very concise overview of these topics, mainly to provide a better understanding of the verification problems described in chapter 4. For more detail, users are encouraged to examine the original manuals.

### 2.1 Water flow in the vadose zone

#### 2.1.1 The water flow equation

Combination of the mass balance equation with the Darcy-Buckingham law results in the Richards equation that describes water flow in variably-saturated porous media. The one-dimensional form of the Richards equation can be written as

$$\frac{\partial \theta(h)}{\partial t} = \frac{\partial}{\partial x} \left[ K(h) \left( \frac{\partial h}{\partial x} + \cos \alpha \right) \right] - S(h) \quad (2.1)$$

where  $h$  is the water pressure head [L],  $\theta$  is the volumetric water content [ $L^3L^{-3}$ ],  $t$  time [T],  $x$  is the spatial coordinate [L] (positive upward),  $S$  is the sink term [ $L^3L^{-3}T^{-1}$ ],  $\alpha$  is the angle between the flow direction and the vertical axis, and  $K$  is the unsaturated hydraulic conductivity [ $LT^{-1}$ ].

Both the water content and the unsaturated hydraulic conductivity are nonlinear functions of the pressure head. Three analytical models are available in HYDRUS-1D to describe these soil hydraulic properties (Brooks and Corey, 1994; van Genuchten, 1980; and Vogel and Cislerova, 1988). Only van Genuchten's functions will be used in the verification problems documented in this manual

$$\theta(h) = \theta_r + \frac{\theta_s - \theta_r}{\left(1 + |\alpha h|^n\right)^m} \quad (2.2)$$

$$K(h) = K_s S_e^l \left[ 1 - \left( 1 - S_e^{1/m} \right)^m \right]^2 \quad (2.3)$$

where  $\theta_r$  is the residual water content [ $L^3L^{-3}$ ],  $\theta_s$  is the saturated water content [ $L^3L^{-3}$ ],  $\alpha$  [ $L^{-1}$ ],  $n$  [-] and  $m (= 1 - 1/n)$  [-] are shape parameters,  $l$  is the pore connectivity parameter [-],  $K_s$  is the saturated hydraulic conductivity [ $LT^{-1}$ ], and  $S_e = (\theta - \theta_r) / (\theta_s - \theta_r)$  is effective saturation. These parameters can be obtained by direct measurement of the  $\theta$ - $h$  or  $K$ - $h$  relationships (e.g., chapters 3.3 and 3.4 in Dane and Topp, 2002), by inverse optimization (Hopmans et al., 2002) or indirect estimation from basic soil textural properties using pedotransfer functions. The latter approach in HYDRUS-1D uses neural network predictions from textural data as implemented in the ROSETTA program of Schaap et al. (1998). The following additional features related to the soil hydraulic properties are also included in HYDRUS-1D: (i) hysteresis in the water retention characteristic and the hydraulic conductivity function, (ii) description of small-scale spatial variability in the soil hydraulic properties by means of scaling factors, and (iii) temperature dependence of the soil hydraulic functions. These additional features are described in sections 2.6, 2.4, and 2.5 of Šimůnek et al. (1998), respectively.

The sink term  $S$  in (2.1) is defined as the volume of water extracted from the soil by the roots. The potential root water uptake rate  $S_p(x)$  is obtained by multiplying a normalized water uptake distribution  $b(x)$  [ $L^{-1}$ ] with the potential transpiration  $T_p$  [ $LT^{-1}$ ]. The  $b(x)$  function is obtained from the root distribution with depth, whereas  $T_p$  depends on climate conditions and vegetation. Both  $b(x)$  and  $T_p$  are input to the HYDRUS-1D model. The actual root water uptake rate  $S(x)$  is obtained by multiplying  $S_p(x)$  with a root water stress response function (e.g., Feddes et al., 1978; van Genuchten, 1987) to account for a possible reduction in root water uptake due to water and salinity stress conditions in the soil profile. Soil water uptake reduction due to the salinity stress can be included using an osmotic head reduction function that can be either additive or multiplicative to water stress. The actual water uptake distribution is then of the form

$$S(h, h_\phi, x) = \alpha(h, h_\phi)b(x)T_p \quad (2.4)$$

where  $S$  is the root water uptake as a function of the pressure head  $h$  (related to water stress), the osmotic head  $h_\phi$  [L] (related to salinity stress), and depth  $x$  (related to the root spatial distribution), while  $\alpha(h, h_\phi)$  defines the reduction in root water uptake due to the water and salinity stress. Root growth can be included using the Verhulst-Pearl logistic growth function, with the assumption of an exponential root distribution with depth.

### 2.1.2 Initial and boundary conditions for water flow

To solve Eq. (2.1), initial and boundary conditions must be specified. Initial conditions can be defined in terms of pressure heads or water contents. Possible system-independent boundary conditions are time series of pressure heads or soil water fluxes at the soil surface and/or the

bottom of the soil profile, and a zero-gradient (free drainage) pressure head boundary condition at the bottom of the soil profile. In addition, system-dependent boundary conditions that depend on the status of the system are also available. When atmospheric conditions (precipitation, evaporation, and transpiration) defining the potential water flux across the top boundary are specified, the actual water flux across this boundary depends also on the soil moisture conditions. When the potential surface flux (precipitation) is larger than the infiltration capacity, any excess water on the soil surface is either assumed to be immediately removed by surface runoff, or is permitted to build up on the soil surface. At the bottom of the soil profile, the following boundary conditions can be implemented: (i) a seepage face boundary condition that assumes a zero-flux when the bottom of the soil profile is unsaturated and a zero pressure head when it is saturated, (ii) a tile drain boundary condition that approximates flow to horizontal subsurface drains using selected analytical solutions, and (iii) a deep drainage boundary condition that uses a functional relationship that relates the water table depth with the deep recharge from the soil profile. Mathematical descriptions of these boundary conditions can be found in section 2.7 of Šimůnek et al. (1998).

## 2.2 Solute transport in the vadose zone

### 2.2.1 The solute transport equation

The HYDRUS-1D code allows simulations of the transport of multiple solutes involved in a sequential first-order decay chain in three phases (liquid, solid, and gaseous) using the physical nonequilibrium advection-dispersion equations. However, many solute transport features of HYDRUS-1D are not used in the coupled HP1 code since they are considered in the PHREEQC module. These include interactions between the liquid and solid phases, degradation/production, and the presence of sequential decay chain reactions. These interactions are defined in PHREEQC using equilibrium or kinetic reactions. In fact, solute transport in the HYDRUS module is modelled as the transport of inert tracers (i.e., no interaction with the solid phase, and no solute sink terms) since reactions are considered in the PHREEQC module. Note, however, that it is still possible to simulate reactive transport with HYDRUS-1D in the coupled model when particular parameters are entered with non zero values. In the present coupled model, interactions with (and thus also diffusion in) the gas phase are not considered.

The general solute transport equations, as given by (3.1) and (3.2) in Šimůnek et al. (1998), for conditions described above reduce to

$$\frac{\partial \theta c_i}{\partial t} = \frac{\partial}{\partial x} \left( \theta D_i^w \frac{\partial c_i}{\partial x} \right) - \frac{\partial q c_i}{\partial x} - S c_{r,i} + R_i \quad (2.5)$$

where  $i$  ( $= 1, \dots, N_m$ ) is the aqueous species number ( $N_m$  is the total number of aqueous species),  $c_i$  is the aqueous concentration of the  $i$ th species [ $\text{ML}^{-3}$ ],  $q$  is the volumetric flux density [ $\text{LT}^{-1}$ ],  $S$  the sink term in the water flow equation (Eq. (2.1)),  $c_r$  the concentration of the sink term [ $\text{ML}^{-3}$ ],  $D^w$  is the dispersion coefficient in the liquid phase [ $\text{L}^2\text{T}^{-1}$ ], and  $R_i$  is the general source/sink term due to geochemical reactions [ $\text{ML}^{-3}\text{T}^{-1}$ ]. This sink/source term contains heterogeneous equilibrium reactions, and homogeneous and heterogeneous kinetic reactions (see section 2.4).

Physical nonequilibrium solute transport is modeled using a two region model that assumes that the liquid phase can be divided into a mobile (flowing) region,  $\theta_m$  [ $\text{L}^3\text{L}^{-3}$ ], and an immobile (stagnant) region,  $\theta_{im}$  [ $\text{L}^3\text{L}^{-3}$ ]. Solutes are exchanged between the mobile and immobile regions by means of a first-order exchange process. The mathematical formulation of this nonequilibrium model is given by (van Genuchten and Wierenga, 1976):

$$\begin{aligned} \frac{\partial \theta_m c_{i,m}}{\partial t} + \frac{\partial \theta_{im} c_{i,im}}{\partial t} &= \frac{\partial}{\partial x} \left( \theta_m D_i^w \frac{\partial c_{i,m}}{\partial x} \right) - \frac{\partial q c_{i,m}}{\partial x} - S c_{r,i} + R_{i,m} \\ \frac{\partial \theta_{im} c_{i,im}}{\partial t} &= \omega_i (c_{i,m} - c_{i,im}) + R_{i,im} \end{aligned} \quad (2.6)$$

where  $c_{i,m}$  and  $c_{i,im}$  are concentrations of the  $i$ th aqueous species in the mobile and immobile regions [ $\text{ML}^{-3}$ ], respectively,  $R_{i,m}$  and  $R_{i,im}$  are the source/sink terms due to geochemical reactions in the mobile and immobile regions [ $\text{ML}^{-3}\text{T}^{-1}$ ], respectively, and  $\omega_i$  is the mass transfer coefficient for the  $i$ th aqueous species [ $\text{T}^{-1}$ ]. Note that HYDRUS-1D can also consider chemical nonequilibrium transport (kinetic adsorption/desorption reactions). However, we strongly suggest not to use this option of HYDRUS-1D, and to simulate chemical nonequilibrium reactions using options in the PHREEQC module.

The dispersion coefficient is given by

$$\theta D_i^w = D_L |q| + \theta D_{i,w} \tau_w \quad (2.7)$$

where  $D_{i,w}$  is the molecular diffusion of the  $i$ th aqueous species in free water [ $\text{L}^2\text{T}^{-1}$ ],  $D_L$  is the longitudinal dispersivity [ $\text{L}$ ], and  $\tau_w$  is a tortuosity factor in the liquid phase [-] that is related to the water content as follows (Millington and Quirk, 1961)

$$\tau_w = \frac{\theta^{7/3}}{\theta_s^2} \quad (2.8)$$

The dependence of the diffusion parameter  $D_i^w$  on temperature can be described using the Arrhenius equation (see section 3.4 of Šimůnek et al., 1998).

### 2.2.2 Initial and boundary conditions for the solute transport equation

To solve Eqs. (2.5) or (2.6), the initial and boundary conditions must be specified. Initial total aqueous concentrations of all aqueous species as a function of depth at time zero in both the mobile and immobile regions must be defined. Concentrations of adsorbed secondary or precipitated species must also be specified at time zero when kinetic adsorption and precipitation/dissolution reactions are considered.

Possible boundary conditions include first-type (or Dirichlet type) boundary conditions defining a prescribed boundary concentration, and third-type (or Cauchy type) boundary conditions defining a prescribed boundary solute flux. At an impermeable boundary (i.e., where  $q=0$ ) or at a boundary where water flows out of the domain, the third-type boundary condition reduces to a second-type (Neumann type) boundary condition.

## 2.3 Heat transport in the vadose zone

### 2.3.1 The heat transport equation

The one-dimensional heat transport equation (neglecting water vapour diffusion) is given by

$$\frac{\partial C_p(\theta)T}{\partial t} = \frac{\partial}{\partial x} \left[ \lambda(\theta) \frac{\partial T}{\partial x} \right] - C_w \frac{\partial qT}{\partial x} - C_w ST \quad (2.9)$$

where  $\lambda(\theta)$  is the apparent thermal conductivity of the soil [ $\text{MLT}^{-3}\text{K}^{-1}$ ], and  $C_p(\theta)$  and  $C_w$  are volumetric heat capacities of the porous medium and the liquid phase, respectively, [ $\text{ML}^{-1}\text{T}^{-2}\text{K}^{-1}$ ]. The volumetric heat capacity of the porous medium is estimated based on its constituents (de Vries, 1963) as follows

$$C_p(\theta) = C_n\theta_n + C_o\theta_o + C_w\theta + C_a\theta_v \quad (2.10)$$

where  $C_n$ ,  $C_o$ , and  $C_a$  are the volumetric heat capacities of the solid phase, the organic matter, and the gas phase, respectively, [ $\text{ML}^{-1}\text{T}^{-2}\text{K}^{-1}$ ], and  $\theta_n$ ,  $\theta_o$ , and  $\theta_v$  are the volumetric fractions of the solid phase, the organic matter, and the gas phase, respectively [ $\text{L}^3\text{L}^{-3}$ ]. The apparent thermal conductivity is defined as (de Marsily, 1986)

$$\lambda(\theta) = \lambda_0(\theta) + \beta_t C_w |q| \quad (2.11)$$

where  $\beta_t$  is the thermal dispersivity [L] and  $\lambda_0(\theta)$  is the thermal conductivity of the soil defined as (Chung and Horton, 1987)

$$\lambda_0(\theta) = b_1 + b_2\theta + b_3\theta^{0.5} \quad (2.12)$$

where  $b_1$ ,  $b_2$ , and  $b_3$  are empirical parameters [ $\text{ML}^{-1}\text{T}^{-2}\text{K}^{-1}$ ].

### 2.3.2 Initial and boundary conditions for heat transport

To solve Eq. (2.9), initial and boundary conditions must be specified. The initial temperature as a function of space at time zero must be defined. Possible boundary conditions again include first-type (or Dirichlet type) boundary conditions defining a prescribed boundary temperature and third-type (or Cauchy type) boundary conditions defining a prescribed heat flux through the boundary. At an impermeable boundary ( $q = 0$ ) or at a boundary where water flows out of the domain, a third-type boundary condition reduces to a second-type (Neumann type) boundary condition.

At the soil surface, the temperature can be represented using a sine function (Kirkham and Powers, 1972)

$$T = T_{avg} + A \sin\left(\frac{2\pi t}{p_t} - \frac{7\pi}{12}\right) \quad (2.13)$$

where  $p_t$  is the period of time necessary to complete one temperature cycle [T],  $T_{avg}$  is the average temperature at the soil surface [K], and  $A$  is the amplitude of the sine wave [K].

### 2.4 Geochemical reactions

In general, species present in a system are related to each other by a set of reaction equations. It is possible to write the various reaction equations in terms of a limited set of independent components. The latter group permits one to define the stoichiometry of the system, and are independent of each other (Morel and Herring, 1993). The species are thus divided in two groups: (i) the components, primary species or master species (in the terminology of PHREEQC), and (ii) the secondary species. The number of master species,  $N_m$ , equals the total number of species minus the number of reactions if the reactions are written stoichiometrically independent (none of the reactions is a linear combination of the others). The number of secondary species,  $N_s$ , is then defined as the number of species minus the number of master species. Thus, each reaction can be written in the canonical form

$$\sum_{j=1}^{N_m} \nu_{ji} A_j^m = A_i \quad (2.14)$$

where  $i = 1, \dots, N_s$ ,  $N_s$  is the number of secondary species,  $A_j^m$  and  $A_i$  are the chemical formula of the master and secondary species, respectively, and  $\nu_{ji}$  are the stoichiometric coefficients in the reaction.

In the remainder of this section we present the mass-actions relations for different reactions (aqueous speciation, ion exchange, mineral precipitation/dissolution), and the activities of the aqueous and exchange species.

#### 2.4.1 Homogeneous aqueous reactions

For an aqueous complexation reaction, Eq. (2.14) is written as

$$\sum_{j=1}^{N_m} \nu_{ji}^l A_j^m = A_i^l \quad (2.15)$$

where the superscript  $l$  indicates the liquid phase,  $i=1, \dots, N_{sa}$ , where  $N_{sa}$  is the number of aqueous secondary species. For equilibrium conditions, the mass-action equation is

$$K_i^l = \gamma_i^l c_i^l \prod_{j=1}^{N_m} (\gamma_j^m c_j^m)^{-\nu_{ji}^l} \quad (2.16)$$

where  $K_i^l$  is the equilibrium constant for reaction (2.15),  $\gamma_i^l$  is the activity coefficient of the  $i$ th aqueous complex, and  $\gamma_j^m$  is the activity coefficient of the  $j$ th master species in solution. The activity coefficients are defined with the Davies equation or the extended Debye-Hückel equation (Langmuir, 1997; Parkhurst and Appelo, 1999).

#### 2.4.2 Heterogeneous ion exchange reactions

In PHREEQC, the ion exchange sites are defined by exchange primary (or master) species ( $X^m$ ) and ion exchange reactions are defined as half reactions. For the Gaines and Thomas convention (Gaines and Thomas, 1953), the half reaction is written as

$$\sum_{j=1}^{N_m} \nu_{ji_e}^e A_j^m + \nu_{j_e}^e X_{j_e}^m = A_{i_e}^e \quad (2.17)$$

where  $j_e=1, \dots, N_X$  ( $N_X$  is the number of master exchangers),  $i_e=1, \dots, N_{s_e}$  ( $N_{s_e}$  is the number of the secondary exchange species), and the superscript  $e$  refers to exchange reactions. Let the activity of an exchange species be defined as

$$a_{i_e} = \gamma_{i_e}^e \beta_{i_e, j_e} \quad (2.18)$$

where  $a$  is the activity,  $\gamma_{i_e}^e$  is the activity coefficient of the  $i_e$ th exchange species, and  $\beta_{i_e, j_e}$  is the equivalent fraction of the  $i_e$ th exchange species on the  $j_e$ th exchanger, defined as  $b_{i_e, j_e} n_{i_e, j_e} / T_{j_e}$  where  $b_{i_e, j_e}$  is the number of equivalents of exchanger  $j_e$  occupied by the  $i_e$ th exchange species,  $n_{i_e, j_e}$  are the moles of the  $i_e$ th exchange species on exchanger  $j_e$ , and  $T_{j_e}$  is the total number of exchange sites for the  $j_e$ th exchanger (in equivalents). Then the mass-action equation for equilibrium conditions can be written as

$$K_{i_e}^e = \gamma_{i_e}^e \beta_{i_e, j_e} \prod_{j=1}^{N_m} (\gamma_j^m c_j^m)^{-v_{j_e}^e} (\gamma_{j_e}^e \beta_{j_e, j_e})^{-v_{j_e}^e} \quad (2.19)$$

The activity coefficients for the exchange species are calculated with the WATEQ Debye-Hückel equation (Toussaint and Jones, 1974), the Davies equation, or are equal to one. Note that in PHREEQC it is also possible to express ion exchange reactions using the Gapon convention (Gapon, 1933; see also Appelo and Postma, 1999).

### 2.4.3 Heterogeneous mineral dissolution/precipitation

For equilibrium precipitation/dissolution reactions of a mineral, Eq. (2.14) is written as

$$\sum_{j=1}^{N_m} \nu_{ji}^p A_j^m = A_i^p \quad (2.20)$$

where  $i=1, \dots, N_p$  ( $N_p$  is the number of minerals), and  $A_i^p$  is the formula of the mineral, while the superscript  $p$  refers to pure phases (minerals). Note that in the database of PHREEQC, dissolution/precipitation can be written in terms of any of the aqueous species. These reactions can always be transformed to a canonical form of Eq. (2.20). For equilibrium conditions, the mass-action equation is

$$K_i^p = \prod_{j=1}^{N_m} (\gamma_j^m c_j^m)^{-\nu_{ji}^p} \quad (2.21)$$

since the activity of a pure phase (mineral) is assumed to be 1.

#### 2.4.4 Kinetic reactions

Both homogeneous and heterogeneous reactions can be treated as kinetic reactions. Homogeneous reactions define the production or consumption of a master species from other master species in the aqueous phase

$$\sum_{j=1}^{N_m} \nu_{ji}^{lk} A_j^m = 0 \quad (2.22)$$

where  $i=1, \dots, N_{lk}$  ( $N_{lk}$  is the number of kinetically-controlled homogeneous reactions in the aqueous phase), the superscript  $lk$  indicates the homogeneous kinetic reaction, and  $\nu_{ji}^{lk}$  are the stoichiometric coefficients involved in the  $i$ th homogeneous kinetic reaction. The rate equation itself can be of any form and be dependent upon the total concentrations of a given master species, on concentrations or activities of the master species, on concentrations or activities of secondary aqueous species, or on external factors such as temperature and biomass. It is possible to define rather complex sequential and parallel kinetic pathways (e.g., Steefel, 2000). This flexibility in PHREEQC is possible due to an embedded BASIC interpreter which permits one to define rate expressions in a general way in the input file (see the section ‘Numerical method and rate expressions for chemical kinetics’ in Parkhurst and Appelo, 1999). Typical examples of homogeneous kinetic reactions are oxidation-reduction reactions, radioactive decay, and degradation reactions. Another type of homogeneous kinetic reaction is the production or consumption of a particular master species (the consumption/production of the specific secondary species is also possible). Only mineral dissolution/precipitation can be considered as a heterogeneous kinetic reaction. The BASIC interpreter in PHREEQC allows one to use a broad range of reaction rate expressions.

#### 2.5 Multicomponent reactive transport

Multicomponent reactive transport system may be viewed as consisting of  $N_m$  transport equations for the master species

$$\frac{\partial \theta c_j}{\partial t} = \frac{\partial}{\partial x} \left( \theta D_j^w \frac{\partial c_j}{\partial x} \right) - \frac{\partial q c_j}{\partial x} - S c_{r,j} + R_j \quad (2.23)$$

( $j=1, \dots, N_m$ ), and  $N_{sa}$  transport equations for the secondary aqueous species

$$\frac{\partial \theta c_i}{\partial t} = \frac{\partial}{\partial x} \left( \theta D_i^w \frac{\partial c_i}{\partial x} \right) - \frac{\partial q c_i}{\partial x} - S c_{r,i} + R_i \quad (2.24)$$

( $i=1, \dots, N_{sa}$ ). The terms  $R_j$  and  $R_i$  include both rapid and slow reactions involving the given species. However, some reactions can be so fast that the rate of the reaction is controlled by the rate of transport of the species to or from the site of the reaction rather than by the reaction itself. For these reactions, equilibrium can be assumed. Consequently, the sink/source term of the geochemical reactions can be divided as

$$\begin{aligned} R_j &= R_j^{eq,hom} + R_j^{eq,het} + R_j^{kin,hom} + R_j^{kin,het} \\ R_i &= R_i^{eq,hom} + R_i^{eq,het} + R_i^{kin,hom} + R_i^{kin,het} \end{aligned} \quad (2.25)$$

where the superscripts *eq*, *kin*, *hom*, and *het* refer to local equilibrium reactions, kinetic reactions, homogeneous reactions, and heterogeneous reactions, respectively. A system involving both local equilibrium and kinetic reactions is in a state of local partial equilibrium (Lichter, 1996). A system of  $N_p + N_{sa}$  transport equations can be reduced to the number of primary species. The  $R_j^{eq,hom}$  can be expressed in terms of the reaction stoichiometry defined by Eq. (2.15)

$$R_j^{eq,hom} = - \sum_{i=1}^{N_{sa}} \nu_{ji} R_i^{eq,hom} \quad (2.26)$$

Substituting Eq. (2.26) in Eq. (2.23) and replacing  $R_i$  by Eq. (2.24) allows the global transport equation for the  $j$ th master species to be written as

$$\begin{aligned} \frac{\partial \theta c_j}{\partial t} + \sum_{i=1}^{N_{sa}} \nu_{ji} \frac{\partial \theta c_i}{\partial t} &= \frac{\partial}{\partial x} \left( \theta D_j^w \frac{\partial c_j}{\partial x} \right) - \frac{\partial q c_j}{\partial x} + \\ + \sum_{i=1}^{N_{sa}} \nu_{ji} \frac{\partial}{\partial x} \left( \theta D_i^w \frac{\partial c_i}{\partial x} \right) &- \sum_{i=1}^{N_{sa}} \nu_{ji} \frac{\partial q c_i}{\partial x} - S c_{r,i} - \sum_{i=1}^{N_{sa}} \nu_{ji} S c_{r,j} + R_{o,j} \end{aligned} \quad (2.27)$$

where  $R_{o,j}$  is the term that includes all other heterogeneous equilibrium and kinetic reactions. Defining  $C_j$  as the total concentration of a master species

$$C_j = c_j + \sum_{i=1}^{N_{sa}} \nu_{ji} c_i \quad (2.28)$$

and  $C_{rj}$  the total concentration in the sink term

$$C_{rj} = c_{rj} + \sum_{i=1}^{N_{sa}} \nu_{ji} c_{ri} \quad (2.29)$$

and assuming that the diffusion coefficients  $D_j^w$  and  $D_i^w$  are all equal ( $=D^w$ ; i.e., species-independent diffusion) and that concentrations of the sink term  $c_{r,j}$  and  $c_{r,i}$  are equal to each other, then the transport equation for the master species becomes

$$\frac{\partial \theta C_j}{\partial t} = \frac{\partial}{\partial x} \left( \theta D^w \frac{\partial C_j}{\partial x} \right) - \frac{\partial q C_j}{\partial x} - S C_{r,i} + R_{o,j} \quad (2.30)$$

Note that it is possible to introduce heterogeneous equilibrium reactions in Eq. (2.30) in a similar way, and thus to define transport equations for the total concentration of the master species using only kinetic reactions as source/sink terms (Lichtner, 1996; Mayer, 1999). However, this is not done here since the solution method for solving the reactive transport equations is based on a sequential non-iterative approach (Steeffel and MacQuarrie, 1996). This means that the transport equation (2.30) is solved without the reaction term  $R_{o,i}$ , whereas the mass-action equations (2.16), (2.19), and (2.21) are solved sequentially (see section 2.6). Note that when  $c_r$  is not equal to zero, a component will be taken up by the roots, but not a species. When  $c_r$  is zero, no solute is removed from the soil solution due to the root uptake. It is, however, still possible to define some active uptake mechanism in PHREEQC, i.e., one that is independent of water uptake (contained in the  $R_{o,i}$  term of Eq. (2.30)).

## 2.6 Coupling procedures

Reactive transport systems as defined in the above sections involve many processes that are interrelated and contain parameters that are dependent upon the state of the system. Without attempting to be complete, the following interactions may occur in natural systems

- Effect of concentration and temperature on flow properties (by affecting the water density and the viscosity, and the surface tension at the air-water interface),
- Effect of temperature on diffusion coefficients,
- Effect of temperature on the equilibrium constants and rate coefficients,
- Effect of water flow on solute and heat transport,
- Effect of mineralogical changes on water flow and solute transport parameters.

Not all of these interactions are included in the present model. The effect of concentration on the flow properties and the effect of mineralogical changes on the water flow, solute and heat transport equations are neglected in the present version of HP1.

Yeh and Cheng (1999) discriminate between strong coupling (in which the governing water flow, solute transport and heat transport equations, as well as the geochemical reactions are solved simultaneously) and weak coupling (in which the governing equations are solved sequentially). In the latter method, state variables obtained after solving a given equation are used to calculate properties and state variables in the next equation. Yeh and Cheng (1999) used the following sequence for this purpose: first solve the water flow equation, then the heat transport equation, and finally the solute transport equation. The approach assumes that (i) the temperature effect on chemical reactions is important so that updated temperature information should be used for the geochemical equilibrium and kinetic calculations, and that (ii) the effect of advection (water flow) in the solute and heat transport equations is larger than the effect of concentration and temperature on the water flow equation. Therefore, the water flow equation should be solved before the solute and heat transport equations. The weak coupling method is also invoked in our modelling approach. The same solutions sequence was used in the original HYDRUS-1D model (Šimůnek et al., 1998), and is followed in HP1 as well.

Different approaches also exist to solve the multicomponent reactive transport equation (2.30). This equation contains terms describing the physical transport of the component (the first three terms on the right hand-side) and a term describing the geochemical reactions (the fourth term on the right hand-side). The physical transport part and the geochemical reactions can be solved either simultaneously (a global-implicit or one-step approach) or sequentially (an operator-splitting, two-step, or sequential approach). For a discussion of these two approaches, the reader is referred to Steefel and MacQuarrie (1996) and Mayer (1999). In our model we use the sequential approach. Following Walter et al. (1994), the solution space has three degrees of freedom: spatial, temporal, and chemical. Physical transport is connected in the spatial and temporal domains, and the geochemical reactions are only connected in the chemical domain. The physical part (coupled in space, uncoupled over the components) is obtained by solving Eq. (2.30) without the reaction term:

$$\frac{\partial \theta C_j}{\partial t} = \frac{\partial}{\partial x} \left( \theta D^w \frac{\partial C_j}{\partial x} \right) - \frac{\partial q C_j}{\partial x} - S C_{r,i} \quad (2.31)$$

and the chemical part (uncoupled in space, i.e., no transport, but coupled over the components) by simultaneously solving the equilibrium and kinetic geochemical reactions.

An overview of the coupled multicomponent reactive transport calculations is shown in Figure 2.1. The symbols used in this figure are:

- $n$  the  $n$ th time step
- H variables related to water flow (pressure heads, fluxes)
- T variables concerning heat transport (temperature)
- C variables dealing with components and species in the system

- G variables concerning the solid phase (mineralogical composition, exchange site, surface site, reactive surfaces)
- $\mathbf{p}^w$  vector of parameters needed to solve the water flow equation (Eq. (2.1))
- $\mathbf{p}^h$  vector of parameters needed to solve the heat transport equation (Eq. (2.9))
- $\mathbf{p}^s$  vector of parameters needed to solve the solute transport equation (Eq. (2.31))
- $\mathbf{p}^{gc}$  vector of parameters needed to solve the geochemical reactions

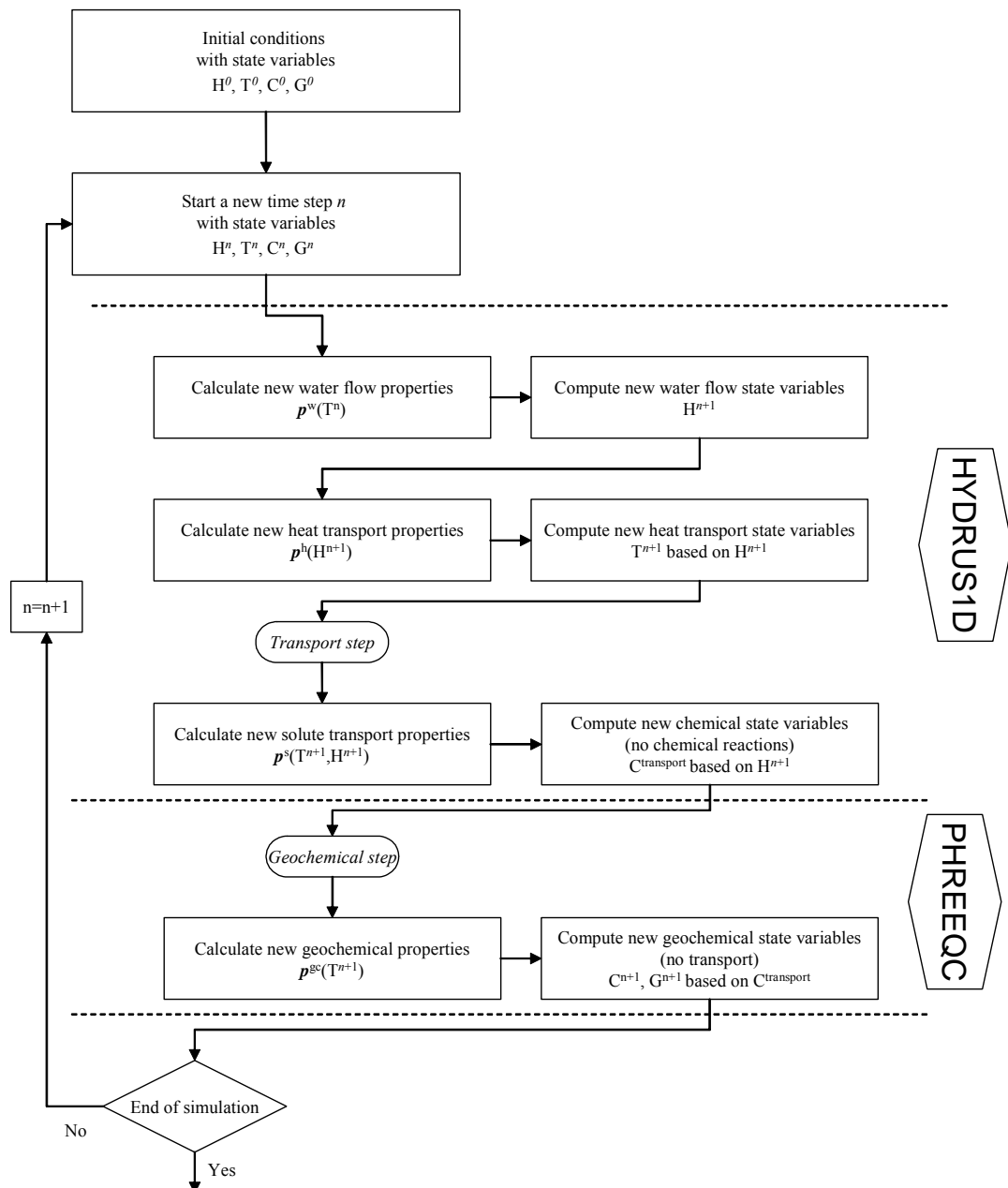


**Figure 2.1** Schematic of the modelling approach of the coupled HPI model.

## 2.7 Model structure

In this section we summarize the changes implemented in both codes. While the Fortran routines of HYDRUS-1D are compiled into Hydrus.dll, the c functions of PHREEQC are compiled into PHREEQC.dll.

### 2.7.1 PHREEQC

The original PHREEQC code contained the following files: Advect.c, Basic.c, Cl1.c, Integr.c, Inverse.c, Kinetics.c, Main.c, Mainsubs.c, Model.c, P2clib.c, Parse.c, Phqalloc.c, Prep.c, Print.c, Read.c, Readtr.c, Spread.c, Step.c, Structur.c, Tidy.c, Transp.c, and Utility.c. In the coupled HP1 we modified mostly only the **main.c** routine, and added a new file **Hydr\_tr.c**

#### **main.c**

From the main routine (main\_Phreeqc) we call first the “**read\_text\_file**” function that reads from the **Species.in** file the names of components to be transported by HYDRUS-1D, and stores these in the vector of strings **cRows** (nRows). Then we call the “**check\_hydrus\_species**” function that checks whether these components are defined in the geochemical database. Then instead of the original “**Transport()**” function, we call “**HYDRUS\_MAIN**” with three parameters, which refer to c functions called from the HYDRUS Fortran code. At the end we call function “**free\_string\_array**”, which deallocates memory from **cRows**.

```
void __stdcall HYDRUS_MAIN(void * run_HYDRUS_reactions, void *
    Get_Concentrations, void * Initialization);
int read_text_file(const char *file_path_name, int *nRows, char ***cRows);
void free_string_array(int nRows, char **cRows);
void check_hydrus_species(int nRows, char **cRows);
```

#### **Hydr\_tr.c**

This file contains four new functions: **Initialization**, **Get\_Concentrations**, **Run\_Hydrus\_reactions**, and **Get\_Names** that are called from HYDRUS. They are described below:

```
void Initialization(int node_number, int lMobil, float * Temperature, float * Theta, float
    ThImob, int max_species_number, int species_number, float * Concentrations,
    float * Im_Concentrations, float TimeInit);
void Get_Concentrations(int node_number, int max_species_number, int species_number,
    float * Concentrations, float * Im_Concentrations, int lMobil, float ThImob);
```

```

void run_HYDRUS_reactions(int node_number, int max_species_number, int
    species_number, float * Concentrations, float time, float *Temperature, float * Theta,
    float * Im_Concentrations, float TimeStep, int iPrint, int Step_No, int IMobil, float
    ThImob);
char * Get_Names(int species_number);

```

### 2.7.2 HYDRUS-1D

The original Hydrus-1D code contained the following files (see section 12 of Šimůnek et al., 1998): Hydrus.for, Input.for, Material.for, Output.for, Sink.for, Solute.for, Temper.for, Time.for, and Watflow.for. We added one additional file (Exports.h) that interfaces Fortran with c. Most of the changes were done in the main HYDRUS file, where the main program was converted into a **HYDRUS\_MAIN** subroutine. From this subroutine we call the following c functions that are located in the Hydr\_tr.c file:

```

    call Initialization(NumNP,IMobil,TempN,ThOld,ThImob,NSD,NS,Conc,
!           Sorb,tInit)
    call Get_Concentrations(NumNP,NSD,NS,Conc,Sorb,IMobil,ThImob)
    call run_HYDRUS_reactions(NumNP,NSD,NS,Conc,t,TempN,ThNew,Sorb,
!           dt,iPrint,TLevel,IMobil,ThImob)

```

and one new Fortran subroutine

```

    call PhreeqcMB(NSD,NS,NumNP,Conc,Conc1,Sorb,Sorb1,x,ThNew,
!           ThImob,PhrExch)

```

The **run\_HYDRUS\_reactions** function calls PHREEQC to carry out all chemical and biological reactions and transfers information from HYDRUS to PHREEQC, the **Get\_Concentrations** function transfers information back to HYDRUS from PHREEQC, the **Initialization** brings initial information from the PHREEQC part, and **PhreeqcMB** calculates mass balances for the main components.

**Table 2.1** Description of variables that are used in both HYDRUS-1D and PHREEQC, or newly defined in HYDRUS-1D.

Fortran variables	c variables	Type	Description
<b>Initialization</b>			
NumNP	node_number	int	Number of nodes
IMobil	IMobil	int	Mobile-immobile water model
TempN	Temperature	float*	Temperatures
ThOld	Theta	float*	Initial water contents
ThImob	ThImob	float	Immobile water content
NSD	max_species_number	int	Max number of components
NS	species_number	int	Number of components
Conc	Concetrations	float*	Concentrations
Sorb	Im_Concetrations	float*	Immobile concentration
tInit	TimeInit	float	Initial time
<b>Get_Concentrations</b> (see definitions above)			
Conc	Concetrations	float*	Concentrations before chemical reactions
Sorb	Im_Concetrations	float*	Immobile concentrations before chemical reactions
Conc1	Concetrations	float*	Concentrations after chemical reactions
Sorb1	Im_Concetrations	float*	Immobile concentrations after chemical reactions
<b>run_HYDRUS_reactions</b>			
t	time	float	Time
ThNew	Theta	float*	Water content
dt	TimeStep	float	Time step
iPrint	iPrint	int	Print time flag
TLevel	Step_No	int	Step Number
<b>PhreeqcMB</b>			
Conc		real*	Component concentrations in the mobile phase before chemical reactions
Conc1		real*	Component concentrations in the mobile phase after chemical reactions
Sorb		real*	Component concentrations in the immobile phase before chemical reactions
Sorb1		real*	Component concentrations in the immobile phase after chemical reactions
x		real*	Nodal coordinates
PhrExch		real*	Change in the mass of a component

### 3 Description of data input

#### 3.1 Input data

The following separate input files are required to run the coupled HP1 model:

#### HYDRUS-1D

<i>selector.in</i>	contains the following blocks:
	A. Basic Information
	B. Water Flow Information
	C. Time Information
	D. Root Growth Information
	E. Heat Transport Information
	F. Solute Transport Information
	G. Root Water Uptake Information
<i>profile.dat</i>	contains the following block:
	H. Nodal Information (except the initial total aqueous concentrations)
<i>atmosph.in</i>	contains the following block:
	I. Atmospheric Information

#### PHREEQC

<i>xxxxxxx.xxx</i>	is the database file containing thermodynamic data for aqueous species, pure phases and exchange reactions (e.g., <i>phreeqc.dat</i> , <i>minteq.dat</i> ).
<i>phreeqc.in</i>	contains information about the geochemical reactions.

#### HP1

<i>species.in</i>	contains a list of master species to be transported.
-------------------	--

The data and format of the different input files and blocks are described in section 10 of the HYDRUS-1D manual (Šimůnek et al., 1998) for input files related to HYDRUS-1D (*selector.in*, *profile.dat*, and *atmosph.in*), and in Parkhurst and Appelo (1999) for input files related to PHREEQC. We recommend that users refer to original manuals in order to complete the data input. Specific guidelines for the coupled HP1 code are:

- The *species.in* file contains on the first line the path to the geochemical database, and then a list of master species to be transported. An example of the *species.in* file is

```
c:\program files\phreeqc\phreeqc.dat
Na
Cl
Ca
Mg
```

where *phreeqc.dat* is the database file. This file forms a link between HYDRUS-1D and PHREEQC. The master species in the file must be written in the same way as they are defined in the **SOLUTION\_MASTER\_SPECIES** block of the *phreeqc.dat* input file (see Parkhurst and Appelo, 1999). The order of the master species in the *species.in* file refers to solute numbers in the *selector.in* files for the HYDRUS-1D model. Note that a check is made whether or not names from the *species.in* file correspond to master species from the geochemical database.

- When the graphical user interface of HYDRUS-1D (discussed later) is used, the number of master species is limited to 10. After the HYDRUS-1D input files are created with the graphical interface, the number of master species can be increased manually by making several changes in the *Selector.in* file described in Table 10.6 of Šimůnek et al. (1998): increase the variable *NS* to the number of master species, add records 9 and 12 for each additional solute, and expand record 16. The *Profile.dat* and *Atmosph.in* files (Table 10.8 and 10.9, respectively) must also be expanded for the specified number of species.
- We suggest to set solute transport parameters describing exchange with the solid or gas phases, or describing degradation, equal to zero. It is important to use the same molecular diffusion coefficient for all master species (see section 2.5). Note that this is not checked in the current version of the model.
- All boundary conditions are specified in the input files of HYDRUS-1D.
- Initial chemical conditions are to be defined in the *phreeqc.in* file. This includes concentrations of all master species. If the initial concentration of a given master species is zero, a very small value (e.g., 1E-20 mol/l) should be given; otherwise it is possible that the master species will be neglected during the simulation. There is no need to define the initial conditions of the total aqueous concentrations in the input files of HYDRUS-1D. Initial conditions for water flow and heat transport are to be defined in *profile.dat*.
- For each node in the HYDRUS-1D finite element mesh, a **SOLUTION** must be defined in the *phreeqc.in* file. The node number at the soil surface is 1 and numbering increases with depth. Solutions at different depths with the same initial composition can be grouped in the *phreeqc.in* input file.
- Since the *phreeqc.in* data file is read prior to the *profile.dat* data file, the amount of initial water for each **SOLUTION** (defined in the *profile.dat* file) is not known when the initial solutions are initialized. Therefore, the water content at each node (and

hence for each solution) should be specified for each **SOLUTION** key word in the *phreeqc.in* file. Alternatively, the **SOLUTION\_SPREAD** key word can be used to define solutions with varying amounts of water and temperatures as a function of depth.

- The input file *phreeqc.in* must contain the keyword **TRANSPORT** together with the option **-cells** indicating the number of cells. No additional information is required after the keyword (e.g., dispersivity and molecular diffusion are all defined in the input files of HYDRUS-1D), although **-punch\_cells** and **-punch\_frequency** can be used to control the output.

The different input files are most conveniently created using the interactive graphic-based user interfaces of the original models. These interfaces are public domain and can be downloaded from the World Wide Web for both the HYDRUS-1D and PHREEQC models. The HYDRUS-1D model is located at [http://www.pc-progress.cz/Fr\\_Hydrus.htm](http://www.pc-progress.cz/Fr_Hydrus.htm). The main part of the input-files required for the water flow, heat and solute transport parts of the problem can be constructed using the HYDRUS-1D interface (section B of Šimůnek et al., 1998). A graphical interface for PHREEQC can be found at <http://www.geo.vu.nl/users/posv/phreeqc/index.html> or at [http://wwwbrr.cr.usgs.gov/projects/GWC\\_coupled/phreeqi/](http://wwwbrr.cr.usgs.gov/projects/GWC_coupled/phreeqi/). This interface is helpful for constructing the *phreeqc.in* input file for the geochemical reactions in the problem.

### 3.2 Running the model and output

An extra file, *path.dat*, must be placed in the same directory as the executable of the HP1 model (i.e., HP1.exe) and two dynamically linked libraries with HYDRUS-1D (i.e., Hydrus.dll) and PHREEQC (i.e., Phreeqc.dll) subroutines and functions. The *path.dat* file specifies the path to the input and output file folder. All input files should be placed in the same folder (except the database file for which the path and name is defined in the *species.in* file). The simulation is started by activating the executable. Output files are created in the same folder as the input files. The content of the output files created by HYDRUS-1D are described in section 11 of Šimůnek et al. (1998). The output file of PHREEQC contains user-defined output data (the **SELECTED\_OUTPUT** key word in the input file, see Parkhurst and Appelo, 1999). Part of the created output can be viewed through the interfaces.



## 4 Verification problems

In this section we describe different test examples of the coupled HP1 model. We present examples having different levels of complexity. The following problems were solved with HP1 for verifying the numerical correctness of the coupling procedure: (i) transport problems with single or multiple components, subject to sequential first-order decay, will be compared with simulations using HYDRUS separately, (ii) multicomponent transport problems for steady-state flow will be compared with simulations using PHREEQC separately, and (iii) several more complicated problems will be compared with simulations using the CRUNCH model. The CRUNCH model was a result of further development of the GIMRT/OS3D codes of Steefel and Yabusaki (1996, see <http://www.csteefle.com>). Several of the verification examples as well as additional applications for transient flow were previously reported by Jacques et al. (2002, 2003).

### 4.1 *Modelling the transport of a single component or decay chain*

This first group of verification problems concerns the transport of one solute (either inert or adsorbing according to the Freundlich isotherm), or of a sequential first-order decay chain. Although these problems can be solved directly with the HYDRUS-1D program, we use them here to verify the coupling of HYDRUS-1D and PHREEQC, with HYDRUS-1D solving the transport part and PHREEQC the reaction part of the problem. First, we will test if the transfer of information (i.e., solute concentrations and water contents) between two modules of the coupled model (i.e., HYDRUS-1D and PHREEQC) is done correctly (section 4.1.1). Second, we will compare the numerical accuracy of both the coupled HP1 model and PHREEQC against the stand-alone HYDRUS-1D using a single-component transport problem involving either equilibrium (using the Freundlich adsorption isotherm) or kinetic (first-order decay) reactions. These geochemical reactions are coupled with transport within HYDRUS-1D using a one-step or global implicit method (i.e., various reactions are directly included into the governing transport equations). In contrast, a non-iterative sequential approach is used in both the PHREEQC and HP1 codes. In section 4.1.2 we will compare results of these three models (i.e., HYDRUS-1D, PHREEQC, and HP1) for different Peclet and Courant numbers. Finally, the transport of three sequential first-order decaying contaminants is simulated for transient flow with both HYDRUS-1D and HP1 (section 4.1.3).

#### 4.1.1 **Physical equilibrium and nonequilibrium transport of chloride**

In this first section we simply test if the transport of an inert solute (Cl) is correctly simulated using HP1 for the following conditions: (i) steady-state flow with no immobile water, (ii) steady-state flow with immobile water, and (iii) transient water flow. Since this example does

not consider any geochemical reactions, all transport processes in the coupled model (HP1) are simulated only with the HYDRUS-1D module. However, since solute concentration and water content values still pass between the two modules, we will evaluate in this example if the transfer of information between the two components of the coupled model is done correctly.

**Verification Problem 1: Steady-state physical (non)equilibrium transport of chloride (EQCL – NEQCL)**

This problem simulates the transport of chloride (i.e., a geochemically inert tracer) during saturated steady-state flow in a 20-cm long soil core. The saturated hydraulic conductivity  $K_s$  is  $1 \text{ cm d}^{-1}$  and the saturated water content is  $0.5 \text{ cm}^3 \text{ cm}^{-3}$ . The following solute parameters were used: a dispersivity ( $D_L$ ) of 8 cm for both the equilibrium and nonequilibrium cases, and for the latter case an immobile water content ( $\theta_{im}$ ) of  $0.1 \text{ cm}^3 \text{ cm}^{-3}$  and a first-order exchange coefficient ( $\omega$ ) of  $0.01 \text{ d}^{-1}$ . Simulation results obtained with HP1 were found to be identical to those obtained with HYDRUS-1D, as illustrated by the outflow concentrations in Figure 4.1.

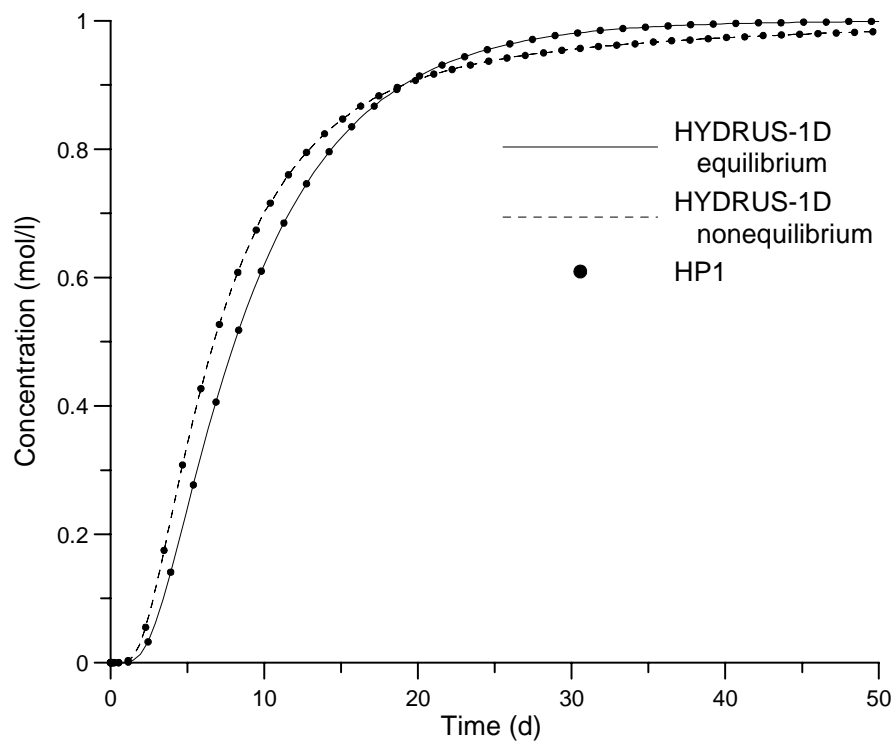


**Figure 4.1** Outflow concentrations for Verification Problem 1. Full and dashed lines are results for physical equilibrium and nonequilibrium transport, respectively, obtained with HYDRUS-1D. Dots are results obtained with HP1.

**Verification Problem 2: Transient physical nonequilibrium transport of chloride (TRANSCL)**

In this second problem we simulate the transport of chloride through a 1-m deep soil profile subject to a transient upper boundary condition given by daily values of precipitation and evaporation over a 300-d period. Physical nonequilibrium (i.e., the presence of immobile water in the soil profile) was considered in this problem. Note again that all transport calculations were done by HYDRUS-1D, which means that the test again applies only to the transfer of concentrations and water contents between HYDRUS-1D and PHREEQC. We used parameters of the soil hydraulic properties typical for a loamy soil ( $\theta_r = 0.078 \text{ cm}^3 \text{ cm}^{-3}$ ,  $\theta_s = 0.43 \text{ cm}^3 \text{ cm}^{-3}$ ,  $\alpha = 0.036 \text{ cm}^{-1}$ ,  $n = 1.56$ , and  $K_s = 24.96 \text{ cm d}^{-1}$  from Carsel and Parish, 1988). Solute transport parameters were as follows: a dispersivity  $D_L$  of 8 cm, an immobile water content  $\theta_{im}$  of  $0.05 \text{ cm}^3 \text{ cm}^{-3}$ , and a first-order exchange coefficient  $\omega$  of  $0.0125 \text{ d}^{-1}$ . Precipitation and evaporation rates were typical for the Campine region in Belgium. The soil profile was discretized into 100 elements of 1 cm each. Chloride was applied during the first 53 days of the simulation with a concentration of  $0.1 \text{ mmol l}^{-1}$ . Results in Figure 4.2 show a perfect match between HYDRUS-1D and HP1. From these results we conclude that the transfer of water contents and concentrations between the transport and reaction modules was done correctly.

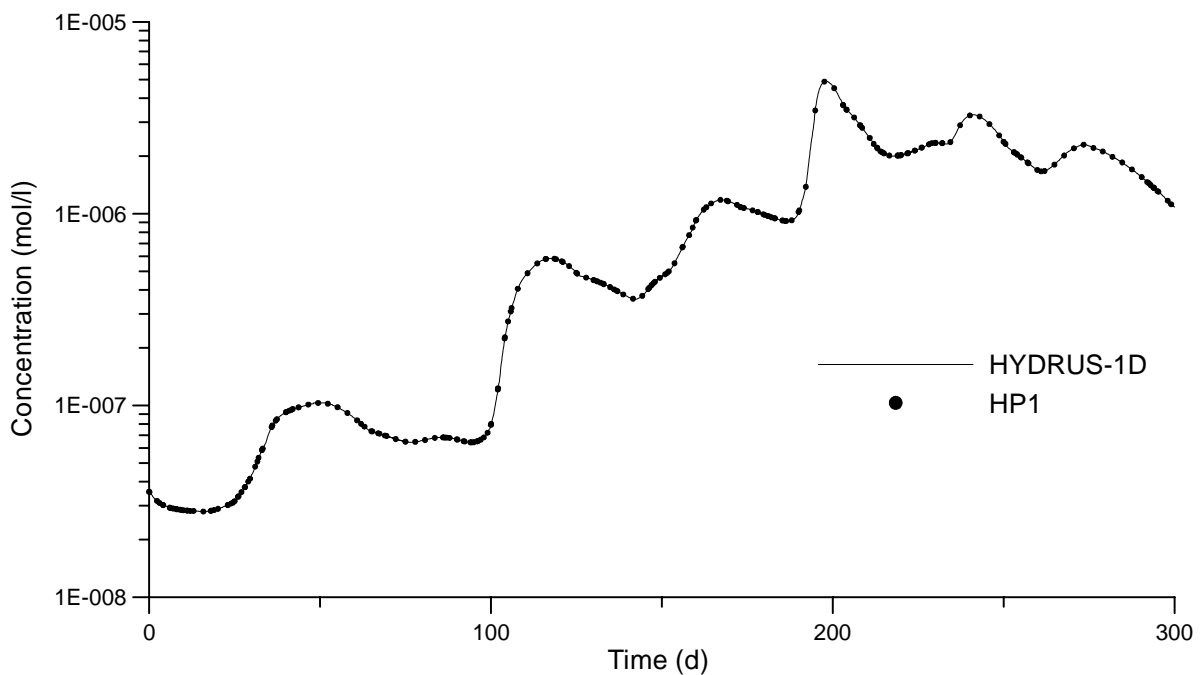


**Figure 4.2** Outflow concentrations for Verification Problem 2. The full line was generated with HYDRUS-1D, while dots were obtained with HP1.

#### 4.1.2 Transport of a nonlinearly adsorbing solute subject to first-order decay

This section considers numerical simulations of a nonlinearly sorbing solute undergoing first-order decay during steady-state water flow. We assume only heterogeneous reactions of a contaminant *Cont* with a sorbing surface *Sor*. Adsorption is assumed to be instantaneous and described with the Freundlich equation:

$$S^s = K_d C^{n_F} \quad (4.1)$$

where  $S^s$  is the adsorbed concentration [ $M_a M_s^{-1}$ ],  $C$  is the aqueous concentration [ $M_a L^{-3}$ ],  $K_d$  is an empirical adsorption coefficient [ $M_a^{(1-n)} L^{3n} M_s^{-1}$ ] and  $n_F$  is the empirical Freundlich coefficient [-]. The contaminant *Cont* is additionally assumed to be subject to first-order degradation:

$$R = \mu_w C \quad (4.2)$$

where  $R$  is the decay rate [ $M_a L^{-3} T^{-1}$ ] and  $\mu_w$  is the first-order rate constant for solutes in the liquid phase [ $T^{-1}$ ].

##### ***Modelling nonlinear Freundlich adsorption with PHREEQC***

To model instantaneous adsorption using the Freundlich adsorption isotherm, we rewrote Eq. (4.1) in terms of the amount adsorbed per unit volume of water:

$$S^w = (K_d \rho) C^{n_F} \quad (4.3)$$

where  $S^w$  is the adsorbed concentration per unit volume of water [ $M_a L^{-3}$ ] and  $\rho$  is the bulk density [ $M_s L^{-3}$ ]. Equation (4.3) corresponds with the following mass action equation:

$$\frac{[SorCont]}{[Sor][Cont]^{n_F}} = (K_d^s \rho) = K_d^w \quad (4.4a)$$

$$[SorCont] = K_d^w [Sor] [Cont]^{n_F} \quad (4.4b)$$

where  $K_d^w$  is the adsorption constant in mass per unit volume of water [ $M_a^{(1-n)} L^{3n} L^{-3}$ ]. In PHREEQC, this sorption reaction is modelled as a surface complexation reaction. The amount of adsorption sites is chosen very large so that  $[Sor]$  in Eq. (4.4b) does not change significantly when the amount of adsorbed species  $[SorCont]$  remains small. An outline of the PHREEQC input file is given in Box 4.1. In this example, the new solution master species

**Box 4.1 PHREEQC input for the Freundlich adsorption isotherm**

```

1  SOLUTION_MASTER_SPECIES
2  Cont Cont 0.0 Cont 1.0

3  SOLUTION_SPECIES
4  Cont = Cont; log_k 0.0

5  SURFACE_MASTER_SPECIES
6  Sor Sor

7  SURFACE_SPECIES
8  Sor = Sor
9  log_k 0

10 Sor + nF Cont = SorCont          #nF Freundlich term
11 -no_check; -mole_balance SorCont
12 log_k K                          #K = Log(Kdw / S)

13 SURFACE 1
14 equilibrate 1
15 -no_edl true
16 Sor S 1 S                        #S Total amount of adsorption sites

```

(*Cont*), its aqueous speciation, and the surface species (*Sor*) are defined on lines 1-6 with the PHREEQC-keywords **SOLUTION\_MASTER\_SPECIES**, **SOLUTION\_SPECIES**, and **SURFACE\_MASTER\_SPECIES**. The definition of the mass action equation of the Freundlich isotherm, Eq. (4.4b), is given on lines 10-12 with the PHREEQC-keyword **SURFACE\_SPECIES**. Two options are included: (1) **-no\_check** since the mole balance of the reaction equation (line 10) is not fulfilled due to nonlinearity of the Freundlich isotherm ( $n_F \neq 1$ ), and (2) **-mole\_balance** to ensure balancing of 1 *Sor* and 1 *Cont*. The association coefficient  $K$  is defined by  $K_d^w/[Sor]$ , which is approximately equal to the total amount of adsorption sites  $S$ , if  $S$  is chosen very large, e.g.  $10^{100} \text{ mol l}^{-1}$  (put  $S = 10^{100}$  in line 16). As an example, for  $K_d^s = 5$ ,  $\rho = 1.5$ , and  $S = 10^{100}$  we obtained a  $K$ -value (=log\_k) of -99.1249.

**Verification Problem 3: Steady-state transport of nonlinearly adsorbed contaminant (STADS)**

In this problem we consider saturated steady-state water flow and single-component (*Cont*) transport through a soil column of 1 m length for a period of 1000 d. Very low initial concentrations of *Cont* are assumed to be present ( $10^{-15} \text{ mol l}^{-1}$ ) in all cases. Transport and simulation parameters as well as Peclet numbers ( $Pe = (q \Delta x)/(\theta D^w)$  with  $\Delta x$  the characteristic length of a finite element), and Courant numbers ( $Cr = (q \Delta t) / (\theta \Delta x)$ , Steefel and MacQuarrie, 1996) are given in Table 4.1. HYDRUS-1D, PHREEQC and HP1 simulations with several different combinations of the Peclet and Courant numbers are compared in

**Table 4.1** Transport and simulation parameters for Verification Problem 3.

Parameters	HYDRUS	PHREEQC			HP1			
	H	P-1	P-2	P-3	HP1-1	HP1-2	HP1-3	HP1-4
$K_s$ (cm d <sup>-1</sup> )	1	-	-	-	1	1	1	1
$\theta_s$ (cm <sup>3</sup> cm <sup>-3</sup> )	0.5	0.5	0.5	0.5	0.5	0.5	0.5	0.5
$q$ (cm d <sup>-1</sup> )	1	2	2	2	1	1	1	1
$\nu$ (cm d <sup>1</sup> )	2	1	1	1	2	2	2	2
$D_L$ (cm)	1	1	1	1	1	1	1	1
$\rho$ (g cm <sup>-3</sup> )	1.5	-	-	-	1.5	1.5	1.5	1.5
$K_d^s$ ()	5	-	-	-	-	-	-	-
$n_F$ (-)	0.8	0.8	0.8	0.8	0.8	0.8	0.8	0.8
$K_d^w$ ()	-	7.5	7.5	7.5	7.5	7.5	7.5	7.5
Log( $Sor$ )	-	100	100	100	100	100	100	100
Log_k	-	-99.125	-99.125	-99.125	-99.125	-99.125	-99.125	-99.125
$\Delta x$ (cm)	1	1	0.5	0.25	1	1	1	1
$\Delta t_{max}$ (d)	1	-	-	-	1	0.25	0.08	0.04
$Pe$	1	1	0.5	0.25	1	1	1	1
$Cr$	2	1.33	0.66	0.33	2	0.5	0.16	0.08

Figure 4.3. Depth profiles of aqueous *Cont*-concentrations are plotted at 3 different times (250, 500, and 750 d). Figure 4.3a compares three simulations carried out with PHREEQC (the solution method is equivalent to SNIA (sequential non-iterative approach) with an explicit time weighting scheme) and HYDRUS-1D (the global implicit method with implicit time weighing).

The concentration front for the P-1 space discretization scheme displayed significant numerical dispersion as compared to the HYDRUS-1D solution. Increasing the number of cells in PHREEQC, and thus decreasing the Peclet number, produced less numerical dispersion (e.g., P-2 and P-3). However, the simulation time became then very large because of the large number of nodal points in the discretization scheme. Results of simulations using HP1 are compared with HYDRUS-1D in Figure 4.3b. While the same spatial discretization was used for all simulations, the maximum time step was decreased. HP1 simulation with a maximum time step of 1 d (corresponding to Courant numbers larger than one) provided less accurate results as compared to HYDRUS-1D. However, the agreement gradually improved with lower maximum time steps and Courant numbers, with the lowest two  $Cr$ -values providing almost identical results. HP1 results were found to be better than those of PHREEQC for the same Peclet and Courant numbers (compare HP-2 and P-1 in Figure 4.3a). To obtain a similar degree of accuracy for both HP1 and PHREEQC, at least 200 cells were needed for the PHREEQC simulation (Figure 4.3a) compared to 100 for HP1. Also the computational time for HP1 was significantly smaller as compared to PHREEQC.

When the accuracy of the HP1-code is evaluated based on the simulation with HYDRUS-1D, HP1 will need smaller time steps (up to 25 times smaller) with the same spatial discretization. Note that a similar analysis can be done when  $\Delta x$  is decreased in the HP1 simulations.

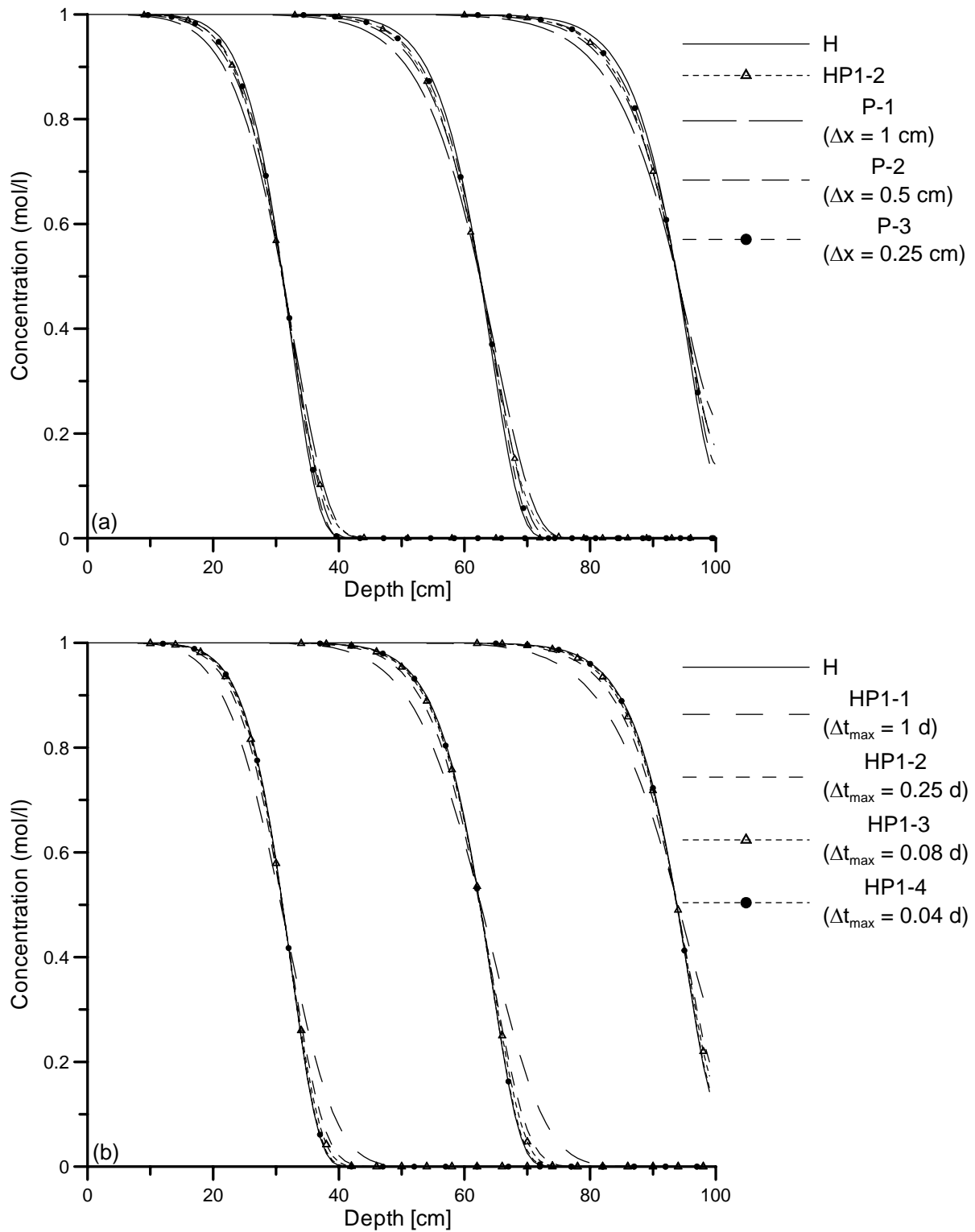


**Figure 4.3** Depth profiles of Cont after 250, 500, and 750 d for different simulations defined in Table 4.1 for Verification Problem 3. Tests consider effects of grid size for PHREEQC (a), and effects of maximum time steps for HP1 (b).

### ***Modelling first-order decay with PHREEQC***

First-order decay (Eq. (4.2)) in PHREEQC is modelled using the keywords **RATES** and **KINETICS**. The implementation in PHREEQC is shown in Box 4.2. The kinetic reaction itself is defined under the keyword **RATES** (lines 1-8). In this example, the reaction is called 'degradation' (line 2). Between **-start** and **-end** a Basic-program is written for the kinetic reaction of the 'phase' degradation consisting of standard Basic-statements (e.g., here only `rem`) and special Basic-statements for PHREEQC (e.g., `MOL`, `SAVE`, `TOT`, and `TIME`). The first statement of the Basic-program (line 4) is only a comment indicating the meaning of the first parameter. The second statement evaluates the rate equation (Eq. (4.2)) with `parm(1)` being the value of  $\mu_w$ , `TOT("water")` the amount of water in the cell (which is included here to have an equivalent problem as in HYDRUS-1D), and `MOL("Cont")` the molality of the solute. The third statement (line 6) integrates the rate over the subinterval with the special variable `TIME`. Finally, the moles of reaction during the time interval are saved with the last special statement `SAVE`. Note the negative sign on line 6 that results in a negative amount of moles saved in the last statement. In general, a positive sign represents decreasing amounts of a phase (i.e., dissolution), whereas a negative sign results in precipitation of that phase. Consequently, elements will enter the solution in the former case (dissolution) and will be removed from the solution in the latter case (i.e., precipitation, degradation, or decay). In this example the imaginary phase 'degradation' is precipitating. This is done to prevent the cessation of the kinetic reaction (i.e., when the phase 'degradation' is completely removed from the system).

The second keyword in Box 4.2 (**KINETICS**) defines the names of the rate expressions related to a specific cell. In this example we have one rate expression called 'degradation'. Since 'degradation' is used here as an imaginary phase (and not a phase defined in the database), the option **-formula** is used to define the elements produced (i.e., when the

#### **Box 4.2** *PHREEQC input for first-order decay reactions*

```

1  RATES
2  degradation
3  -start
4  10 rem parm(1) first-order degradation coefficient (sec-1)
5  20 rate = parm(1)*TOT("water")*MOL("Cont")
6  30 moles = - rate * TIME
7  40 SAVE moles
8  -end

9  KINETICS 1
10 degradation
11 -formula Cont 1; -parms 2.3148E-7

```

product of the stoichiometric element coefficient (i.e., 1 in the formula option) multiplied by the moles of reaction during a particular time step is positive) or consumed (i.e., when the product is negative) during the kinetic reaction. Since in this example the coefficient for the element *Cont* is 1 (line 11) and the reaction progress is negative, the concentration of *Cont* will decrease with the formation of the imaginary phase 'degradation'. Note that we could write the input also with a negative coefficient and a positive reaction progress (i.e., dissolution of the phase). However, in that case we could reach complete dissolution of the phase and, consequently, termination of the decay reactions. The last option under KINETICS in Box 4.2 is **-parms** for the purpose of defining parameters in the rate expression.

***Verification Problem 4: Steady-state transport of nonlinearly adsorbing contaminant with first-order decay (STDECAY)***

This verification problem is the same as the previous one (i.e., Verification Problem 3) but with the inclusion of first-order decay. All transport and simulation parameters are equal to those of Verification Problem 3 (see Table 4.1). However, we did not perform the P-3 and HP-1 simulations because the former (P-3) was computationally inefficient and the latter (HP-1) produced relatively high amount of numerical dispersion. The first-order rate constant was chosen equal to  $0.2 \text{ d}^{-1}$  (or  $2.31 \cdot 10^{-6} \text{ sec}^{-1}$ ). We again compare HYDRUS-1D results with PHREEQC simulations using different spatial discretizations, and HP1 simulations using different maximum time steps (Figure 4.4). The latter code is the reference.

Results of simulations with mixed equilibrium (Freundlich adsorption) and kinetic (first-order decay) reactions were very similar for all three models, thus supporting the same conclusions as in the previous case. The transport of a nonlinearly adsorbing, first-order decaying contaminant was accurately modelled with HP1 when Courant numbers were reasonably small ( $Cr$  smaller than 0.2, i.e. 10 times smaller than  $Cr$  from HYDRUS-1D). Furthermore, results obtained with HP1 were somewhat better compared to results obtained with PHREEQC for the same Peclet and Courant numbers.

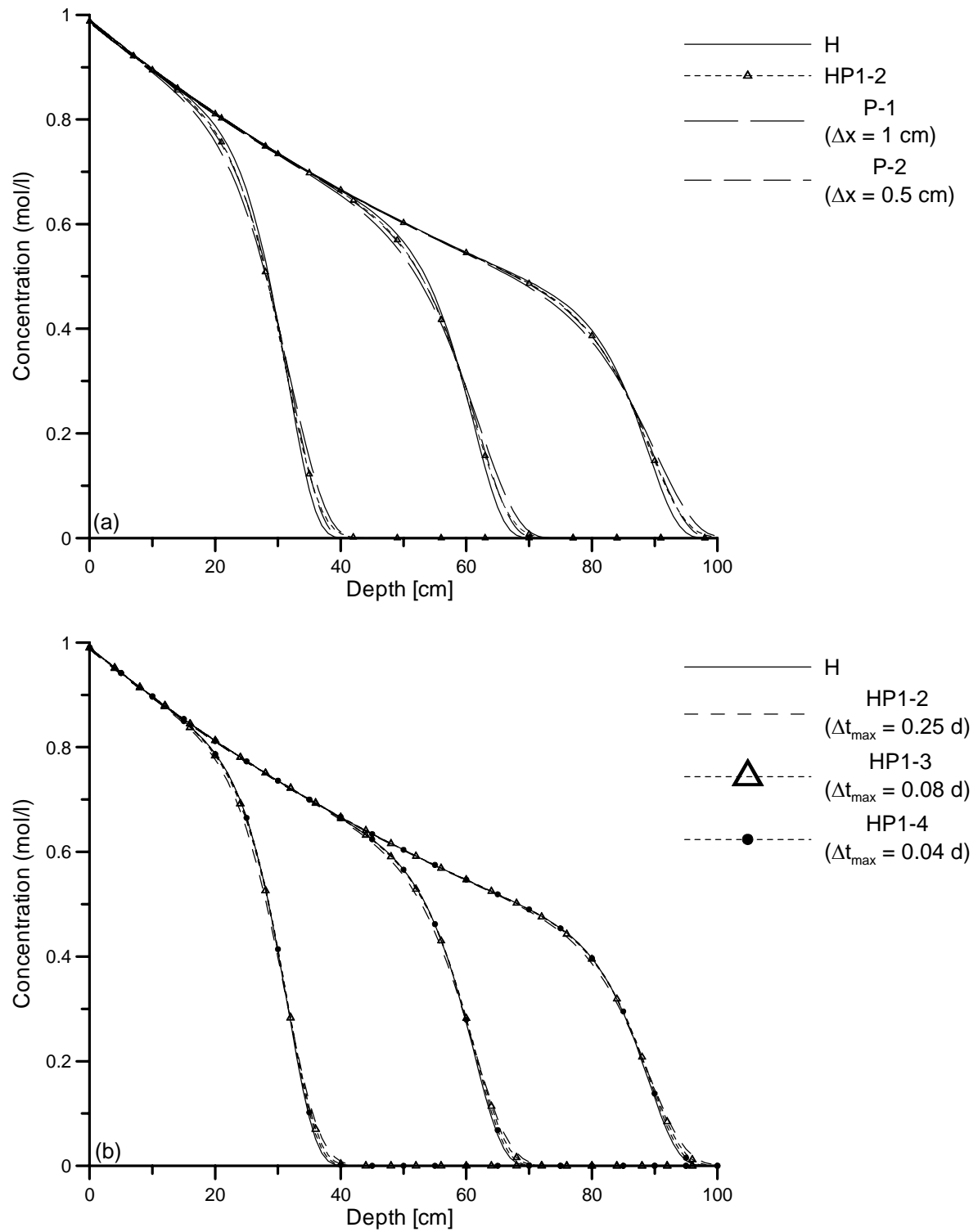
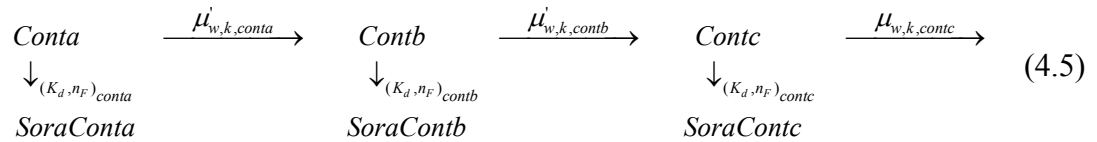


**Figure 4.4** Depth profiles of Cont after 250, 500, and 750 d for different simulations defined in Table 4.1 (Verification Problem 4 with a first-order decay coefficient of  $0.2 \text{ d}^{-1}$ ).

### 4.1.3 Transport of first-order decay chain of nonlinearly adsorbing contaminants during transient flow

#### *Problem definition*

In this example we consider the transport of three (non)linearly adsorbing contaminants, *Conta*, *Contb*, and *Contc* that are involved in a sequential first-order decay chain defined as:



where  $\mu'_{w,k}$  are the first-order rate constants connecting two contaminants,  $\mu_{w,k}$  is the first-order rate constant for *Contc*,  $K_d$  and  $n_F$  are the Freundlich isotherm parameters for the three contaminants, and *SoraConta*, *SorbContb*, and *SorcContc* are the three surface species related to *Conta*, *Contb*, and *Contc* on three surfaces *Sora*, *Sorb*, and *Sorc*, respectively. Reaction parameters for the three contaminants are given in Table 4.2. Model simulations were carried out for a 1-m deep homogeneous soil profile during 1000 d assuming transient flow. Upper boundary conditions were taken as daily precipitation rates representative of the Campine Region in Belgium. Evaporation was neglected during the simulations. The lower boundary condition was defined as free drainage. A uniform initial pressure head of  $-60$  cm was assumed for the entire soil profile. For solute transport, the following initial and boundary conditions were considered: (1) low initial concentrations ( $10^{-15}$  mole  $\text{l}^{-1}$ ) for all three contaminants, (2) third-type solute fluxes as the top boundary conditions with 1, 0.1, and 0 mol  $\text{l}^{-1}$  for *Conta*, *Contb*, and *Contc*, respectively, and (3) zero-gradient bottom boundary condition.

#### *Modelling the decay chain with HPI*

The decay chain was modelled by defining the rates of three kinetic reactions (*degrad\_conta*, *degrad\_contb*, and *degrad\_contc*) to model the degradation of solutes *Conta*, *Contb*, and *Contc*, respectively. The definition of degradation rates is similar as in Verification Problem 4. To model the degradation of *Conta* into *Contb*, the option **-formula** for keyword **KINETICS** (line 11) is changed to **-formula** *Conta* 1 *Contb* -1, which indicates that when 1 mole of the imaginary phase *degrad\_conta* precipitates (a negative rate), 1 mole of *Conta* disappears and 1 mole of *Contb* appears. A similar kinetic rate reaction is written for the transformations of *Contb* into *Contc*.

**Verification Problem 5: First-order decay chain of nonlinearly adsorbing contaminants during unsteady flow (SEASONCHAIN)**

We now compare HYDRUS-1D results with four HP1 runs using different time-stepping schemes. The first two simulations were carried out with maximum time steps of 30,000 s (HP1-1) and 10,000 s (HP1-2) in order to obtain Courant numbers smaller than 1 (based on flow velocities at the top boundary). For the other two simulations we used the stabilisation criterion defined by Perrochet and Berod (1993) and implemented in HYDRUS-1D:

$$Pe \bullet Cr_v \leq \omega_s \quad (4.6)$$

where  $\omega_s$  is the performance index [-]. Simulations were performed with  $\omega_s = 0.4$  (HP1-3) and 0.2 (HP1-4). The HYDRUS-1D module of HP1 automatically adjust the time stepping to fulfil this stabilization criterion. Transport parameters are given in Table 4.2 and simulation parameters (i.e., temporal and spatial steps, and performance index) in Table 4.3.

Distributions of *Conta*, *Contb*, and *Contc* versus depth are shown in Figure 4.5 at three times (250, 500, and 1000 d). Simulations obtained with HP1-1 were identical to the HYDRUS-1D results for *Conta* and *Contb*, except at the leading edge of the concentration profile for the first print time for *Conta*. Results for HP1-3 and HP1-4 shown a better agreement between the simulations than those of HP1-1 and HP1-2. Concentration profiles for *Contc* were also in very good agreement between different runs, except for the peak concentrations, which were smaller than those obtained with HYDRUS-1D. Note again that simulations for HP1-3 and HP1-4 runs shows a better agreement than those for HP1-1 and HP1-2 runs.

**Table 4.2** Soil hydraulic, transport, and reaction parameters for Verification Problem 5.

	Parameter	Value	<i>Conta</i>	<i>Contb</i>	<i>ContC</i>
Hydraulic parameters	$\theta_r$ (cm <sup>3</sup> cm <sup>-3</sup> )	0.078			
	$\theta_s$ (cm <sup>3</sup> cm <sup>-3</sup> )	0.43			
	$\alpha$ (cm <sup>-1</sup> )	0.036			
	$n$ (-)	1.56			
	$K_s$ (cm d <sup>-1</sup> )	24.96			
Transport parameters	$D_L$ (cm)	1			
	$\rho$ (g cm <sup>-3</sup> )	1.5			
Reaction parameters	$K_d$		0.5	2.5	5
	$n_F$ (-)		1	0.9	0.8
	Log_k *		-100.12	-99.43	-99.12
	$\mu'_{w,k}$ (d <sup>-1</sup> )		0.005	0.06	-
	$\mu_{w,k}$ (d <sup>-1</sup> )		-	-	0.02

\* Input for HP1 assuming the amount of adsorption sites  $S = 10^{100}$ .

**Table 4.3** Input simulation parameters and numerical results for Verification Problem 5.

Parameter	HYDRUS1D*	HP1			
		HP1-1	HP1-2	HP1-3	HP1-4
<i>Input simulation parameters</i>					
$\Delta t_{init}$ (sec)	864	864	864	864	864
$\Delta t_{min}$ (sec)	0.0864	0.0864	0.0864	0.0864	0.0864
$\Delta t_{max}$ (sec)	86400	30000	10000	86400	86400
$\omega_s$	2	2	2	0.4	0.2
$\Delta x$ (cm)	1	1	1	1	1
<i>Simulation results</i>					
$N^{**}$	9070	9960	13585	9761	11775
$\Delta t_{min}$ (sec)	864	864	864	864	864
$\Delta t_{max}$ (sec)	86400	30000	10000	86400	57600
$Pe_{max}$	1.09	1.20	1.17	1.08	1.04
$Cr_{max}$	0.47	0.99	0.89	0.47	0.24

\* Note that Courant numbers are calculated differently ( $R$  is included in the denominator).

\*\* Number of time steps for the complete simulation.

An overview of different numerical criteria is given in Table 4.3. The HP1 simulation parameters (temporal and spatial steps) for this particular problem had no significant influence on the accuracy of the simulation results. For purposes of computational efficiency, it is however always better to use the stability criterion based on the performance index  $\omega_s$ . This stability criterion ensures that small time steps are used when flow is rapid, but allows for larger time steps when flow is slow. This is done by modifying time steps such that the Courant number obeys the inequality given by Eq. (4.6). Note that HP1 requires a lower performance index (five times smaller) than HYDRUS-1D to obtain similar results.

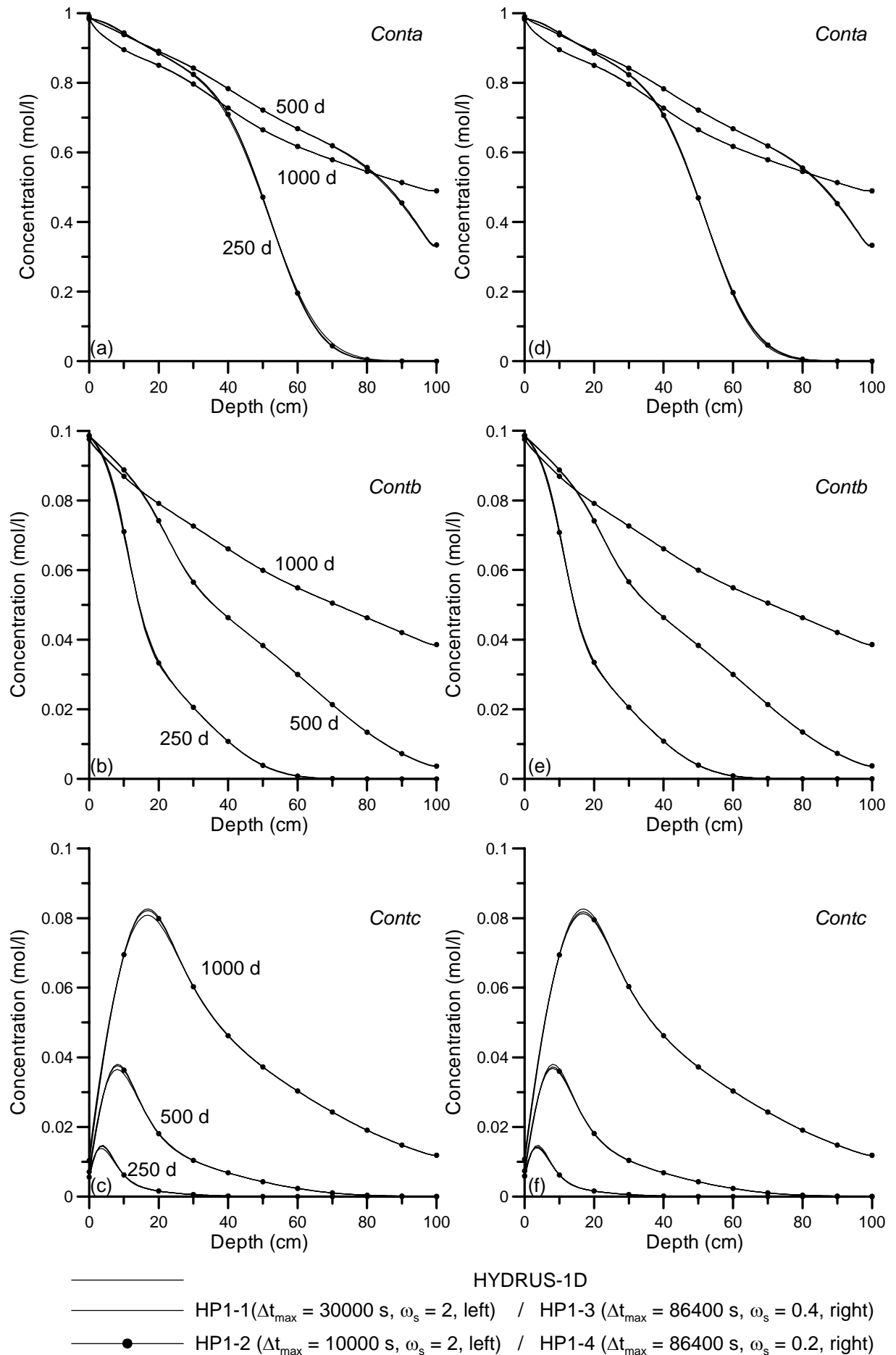


**Figure 4.5** Distribution of *Conta*, *Contb*, and *Contc* versus depth after 250, 500, and 1000 d for different simulations as defined in Table 4.3 (Verification Problem 5).

## 4.2 Multicomponent transport during steady-state flow

In this section we test different keywords of the PHREEQC program while using the coupled HP1 model. The following specific reactions are tested: (1) cation exchange (**EXCHANGE**) and (2) equilibrium and kinetic dissolution / precipitation of minerals (**EQUILIBRIUM-PHASES**). The key words **TRANSPORT** and **KINETICS** were tested in the previous section.

### 4.2.1 Cation exchange reactions

#### *Verification Problem 6: Transport of heavy metals subject to multiple cation exchange (CATEXCH)*

In this problem, the transport of ten ions (Al, Br, Ca, Cd, Cl, K, Mg, Na, Pb, Zn) through a soil column is modelled. Initial and inflow concentrations of the ions are given in Table 4.4. The cation exchange capacity is equal to 0.011 mol / cell. The soil core has a length of 8 cm and is discretized into 40 cells of 0.2 cm. The flow velocity is 2 cm d<sup>-1</sup> and the dispersivity is 2 cm. Simulations were performed for 15 days. The maximum time step used in HP1 was 0.015 d.

Distribution versus depth after three days and outflow concentrations during 15 days for selected output variables (ions and pH) are shown in Figure 4.6 and Figure 4.7, respectively, for simulations carried out with PHREEQC and HP1. Only small differences between the two simulations were present in the concentration profiles (Figure 4.6). Deviations may be due to increased numerical dispersion in PHREEQC, as noted in the Cl concentration profile. As discussed in the previous section, simulations with PHREEQC showed a larger dispersion compared to the simulations with HYDRUS-1D and HP1 if the same spatial discretization was used (e.g., Figure 4.3a and Figure 4.4a). If the spatial discretization in PHREEQC was

**Table 4.4** Initial and inflow concentrations for Verification Problem 6.

mmol l <sup>-1</sup>	Initial pore water composition	Initial concentrations of exchangeable cations*	Inflow concentrations
Al	0.5	0.92	0.1
Ca	1 10 <sup>-4</sup>	2.88 10 <sup>-4</sup>	5
Cd	0.09	0.17	0
K	2	1.06	0
Mg	0.75	1.36	1
Na	6	0.62	0
Pb	0.1	0.34	0
Zn	0.25	0.76	0
Br	11 <sup>+</sup>	-	3.7
Cl	1 10 <sup>-4</sup>	-	10
pH	5.5	-	2.9

\* Calculated in equilibrium with the initial pore water composition.

<sup>+</sup> Br is used to impose a charge balance at pH of 5.5.

reduced to 0.0005 m (i.e., 160 cells), PHREEQC converged towards the numerical simulations obtained with HP1 (Figure 4.6). Small differences between HP1 and PHREEQC exist when a spatial discretization of  $\Delta x = 0.002$  m is used (Figure 4.7). If  $\Delta x$  is decreased to 0.0005 m, no significant differences between the two simulations were present at the end of the column and in the outflow concentrations. We conclude that the keyword **EXCHANGE** is correctly coupled in HP1.

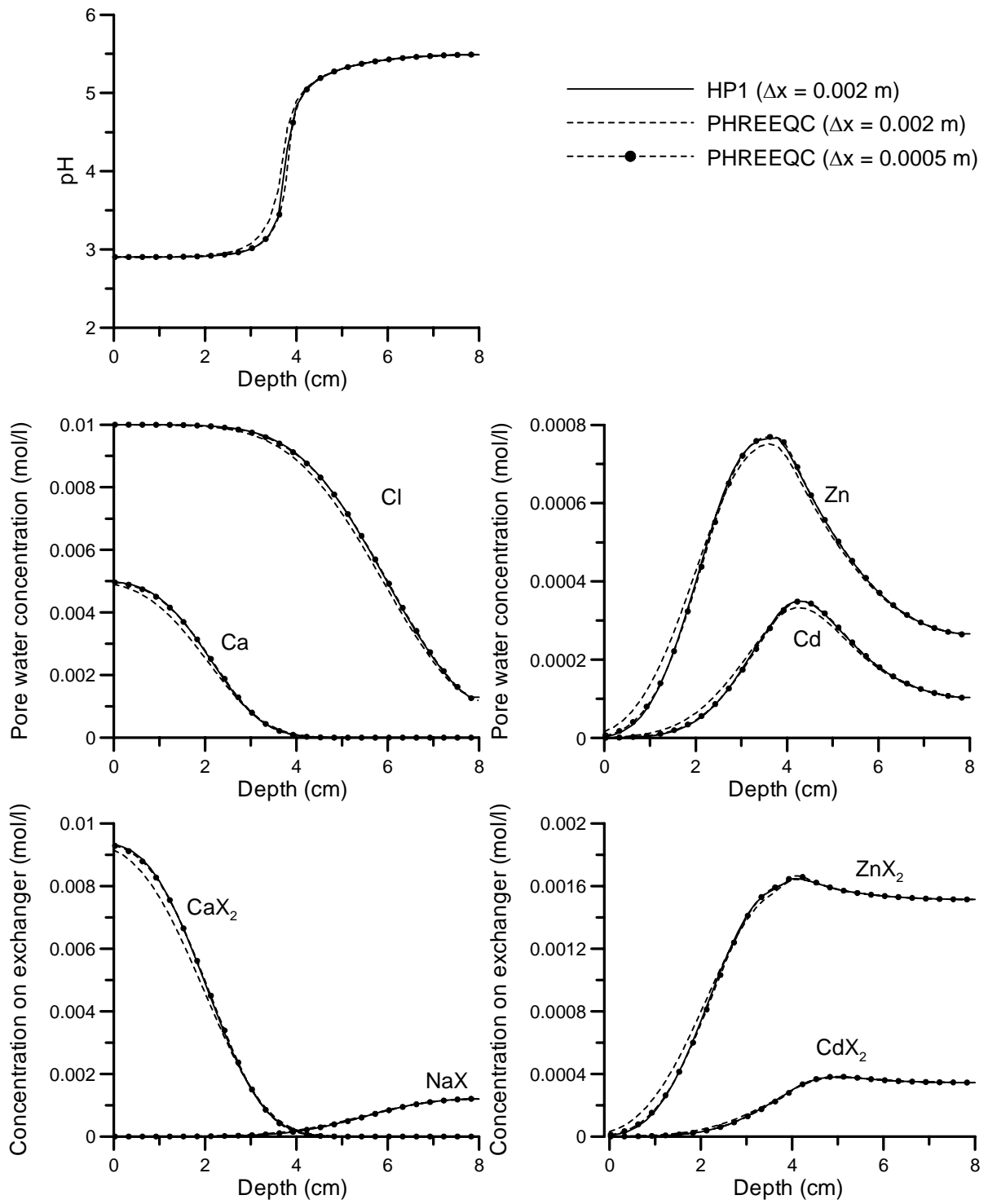


**Figure 4.6** Distribution of pH, dissolved Ca, Cl, Zn, and Cd concentrations, exchangeable Ca, Na, Zn, and Cd concentrations versus depth after three days of infiltration for Verification Problem 6.

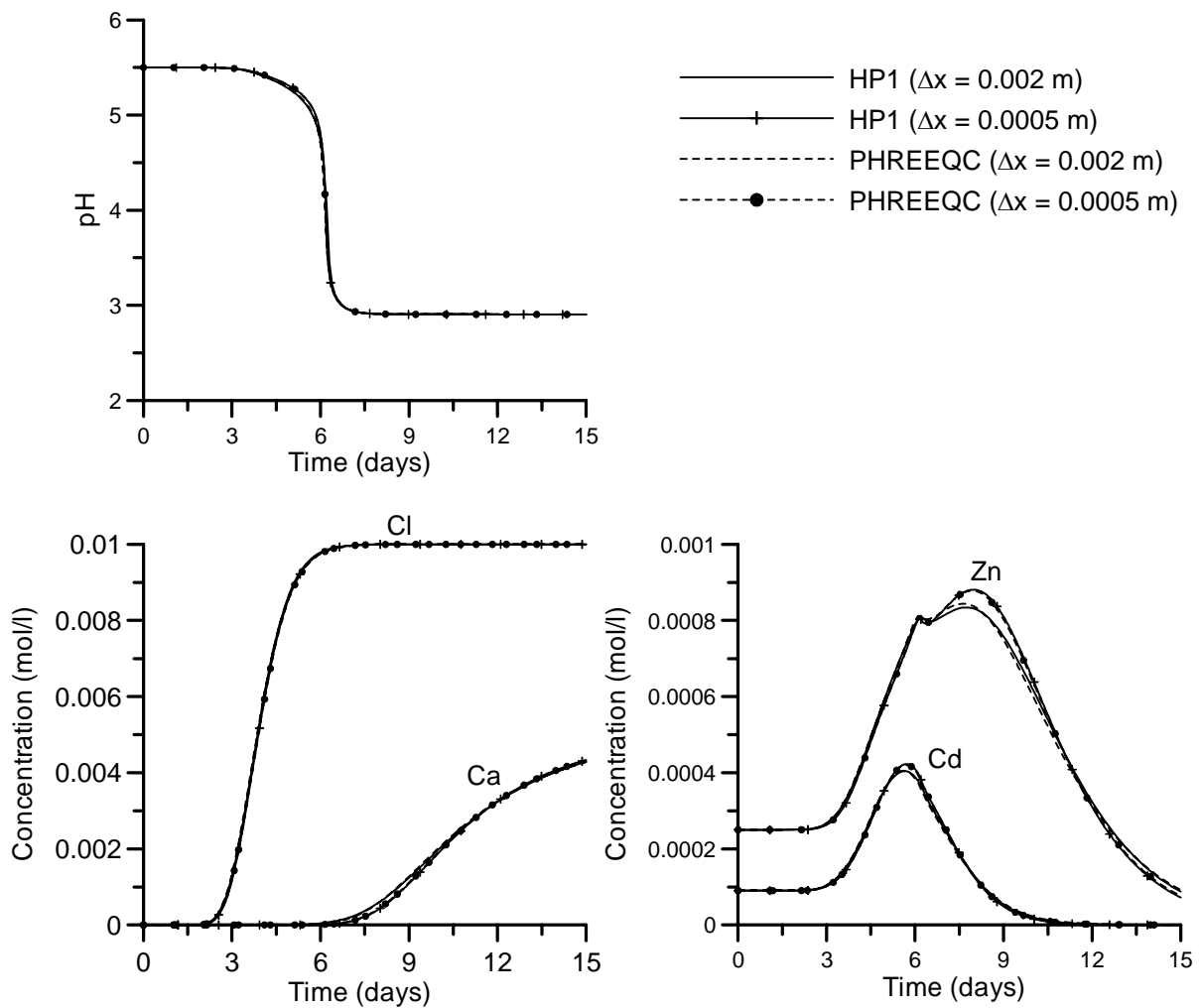


**Figure 4.7** pH, Ca, Cl, Zn, and Cd concentrations in the effluent for Verification Problem 6 (Full line: HP1, dashed line: PHREEQC).

#### 4.2.2 Mineral dissolution

##### *Verification Problem 7: Transport with mineral dissolution (MINDIS)*

A 100-cm long soil column, consisting of amorphous  $\text{SiO}_2$  and gibbsite ( $\text{Al}(\text{OH})_3$ ), is leached with a solution containing  $5 \cdot 10^{-7} \text{ mol l}^{-1}$  Si,  $1 \cdot 10^{-6} \text{ mol l}^{-1}$  Al, and  $1 \cdot 10^{-3} \text{ mol l}^{-1}$  Na (to obtain an inflow pH of 11.15). Initial concentrations were  $1.76 \cdot 10^{-3} \text{ mol l}^{-1}$  Si,  $8.87 \cdot 10^{-9} \text{ mol l}^{-1}$  Al, and  $1 \cdot 10^{-12} \text{ mol l}^{-1}$  Na, corresponding to a pH of 6.33. In each 1-cm cell, 0.015 mol amorphous  $\text{SiO}_2$  and 0.005 mol gibbsite is present. The flow velocity is 2 cm/day and the dispersivity is 1 cm. Simulations are again carried out with both PHREEQC and HP1.

Distribution of pH, Si, Al, amorphous  $\text{SiO}_2$ , and gibbsite versus depth after 150 days of simulation are presented in Figure 4.8. No significant differences between PHREEQC and HP1 were apparent for pH, Si, Al, amorphous  $\text{SiO}_2$  and gibbsite. The keyword **EQUILIBRIUM-PHASES** hence was coupled correctly in HP1.

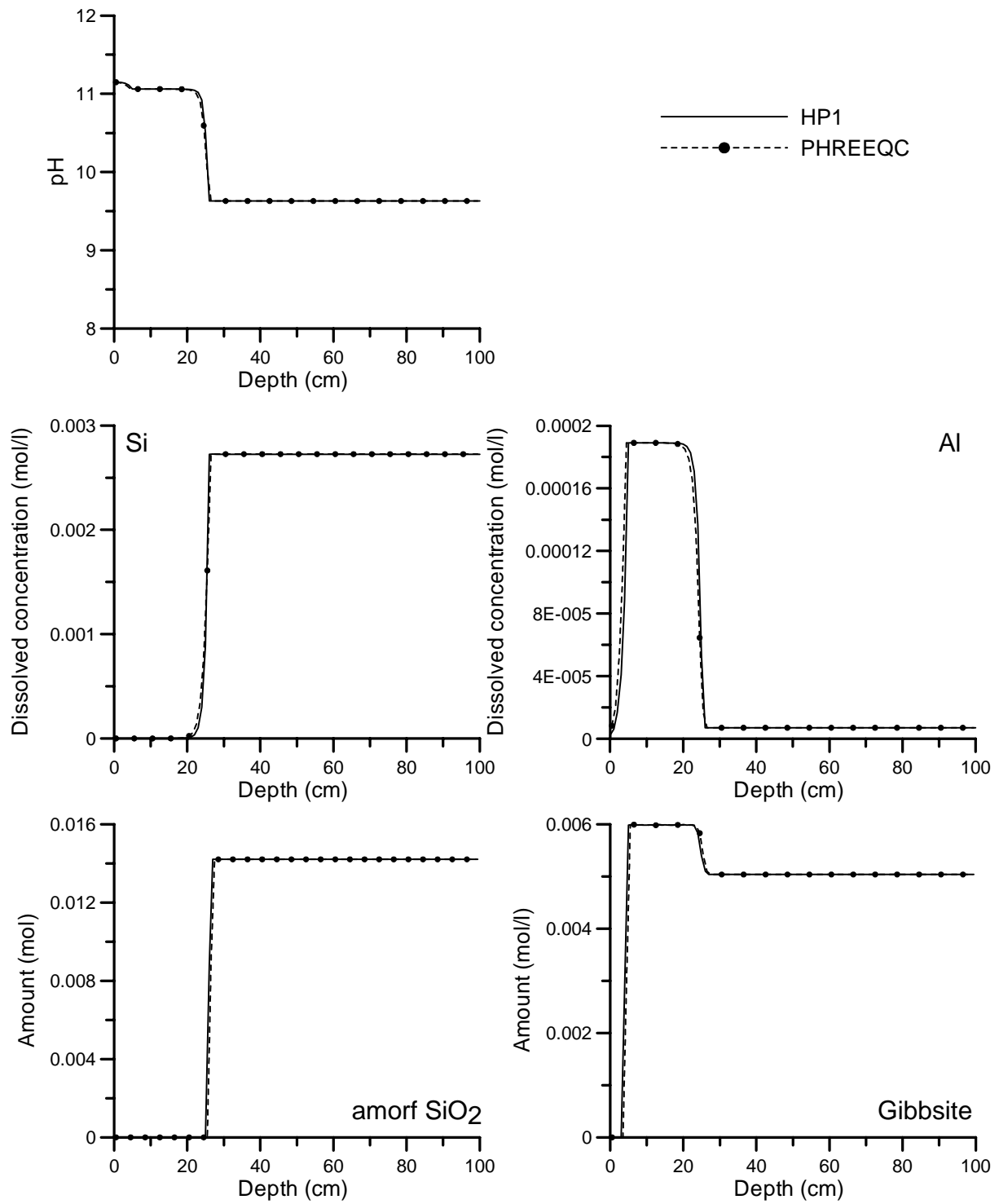


**Figure 4.8** Distribution of pH, Si, Al, amorphous SiO<sub>2</sub>, and Gibbsite versus depth after 150 days of infiltration for Verification Problem 7 (Full line: HP1, dashed line: PHREEQC).

### 4.3 *More complicated verification problems of HP1 model*

Examples presented in this chapter compare the combined HP1 model against a different computer program, CRUNCH, that also simulates multicomponent reactive transport in porous media, with the limitation that only steady-state flow can be invoked. CRUNCH is based on the GIMRT/OS3D package (Steeffel and Yabuski, 1996; Steeffel, 2000). The geochemical reactions and transport in CRUNCH are coupled in one of two ways: (1) a global implicit approach (GIMRT) that simultaneously solves the transport and reaction equations, or (2) SNIA. GIMRT generally leads to smaller numerical errors. A comparison between HP1 and CRUNCH-GIMRT allows one to assess numerical discretization errors of the SNIA coupling as a function of the maximum Courant number,  $Cr$ .

#### 4.3.1 **Heavy metal transport in a medium with a pH-dependent cation exchange complex (Verification Problem 8 – MCATEXCH)**

##### 4.3.1.1 *Problem definition and governing chemical reactions*

Cation adsorption to negatively charged soil solid phases can greatly affect the migration of cations in soils. In HYDRUS-1D, equilibrium isotherms, such as the linear, Freundlich or Langmuir isotherms, describe the adsorption/desorption of cations. The use of such isotherms assumes that the adsorption of a particular cation is independent of the presence of other elements in the soil solution or on the soil solid phases. Their coefficients are constant and independent of pH, other cations, complexing elements, and ligands in the soil solution. Unlike HYDRUS-1D, the coupled HP1 code can include the effect of these factors on adsorption, and consequently, on the migration of multiple cations, by using the ion-exchange reactions of PHREEQC.

In this example we consider the transport of several major cations (Na, K, Ca, and Mg) and three heavy metals (Cd, Zn, Pb) through a 50-cm-deep **multi-layered soil profile** during **unsaturated** steady-state flow. Each soil layer has different soil hydraulic properties and cation exchange capacities (CEC) (Table 4.5). The top 28 cm of the soil is assumed to be contaminated with the three heavy metals (initial pH 8.5), while an acid metal-free solution (pH 3) infiltrates into the soil (Table 4.6). Assuming that the cation exchange complex is associated solely with organic matter, CEC increases significantly with increasing pH due to the acid-base properties of its functional groups. The higher the pH, the more functional groups of the organic matter are deprotonated and thus the higher the cation exchange capacity. This behaviour is represented by a **multi-site cation exchange complex** consisting of six sites, each having a different selectivity coefficient for the exchange of protons (see Appelo et al., 1998). Finally, chloride is present in the soil solutions resulting in the formation of **aqueous complexes** with the heavy metals.

**Table 4.5** Soil hydraulic properties and cation exchange capacities of five soil layers.

Horizon	Layer thickness (cm)	$\theta_r$	$\theta_s$	$\alpha$ (cm <sup>-1</sup> )	$n$	$K_s$ (cm day <sup>-1</sup> )	$l$	Cation exchange capacity (eq / 1000 cm <sup>3</sup> soil)
A	13	0.065	0.476	0.016	1.94	93	0.5	0.0183
E	10	0.035	0.416	0.015	3.21	311	0.5	0.0114
Bh1	5	0.042	0.472	0.016	1.52	39	0.5	0.0664
Bh2	5	0.044	0.455	0.028	2.01	860	0.5	0.0542
Bh/C	17	0.039	0.464	0.023	2.99	1198	0.5	0.0116

**Table 4.6** pH and solution concentrations used in the simulation ( $\mu\text{mol l}^{-1}$ ).

Solution	pH	Na*	K	Ca	Mg	Br	Cl	Cd	Pb	Zn
0-28 cm depth	8.5	401.9	120	98	5	780	0	0.8	2.5	50
28-50 cm depth	8.5	454.0	120	98	5	780	0	0.0	0	0
Applied water	3.5	127.5	120	98	5	780	0	0.0	0	0

\* Concentration of Na is adjusted to obtain the desired pH.

The soil profile is assumed to contain five distinct layers with different soil hydraulic properties and cation exchange capacities. Table 4.5 gives thicknesses of the different horizons, parameters of van Genuchten's equations for the water retention and hydraulic conductivity functions, and the total cation exchange capacities. The higher exchange capacities of the Bh1 and Bh2 horizons reflect their enrichment with immobilized organic matter. Flow is assumed to be steady at a constant flux of 0.05 m day<sup>-1</sup> (18.25 m year<sup>-1</sup>), which causes the soil profile to be unsaturated (water contents vary between 0.37 and 0.15 as a function of depth). The bottom boundary condition for water flow is free drainage. HYDRUS-1D was used to calculate the steady-state water content profile corresponding to these boundary conditions. The dispersivity and diffusion coefficient were taken to be 0.05 m and  $9.2 \cdot 10^{-10} \text{ m}^2 \text{ s}^{-1}$ , respectively.

**Table 4.7** Overview of aqueous equilibrium reactions and corresponding equilibrium constants (data from phreeqc.dat database, Parkhurst and Appelo, 1999).

Nr	Aqueous speciation reaction	Log K		
(1)	$\text{H}_2\text{O} = \text{OH}^- + \text{H}^+$	-14		
(2)	$\text{Na}^+ + \text{H}_2\text{O} = \text{NaOH} + \text{H}^+$	-14.18		
(3)	$\text{K}^+ + \text{H}_2\text{O} = \text{KOH} + \text{H}^+$	-14.46		
(4)	$\text{Ca}^{2+} + \text{H}_2\text{O} = \text{CaOH}^+ + \text{H}^+$	-12.78		
(5)	$\text{Mg}^{2+} + \text{H}_2\text{O} = \text{MgOH}^+ + \text{H}^+$	-11.44		
		Cd	Pb	Zn
(6)	$\text{X}^{2+} + \text{H}_2\text{O} = \text{XOH}^+ + \text{H}^+$	-10.08	-7.71	-8.96
(7)	$\text{X}^{2+} + 2 \text{H}_2\text{O} = \text{X(OH)}_2 + 2 \text{H}^+$	-20.35	-17.12	-16.90
(8)	$\text{X}^{2+} + 3 \text{H}_2\text{O} = \text{X(OH)}_3 + 3 \text{H}^+$	-33.30	-28.06	-28.40
(9)	$\text{X}^{2+} + 4 \text{H}_2\text{O} = \text{X(OH)}_4^{2-} + 4 \text{H}^+$	-47.35	-39.70	-41.20
(10)	$\text{X}^{2+} + \text{Cl}^- = \text{XCl}^+$	1.98	1.60	0.43
(11)	$\text{X}^{2+} + 2 \text{Cl}^- = \text{XCl}_2$	2.60	1.80	0.45
(12)	$\text{X}^{2+} + 3 \text{Cl}^- = \text{XCl}_3$	2.40	1.70	0.5
(13)	$\text{X}^{2+} + 4 \text{Cl}^- = \text{XCl}_4^{2-}$	-	1.38	0.2

**Table 4.8** Log *K* parameters for multi-site exchange complex.

Y-exchanger <sup>(1)</sup>	NaY	KY	MgY <sub>2</sub>	CaY <sub>2</sub>	CdY <sub>2</sub>	PbY <sub>2</sub>	ZnY <sub>2</sub>
HY <sup>(2)</sup>	HYa	HYb	HYc	HYd	HYe	HYf	
	1.65	3.3	4.95	6.85	9.6	12.35	

<sup>(1)</sup> The value for NaY is taken from Appelo et al. (1998). Values for the other complexes are taken from the phreeqc.dat database (Parkhurst and Appelo, 1999) and adapted relative to the *K* for NaY.

<sup>(2)</sup> Values taken from Appelo et al. (1998).

An overview of the considered aqueous equilibrium reactions is given in Table 4.7. The role of chloride as a complexing agent is described by reactions (10) through (13). Other geochemical reactions that are considered are the heterogeneous multi-site ion-exchange reactions. The exchange coefficients for major cations and heavy metals were assumed to be the same for all exchange sites. Table 4.8 gives parameters for this multi-site exchange complex.

#### 4.3.1.2 Database and model input

##### HP1

Chemical reactions and their equilibrium constants are stored in the database **phreeqc.dat**. The following keywords are used for this problem: **SOLUTION\_MASTER\_SPECIES**, **SOLUTION\_SPECIES**, **EXCHANGE\_MASTER\_SPECIES**, and **EXCHANGE\_SPECIES**. The input file for water flow and solute transport is relatively straightforward and can be easily created the standard way with the graphical interface of HYDRUS-1D. The problem involves 9 components that are transported, i.e., Na, K, Mg, Ca, Cl, Br, Cd, Zn, and Pb. Only parameters related to solute transport (i.e., the dispersivity and the aqueous diffusion coefficient) are defined in HYDRUS-1D. All other solute transport parameters, except for the Freundlich exponent which is equal to one, are set to zero. This information is stored in the HYDRUS-1D input files **Selector.in** and **Profile.dat**. Note that these files also contain information about the steady-state flux (0.05 cm day<sup>-1</sup>), the boundary concentrations of the nine components in the incoming water, and spatial and temporal discretization parameters of the numerical problem. The link between HYDRUS-1D and PHREEQC is defined in the **Species.in** input file that contains names of nine elements, the names of which must be the same as in the Phreeqc.dat database. Finally, the initial solutions and exchange complexes are defined in the **Phreeqc.in** input file. Since the transport problem involves variable water contents with depth, a **SOLUTION**-keyword needs to be defined for nearly each cell. In addition, the cation exchange complex for each soil layer must be defined using the keyword **EXCHANGE**, with each layer containing six exchange sites. Also included in the input file are the keywords **TRANSPORT** to indicate that HYDRUS-1D will be used for transport modelling, and **SELECTED\_OUTPUT** to specify the desired output. Details about the keywords used in **Phreeqc.in** can be found in the PHREEQC-2 manual (Parkhurst and Appelo, 1999).

## CRUNCH

The database contains chemical reactions and equilibrium constants for the aqueous speciation reactions (between **end of primary** and **end of secondary**) and the exchange reactions (between **begin of exchange** and **end of exchange**). The input file **reactive.in** defines the initial conditions for the five layers and the inflowing water (**CONDITION**), primary, secondary, and exchange species (**PRIMARY\_SPECIES**, **SECONDARY\_SPECIES**, and **ION\_EXCHANGE**), the discretization, and the initial and boundary conditions (**DISCRETIZATION**, **INITIAL\_CONDITIONS**, and **BOUNDARY\_CONDITIONS**), flow and transport properties (**FLOW**, and **TRANSPORT**), and output (**OUTPUT**). The keyword **POROSITY** defines the porosity. Since the porosity is different for each soil layer, porosities are read from the **porosity1.dat** input file. Numerical issues for solving the equations are defined in **RUNTIME**. The **read\_saturation** identifies the file containing the saturation degree for each cell. Information for this file (**saturation1.dat**) was obtained from an initial HYDRUS-1D run to find the steady-state water content profile.

### 4.3.1.3 Comparison between CRUNCH-GIMRT, CRUNCH-OS, and HP1

Simulations were performed with three different models: (1) the global implicit option in the CRUNCH-model (CRUNCH-GIMRT), (2) the sequential non-iterative option in the CRUNCH-model (CRUNCH-OS), and (3) the coupled HP1 model which also runs in a sequential non-iterative mode. The maximum time step for the latter two simulations was chosen such that both were run at a similar Courant number (0.5). Figure 4.9 shows selected simulation results.

Infiltration of the low-pH solution causes a decrease in the cation exchange capacity (i.e., an increase in the number of protonated sites on the six cation exchange complexes) (see Figure 4.9e). This relation between pH in the soil solution and the deprotonated sites on the multi-site cation exchange complex is apparent when comparing Figure 4.9c and Figure 4.9e. This leads to a desorption of Cd (and other heavy metals) and their subsequent leaching from the soil profile. Cd leaching peaks after about 0.3 y (Figure 4.9b), with most Cd leached from the profile after 1 y.

Results obtained with CRUNCH-OS and HP1 using  $Cr = 0.5$  showed very good agreement, especially for the outflow curves. This indicates that the coupling between HYDRUS-1D and PHREEQC was done correctly since the coupled model was tested in this relatively complicated example with a completely independent reactive transport model (in contrast to the verification problems discussed earlier in sections 4.1 and 4.2). However, the pH-outflow (Figure 4.9a) and the concentration distributions versus depth (Figure 4.9c-f) showed a small

increase in numerical dispersion as compared to simulations using the global implicit approach (CRUNCH-GIMRT).

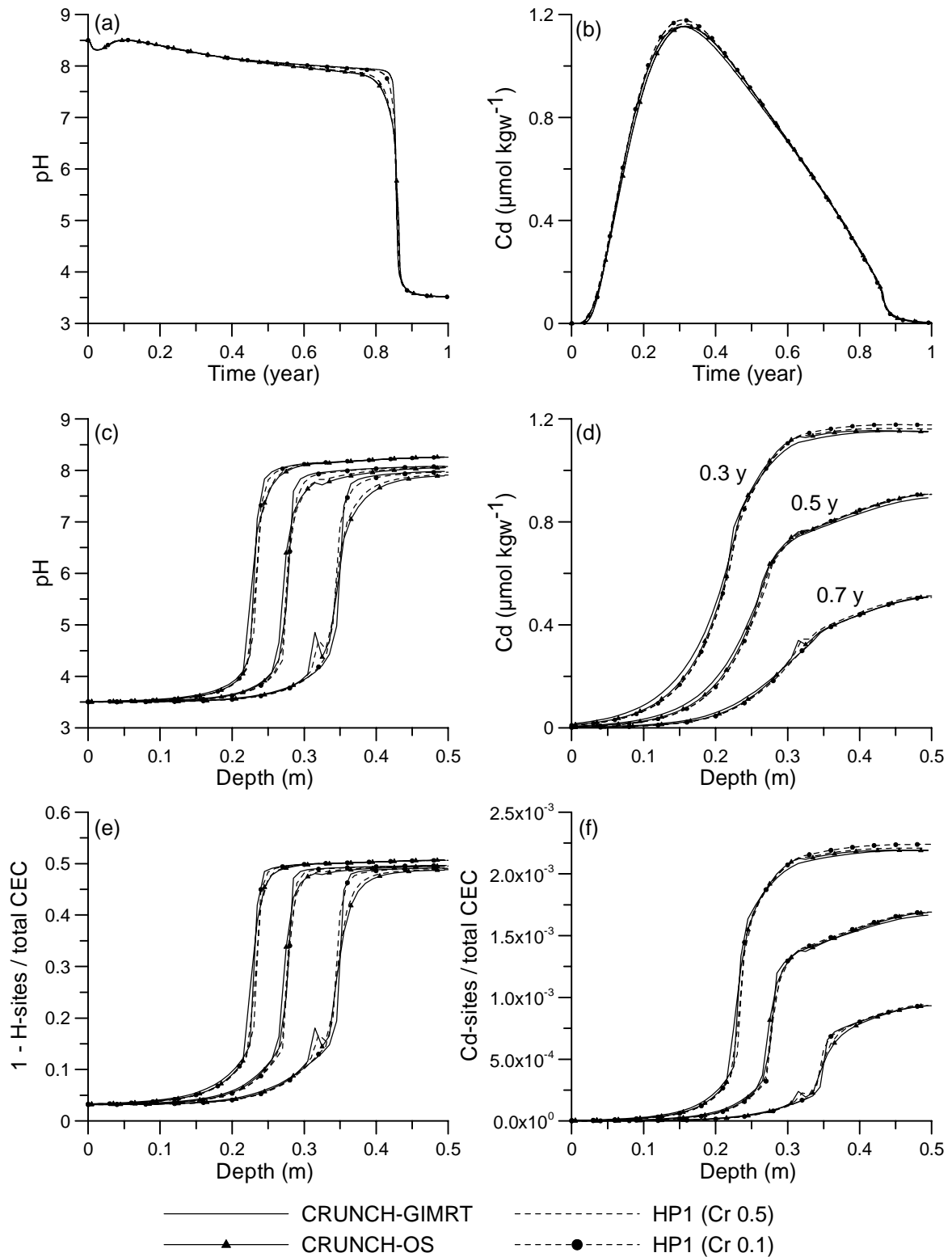


**Figure 4.9** Selected results for cation and heavy metal transport with a pH-dependent cation exchange complex. (a) and (b) pH and Cd concentrations in outflow at 50 cm depth, respectively; (c) and (d) distributions of pH and Cd concentrations versus depth after 0.3, 0.5, and 0.7 y, respectively; (e) and (f) distribution of the fraction of deprotonated sites ( $1 - H\text{-sites}$ ) and sites with Cd versus depth after 0.3, 0.5, and 0.7 y, respectively.

Furthermore, at the boundary between the fourth and fifth layer, the pH shows a small increase for both models using the sequential non-iterative solution approach. This increase seems to be an artefact of the implemented time step. Reducing  $Cr$  to 0.1 in HP1 produced very good agreement with CRUNCH-GIMRT, with the artefact being no longer present (Figure 4.9). Overall, differences in results obtained with Courant numbers of 0.1 (at least one order of magnitude smaller than typical values for  $Cr$ ) and 0.5 were quite small (especially for breakthrough curves), with both runs providing acceptable results.

To illustrate the effect of a decreasing cation exchange capacity with decreasing pH on Cd transport, we changed concentrations of the infiltrating water to those found in the 28–50 cm horizon, i.e., with a pH of 8.5 (see Table 4.6). Simulations were carried out with CRUNCH-GIMRT and HP1 using a Courant number of 0.5; this since no considerable differences were observed for the Cd breakthrough curve in previous calculations. As shown in Figure 4.10, the Cd breakthrough is significantly retarded compared to that produced with the low-pH infiltration water. Finally, to evaluate the effect of heavy metals complexation with  $Cl^-$  ions, we increased  $Cl$  concentration in the infiltrating water to 780  $\mu\text{mol}$  per kilogram of water (and decreased  $Br$  concentration to 0  $\mu\text{mol}$  per kilogram of water). Only a small increase in the Cd breakthrough was obtained (Figure 4.10) compared with the previous case. All three cases produced essentially the same results using both CRUNCH-GIMRT and HP1.

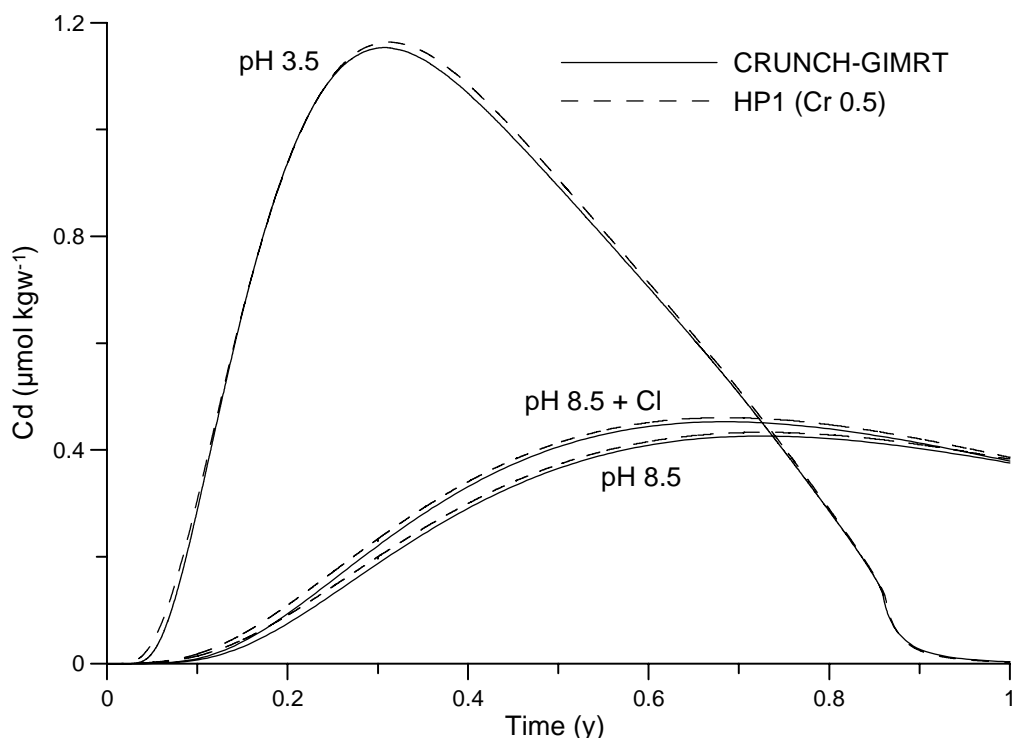


**Figure 4.10** Effect of pH and  $Cl$  concentration on Cd concentrations of leaching water at the 50-cm depth.

### 4.3.2 Infiltration of a hyperalkaline solution in a clay sample (Verification Problem 9 – ALKALINE)

#### 4.3.2.1 Problem definition and governing chemical reactions

Adler (2001) described a column experiment, in which a high-pH-Na-Ca-OH solution infiltrated into a core containing Opalinus Clay. This clay is investigated in Switzerland as a potential host formation for long term disposal of high level radioactive waste (Thury and Bossart, 1999). Adler (2001) also defined a conceptual geochemical model to describe the outflow concentrations of this experiment. A slightly adapted version of this conceptual geochemical model is used here as a benchmark comparison between CRUNCH and HP1<sup>1</sup>.

Infiltration of a high pH plume into the clay core leads to different reactions. First, the **cation exchange complex** associated with the clay minerals will interact with the compositional change in the aqueous solution. Due to the high pH, primary minerals in the clay will become unstable and may dissolve. Dissolution of primary minerals is described with **kinetic dissolution rate equations**. The infiltration of Na-Ca-rich water and the increase of Al and Si from mineral dissolution will cause **the precipitation of secondary minerals**.

The infiltration of a hyperalkaline solution in a 7.4-cm-long clay core was simulated for a period of 1.1 year. The flow domain was discretized in 100 cells of  $7.4 \cdot 10^{-2}$  cm each. The effective porosity of the Opalinus Clay was kept constant at a value of 0.13 during the simulations. A constant flux of  $2.403 \cdot 10^{-9}$  m sec<sup>-1</sup> ( $7.58$  cm y<sup>-1</sup>) was applied, resulting in a solute transport velocity of  $1.85 \cdot 10^{-8}$  m sec<sup>-1</sup>. The diffusion coefficient was  $0.5 \cdot 10^{-9}$  m sec<sup>-2</sup> and the dispersivity zero.

The mineralogical composition of Opalinus Clay is given in Table 4.9. Due to the intrusion of the high pH plume, primary minerals of the clay will become unstable and gradually dissolve. The dissolution rate depends on the chemical composition of the aqueous phase and is described with a ‘transition state’ based dissolution model (Aagaard and Helgeson, 1981; Parkhurst and Appelo, 1999):

$$R_m = A_{m,0} \left( \frac{M_m}{M_{m,0}} \right)^{2/3} \{OH^-\}^n k_{0,m} [1 - Q_m / K_m] \quad (4.7)$$

where  $R_m$  is the dissolution rate of mineral  $m$  (mol sec<sup>-1</sup>),  $A_{m,0}$  is the initial reactive surface area of mineral  $m$  (m<sup>2</sup> for HP1, m<sup>2</sup> m<sup>-3</sup> for CRUNCH),  $(M_m / M_{m,0})^{2/3}$  is a factor accounting for

<sup>1</sup> The conceptual geochemical model used here is somewhat simplified compared to the model described by Adler (2001, p. 55-60). In this report, the same model is used in both CRUNCH and HP1.

**Table 4.9** Mineralogical reactions,  $\text{Log}(K)$ , molar volume, volume percent and moles present in Opalinus Clay, and secondary minerals considered.

mineral	Reaction	Log $K$	Molar volume	Volume % <sup>(1)</sup>	Moles <sup>(2)</sup>
<i>Primary minerals</i>					
Kaolinite	$\text{Al}_2\text{Si}_2\text{O}_5(\text{OH})_4 + 6 \text{H}^+ = 2 \text{Al}^{+3} + 2 \text{SiO}_2 + 5 \text{H}_2\text{O}$	6.36	99.520	23	2.31
Illite	$\text{K}_{0.6}\text{Mg}_{0.25}\text{Al}_{2.3}\text{Si}_{3.5}\text{O}_{10}(\text{OH})_2 + 8 \text{H}^+ = 0.6 \text{K}^+ + 0.25 \text{Mg}^{2+} + 2.3 \text{Al}^{+3} + 3.5 \text{SiO}_2 + 5 \text{H}_2\text{O}$	8.51	-	19	0.38
Quartz	$\text{SiO}_2 = \text{SiO}_2$	-3.91	22.680	11.5	5.06
Calcite	$\text{CaCO}_3 = \text{Ca}^{+2} + \text{CO}_3^{2-}$	-8.51	36.934	13.5	3.655
Dolomite	$\text{CaMg}(\text{CO}_3)_2 = \text{Ca}^{+2} + \text{Mg}^{+2} + 2 \text{CO}_3^{2-}$	-16.71	64.365	2.0	0.31
Gypsum	$\text{CaSO}_4 \cdot 2\text{H}_2\text{O} = \text{Ca}^{+2} + \text{SO}_4^{2-} + 2 \text{H}_2\text{O}$	-4.48	74.69	0.02	0.00268
<i>Secondary minerals</i>					
Hydrotalcite	$\text{Mg}_4\text{Al}_2\text{O}_4(\text{OH})_6 + 14 \text{H}^+ = 4 \text{Mg}^{2+} + 2 \text{Al}^{+3} + 10 \text{H}_2\text{O}$	75.44	207.57	0.00	0.0
Sepiolite	$\text{Mg}_4\text{Si}_6\text{O}_{15}(\text{OH})_2 \cdot 6\text{H}_2\text{O} + 8 \text{H}^+ = 4 \text{Mg}^{2+} + 6 \text{SiO}_2 + 11 \text{H}_2\text{O}$	29.96	285.60	0.00	0.00

<sup>(1)</sup> Used as input in CRUNCH.<sup>(2)</sup> Used as input in HP1.

a lower reactive surface area during dissolution,  $M_{m,0}$  and  $M_m$  are the initial and current numbers of moles (in HP1) and volume percentages (in CRUNCH) of mineral  $m$ ,  $n$  is the reaction order of the OH<sup>-</sup> dependency of the reaction rate,  $k_{0,m}$  is the intrinsic rate constant of mineral  $m$  ( $\text{mol m}^{-2} \text{sec}^{-1}$ ),  $K_m$  is the equilibrium constant of the reaction, and  $Q_m$  is the ion activity product. Table 4.10 lists the parameters of Eq. (4.7). Due to the stiffness of the system (a combination of high and low rate constants), not all dissolution processes of the primary minerals were treated as kinetic reactions in HP1 (equilibrium was assumed for calcite). Eq. (4.7) was also used to describe the kinetic precipitation of two secondary minerals (see Table 4.9) in CRUNCH. These minerals were treated as being in equilibrium with the solution in HP1. Quartz, kaolinite, and illite were not allowed to precipitate in either model.

**Table 4.10** Parameters for the kinetic dissolution reactions (Eq. (4.7)).

Mineral	Log $k_0$ ( $\text{mol m}^{-2} \text{sec}^{-1}$ )	$n$	$A_0$ ( $\text{m}^2 \text{m}^{-3}$ )
Kaolinite <sup>1</sup>	-10.88	0.54	$1.00 \cdot 10^7$
Illite <sup>1</sup>	-13.91	0.22	$0.33 \cdot 10^7$
Quartz <sup>1</sup>	-10.20	0.30	$2.00 \cdot 10^5$
Calcite <sup>2</sup>	-1.00	0.00	$2.00 \cdot 10^3$
Dolomite <sup>1</sup>	-7.70	0.00	$2.00 \cdot 10^3$
Gypsum <sup>1</sup>	-8.00	0.00	$2.00 \cdot 10^3$
Hydrotalcite <sup>2</sup>	-1.00	0.00	$1.00 \cdot 10^2$
Sepiolite <sup>2</sup>	-1.00	0.00	$1.00 \cdot 10^2$

<sup>1</sup> Data from Table 5, Part III, Adler (2001)<sup>2</sup> Minerals are assumed to be in equilibrium in HP1. High dissolution constants are used in CRUNCH.

**Table 4.11** Overview of aqueous equilibrium reactions, and cation exchange half reactions with corresponding equilibrium constant.

Nr	Reaction	Log K
<i>Aqueous speciation reactions</i>		
(1)	$\text{H}_2\text{O} = \text{OH}^- + \text{H}^+$	-14.0
(2)	$\text{HCO}_3^- + \text{H}^+ = \text{CO}_2 + \text{H}_2\text{O}$	6.3447
(3)	$\text{HCO}_3^- = \text{CO}_3^{2-} + \text{H}^+$	-10.3288
(4)	$\text{Al}^{3+} + \text{H}_2\text{O} = \text{AlOH}^{2+} + \text{H}^+$	4.9571
(5)	$\text{Al}^{3+} + 2 \text{H}_2\text{O} = \text{Al}(\text{OH})_2 + 2 \text{H}^+$	-10.5945
(6)	$\text{Al}^{3+} + 2 \text{H}_2\text{O} = \text{AlO}_2^- + 4 \text{H}^+$	-22.8833
(7)	$\text{Al}^{3+} + 2\text{H}_2\text{O} = \text{HAlO}_2 + 3 \text{H}^+$	-16.4329
(8)	$\text{Al}^{3+} + \text{SO}_4^{2-} = \text{AlSO}_4^+$	3.01
(9)	$\text{Al}^{3+} + \text{Na}^+ + 2 \text{H}_2\text{O} = \text{NaAlO}_2 + 4 \text{H}^+$	-23.6266
(10)	$\text{Al}^{3+} + 2 \text{SO}_4^{2-} = \text{Al}(\text{SO}_4)_2$	4.9
(11)	$\text{Ca}^{2+} + \text{H}_2\text{O} = \text{CaOH}^+ + \text{H}^+$	-12.78
(12)	$\text{Ca}^{2+} + \text{HCO}_3^- = \text{CaCO}_3 + \text{H}^+$	-7.0017
(13)	$\text{Ca}^{2+} + \text{HCO}_3^- = \text{CaHCO}_3^+$	1.0467
(14)	$\text{Ca}^{2+} + \text{Cl}^- = \text{CaCl}^+$	-0.6956
(15)	$\text{Ca}^{2+} + 2 \text{Cl}^- = \text{CaCl}_2$	-0.6436
(16)	$\text{Ca}^{2+} + \text{SO}_4^{2-} = \text{CaSO}_4$	2.111
(17)	$\text{Cl}^- + \text{H}^+ = \text{HCl}$	0.67
(18)	$\text{K}^+ + \text{H}_2\text{O} = \text{KOH} + \text{H}^+$	-14.46
(19)	$\text{K}^+ + \text{Cl}^- = \text{KCl}$	-1.4946
(20)	$\text{K}^+ + \text{SO}_4^{2-} = \text{KSO}_4$	0.8796
(21)	$\text{K}^+ + \text{H}^+ + \text{SO}_4^{2-} = \text{KHSO}_4$	0.8136
(22)	$\text{Mg}^{2+} + \text{H}_2\text{O} = \text{MgOH}^+ + \text{H}^+$	-11.44
(23)	$\text{Na}^+ + \text{H}_2\text{O} = \text{NaOH} + \text{H}^+$	-14.18
(24)	$\text{Na}^+ + \text{HCO}_3^- = \text{NaHCO}_3$	0.1541
(25)	$\text{Na}^+ + \text{HCO}_3^- = \text{NaCO}_3 + \text{H}^+$	-9.8144
(26)	$\text{Na}^+ + \text{Cl}^- = \text{NaCl}$	-0.777
(27)	$\text{Na}^+ + \text{SO}_4^{2-} = \text{NaSO}_4$	0.82
(28)	$\text{SO}_4^{2-} + \text{H}^+ = \text{HSO}_4^-$	1.9794
(29)	$\text{SO}_4^{2-} + 2 \text{H}^+ = \text{H}_2\text{SO}_4$	-1.0209
(30)	$\text{SiO}_2 + 2 \text{H}_2\text{O} = \text{H}_2\text{SiO}_4^{2-} + 2 \text{H}^+$	-22.96
(31)	$\text{SiO}_2 + \text{H}_2\text{O} = \text{HSiO}_3^- + \text{H}^+$	-9.9525
(32)	$\text{SiO}_2 + \text{Na}^+ + \text{H}_2\text{O} = \text{NaHSiO}_3 + \text{H}^+$	-8.3040
<i>Cation exchange half reactions (X<sup>-</sup> is the exchange site)</i>		
(33)	$\text{Na}^+ + \text{X}^- = \text{NaX}$	0.00
(34)	$\text{K}^+ + \text{X}^- = \text{KX}$	0.757
(35)	$\text{Ca}^{2+} + 2 \text{X}^- = \text{CaX}_2$	0.604
(36)	$\text{Mg}^{2+} + 2 \text{X}^- = \text{MgX}_2$	0.505

An overview of the considered aqueous equilibrium reactions and the ion exchange reactions is given in Table 4.11. The total cation exchange capacity of Opalinus Clay is 120 meq per kg of rock. The initial concentrations and concentrations in the infiltrating water are given in Table 4.12.

#### 4.3.2.2 Database and model input

##### HP1

The chemical reactions and their equilibrium constants are stored in the database **phreeqc.dat**. This problem uses the following keywords: **SOLUTION**

**Table 4.12** Chemical composition of the initial pore water and the inflowing alkaline solution.

Element	Initial composition of the pore water (mol kgw <sup>-1</sup> ) <sup>1</sup>	Composition of the inflowing alkaline solution (mol kgw <sup>-1</sup> ) <sup>2</sup>
K	5.42 10 <sup>-3</sup>	1.61 10 <sup>-1</sup>
Na	3.28 10 <sup>-1</sup>	6.52 10 <sup>-2</sup>
Ca	2.16 10 <sup>-2</sup>	2.24 10 <sup>-3</sup>
Mg	3.57 10 <sup>-2</sup>	1.00 10 <sup>-30</sup>
Cl	2.64 10 <sup>-1</sup>	1.00 10 <sup>-30</sup>
S	9.20 10 <sup>-2</sup>	1.00 10 <sup>-30</sup>
Al	1.00 10 <sup>-6</sup>	1.00 10 <sup>-30</sup>
Si	4.40 10 <sup>-5</sup>	1.00 10 <sup>-30</sup>
C	3.96 10 <sup>-4</sup>	4.21 10 <sup>-5</sup>
pH	7.90	13.20

<sup>1</sup>: From Table 2; Part III, Adler (2001)

<sup>2</sup>: From Table 6, Part III, Adler (2001)

**\_MASTER\_SPECIES**, **SOLUTION\_SPECIES**, **EXCHANGE\_MASTER\_SPECIES**, **EXCHANGE\_SPECIES**, **PHASES**, and **RATES**. The last keyword is used to define the specific rate reactions for the dissolution of primary minerals (except calcite) with Eq. (4.7) translated into the BASIC-programming language for each mineral (for details, see the PHREEQC-2 manual; Parkhurst and Appelo, 1999).

The input file for water flow and solute transport can again be easily created with the graphical interface of HYDRUS-1D. Nine components (i.e., Ca, K, Na, C, S, Cl, Mg, Si, and Al) are transported in this problem. Only parameters related to transport are defined in HYDRUS-1D, i.e., the dispersivity, and the aqueous diffusion coefficient. This information is stored in input files **selector.in** and **profile.dat**. Note that these files also contain information for the steady-state inflow flux and concentrations of the nine components in the infiltrating water.

The link between HYDRUS-1D and PHREEQC is defined in the input file **species.in**, which contains names of the 9 components. The **phreeqc.in** file contains chemical information for the reactive transport problem. Initial mineralogical and chemical conditions for each cell are defined with the following keywords: **SOLUTION** (initial chemical composition of the aqueous phase), **EXCHANGE** (size and initial composition of the cation exchange complex), **EQUILIBRIUM\_PHASES** (identifies the minerals in equilibrium with the aqueous phase and their initial amount), **KINETICS** (identifies the kinetic reactions with their parameters and their initial amount), **TRANSPORT** (to indicate that HYDRUS-1D is used for transport modelling), and **SELECTED\_OUTPUT** (to specify the desired output). Details on the keywords used in **phreeqc.in** can be found in the PHREEQC-2 manual (Parkhurst and Appelo, 1999).

## CRUNCH

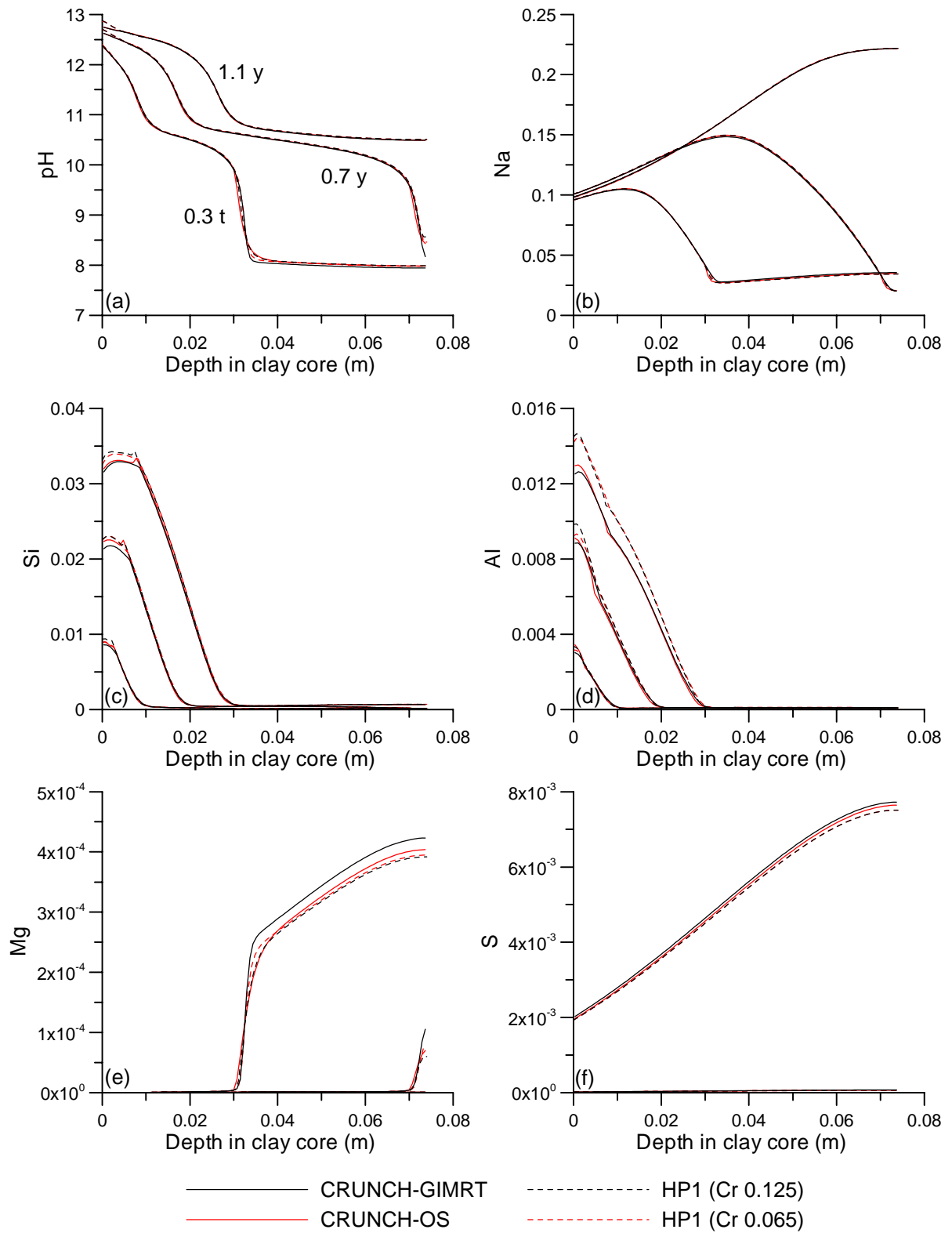
The database contains chemical reactions and equilibrium constants for the aqueous speciation reactions (between **end of primary** and **end of secondary**), the minerals (between **end of secondary** and **end of minerals**), the kinetic dissolution or precipitation reactions of the minerals (between **begin of mineral kinetics** and **end of mineral kinetics**), and the exchange reactions (between **begin of exchange** and **end of exchange**). The input file **reactive.in** defines the initial conditions for the clay and the inflowing water (**CONDITION**), the primary, secondary, and/or exchange species, and the minerals (**PRIMARY\_SPECIES**, **SECONDARY\_SPECIES**, **ION\_EXCHANGE**, and **MINERALS**), the discretization, and the initial and boundary conditions (**DISCRETIZATION**, **INITIAL\_CONDITIONS**, and **BOUNDARY\_CONDITIONS**), the flow and transport properties (**FLOW**, and **TRANSPORT**), and the output (**OUTPUT**). The keyword **POROSITY** defines the porosity which is fixed in this simulation. Numerical information for solving the equations are defined in **RUNTIME**.

### 4.3.2.3 Comparison between CRUNCH-GIMRT, CRUNCH-OS, and HP1

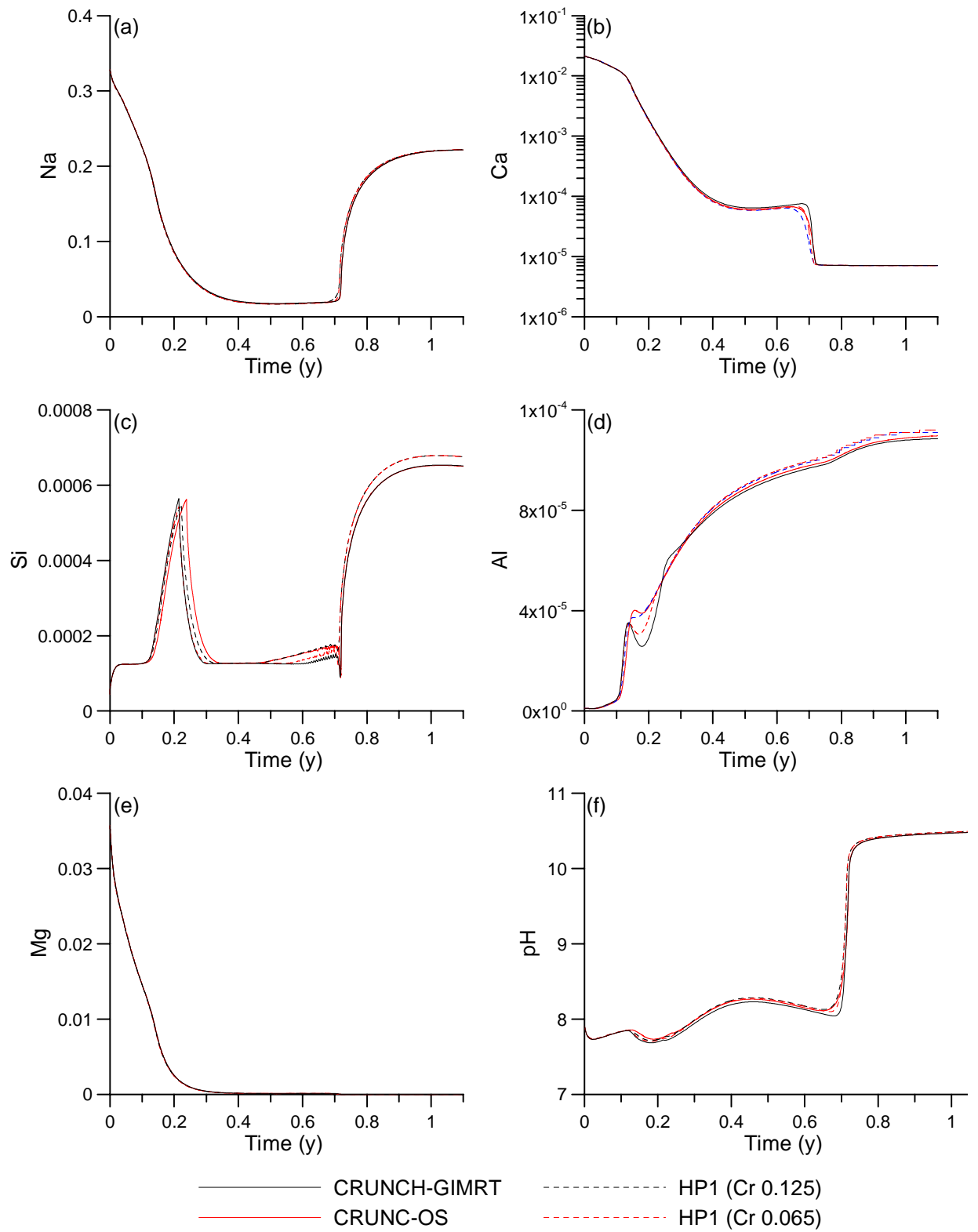
Simulations were performed with two different codes (HP1 and CRUNCH) where CRUNCH was applied in two different modes: the global implicit option in the CRUNCH model (CRUNCH-GIMRT), and the sequential non-iterative option in the CRUNCH model (CRUNCH-OS). The coupled HP1 model runs in a sequential non-iterative mode. For the latter model, different maximum time steps (corresponding to different Courant numbers: 0.125 and 0.065) were used. The maximum allowed Courant number of the CRUNCH-OS simulation was set to 0.125.

Figure 4.11 shows distributions of pH and selected elements after 0.3, 0.7, and 1.1 y. Outflow curves are shown in Figure 4.12. In general, correspondence between the different modelling results is relatively good. Very good agreement was obtained for the propagation of both high pH and elements that are only influenced by cation exchange (Na and K, the latter not shown) (Figure 4.11a, b and Figure 4.12b). The pH near the inlet, as obtained with HP1 was slightly larger than the pH of the CRUNCH simulations. The positions of the propagation waves of Si, Al, and Mg (Figure 4.11c-e) and Ca (similar to Mg, not shown) were identical for the different models, although a slight difference occurred in the concentration of these elements. The reason for this is not clear; it might be due to difference in the precipitation kinetics of the secondary minerals (hydrotalcite and sepiolite). Precipitation of these minerals in HP1 is governed by thermodynamic equilibrium, whereas kinetic precipitation is assumed in the CRUNCH simulations. Due to this equilibrium assumption, Mg concentrations as calculated with HP1 should be slightly smaller than those obtained with CRUNCH. The Si or Al concentrations are consequently also slightly larger. Other minor differences between the two models (e.g., the exact activity coefficients) may have contributed also to this difference.

Compared to cation exchange problems (see section 4.3.1), problems involving (kinetic) dissolution/precipitation of minerals generally require somewhat smaller time steps if a sequential non-iterative coupling method is used. Nevertheless, acceptable results were obtained compared to those using the global implicit method.



**Figure 4.11** Distribution of pH and selected elements versus depth (mol/l) after 0.3, 0.7, and 1.1 y of infiltration of a high pH solution in an Opalinus Clay core.



**Figure 4.12** Outflow curves of selected elements (mol/l) during infiltration of a high pH-solution in an Opalinus Clay core.



## 5 Example

This section considers an example that combines transient variably-saturated water flow, solute transport, and geochemical reactions. The example is used to illustrate some of the capabilities of HP1.

### 5.1 Long term transient flow and transport of major cations and heavy metals in a soil profile (HEAVMET)

#### 5.1.1 Problem definition and governing chemical reactions

This example considers similar processes as those discussed in Verification Problem 8. The problem involves the transport of major cations (Na, K, Ca, and Mg) and heavy metals (Cd, Zn, and Pb) in a 1-m deep multi-layered soil profile subject to atmospheric boundary conditions. While steady-state water flow was considered in Verification Problem 8, in this example the upper boundary condition varies with time and consists of daily values of precipitation and evaporation (no plants are assumed to be present, and transpiration and root water uptake are not considered).

Soil hydraulic and physical parameters (Table 5.1) of the dry Spodosol located at the “Kattenbos” site near Lommel, Belgium were taken from Seuntjens (2000, Tables 3.1 and 7.1). The cation exchange complex was assumed to be associated solely with organic matter. The cation exchange capacity hence is directly related to the amount of exchangeable protons on the organic matter, taken to be 6 meq/g of the organic matter (proton dissociating groups on fulvic acids are 6 – 10 meq/g and 4 – 6 meq/g on humic acids, Tipping, 2002). The cation exchange complex was assumed to consist of six different exchange sites as defined in Table 4.8.

The upper boundary condition (precipitation and evaporation) was defined using meteorological data from the Brogel station (Belgium) for a period of 10 years (1972-1981).

**Table 5.1** Soil hydraulic and other properties of six soil horizons.

Horizon	Depth (cm)	$\rho$ (g cm <sup>3</sup> )	Organic Carbon %	$\theta_r$	$\theta_s$	$\alpha$ (m <sup>-1</sup> )	$n$	$K_s$ (ms <sup>-1</sup> )
A	0 – 7	1.31	2.75	0.065	0.48	1.6	1.94	1.1 10 <sup>-5</sup>
E	7 – 19	1.59	0.75	0.035	0.42	1.5	3.21	3.6 10 <sup>-5</sup>
Bh1	19 – 24	1.3	4.92	0.042	0.47	1.6	1.52	4.5 10 <sup>-6</sup>
Bh2	24 – 28	1.38	3.77	0.044	0.46	2.8	2.01	1.0 10 <sup>-4</sup>
BC	28 – 50	1.41	0.89	0.039	0.46	2.3	2.99	1.0 10 <sup>-4</sup>
C1	50 – 75	1.52	0.12	0.03	0.42	2.1	3.72	1.0 10 <sup>-4</sup>
C2	75 – 100	1.56	0.08	0.021	0.39	2.1	4.33	1.0 10 <sup>-4</sup>

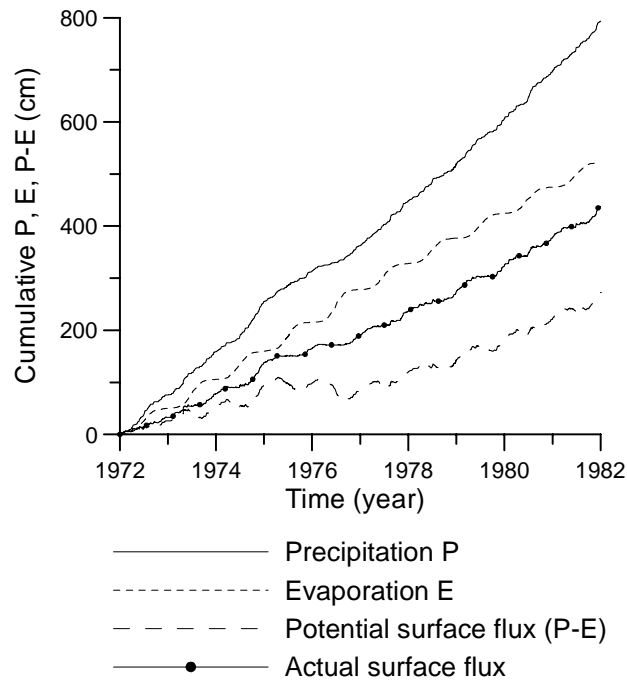


**Figure 5.1** Cumulative precipitation, evaporation and surface flux into the soil between 1972 and 1982.

Figure 5.1 shows precipitation  $P$ , potential evaporation  $E$ , and potential flow across the upper boundary ( $P - E$ ). Since the amount of water available in the soil profile for evaporation was smaller than that required for potential evaporation, the actual evaporation rate will be smaller than the potential evaporation rate. Consequently, the actual surface flux was larger than the potential surface flux (see Figure 5.1). For the considered 10-year period, the actual surface flux (around 45 cm/year) was somewhat larger than expected for this region of Belgium. This is because no water uptake by plant roots was considered in this example. Element concentrations in the precipitation (incoming water) were obtained from Stolk (2001) for station 231 located in Gilze-Rijen (the Netherlands) close to the Belgian border. The composition was based on the average of 13 measurements during 1999 (Table A5 in Stolk, 2001) (Table 5.2).

**Table 5.2** Chemical composition of the rain water (from Stolk, 2001) and in the initial soil solution.

Concentration ( $\mu\text{mol/l}$ )	pH	Cl	Br*	Na	K	Ca	Mg	Cd	Zn	Pb
Rain water	5.25	69	32	64	4	6	8	0	0	0
Initial soil solution										
A	3.4	69	727	64	4	97	8	0.80	50	2.5
E	3.5	69	521	64	4	65	8	0.38	24	1.2
Bh1	3.6	69	398	64	4	39	8	0.43	23	1.1
Bh2	3.8	69	287	64	4	33	8	0.41	21	1.0
BC	4.4	69	235	64	4	55	8	0.63	33	1.6
C1	4.4	69	252	64	4	76	8	0.33	21	1.0
C2	4.5	69	131	64	4	27	8	0.20	14	0.7

\*: Br is used as charge balance

The initial water content was estimated by assuming a constant flux of 0.1206 cm/day (corresponding to the long term actual infiltration rate). Initial concentrations of Na, K, Mg were assumed to be equal to the concentration in the precipitation, while initial concentrations of Ca, Cd, and Zn were obtained from Seuntjens (2000; Table 5.2). Pb concentrations were arbitrarily set to be 20 times smaller than the Zn concentrations (no data available).

The simulation was carried out using the following numerical guidelines: a spatial discretization of 1 cm, a performance index of 0.1, and a maximum time step of 0.125.

## 5.1.2 Analysis of the simulation results

### 5.1.2.1 Accuracy analysis

To assess the accuracy of the simulation, the mass balance was evaluated in terms of the following two variables as a function of time:

$$Q_{in}^j - Q_{out}^j = \left( \int_0^t q_{s0}^j dt - \int_0^t q_{sN}^j dt \right) \quad (5.1)$$

$$M_t^j - M_0^j = \sum_{i=1}^{N_{cells}} \left[ \left( (C_j)_{i,t} + \sum_{k=1}^{N_X} [A_j^m (X_j^m)_{v_j}] \right) \theta_{i,t} - \left( (C_j)_{i,0} + \sum_{k=1}^{N_X} [A_j^m (X_j^m)_{v_j}] \right) \theta_{i,0} \right] \Delta x \quad (5.2)$$

where  $j = 1, \dots, N_m$ ,  $Q_{in}^j$  and  $Q_{out}^j$  are the cumulative inflow and outflow rates of the  $j$ th master species [moles L<sup>-2</sup>], respectively;  $q_{s0}^j$  and  $q_{sN}^j$  are solute flux boundary conditions at the bottom and surface of the soil profile [moles T<sup>-1</sup> L<sup>-2</sup>], respectively;  $M_t^j$ ,  $M_0^j$  are total amounts of the  $j$ th master species in the flow region at time  $t$  and at the beginning of the simulation [moles L<sup>-2</sup>], respectively, and  $v_j$  is the charge of the  $j$ th master species. All other symbols were defined in section 2.  $M_t^j$  and  $M_0^j$  in Eq. (5.2) consist of the total amount of the  $j$ th master species in the aqueous phase,  $\theta C_j$  (see Eq. 2.28), and the sum of the amounts adsorbed on six cation exchange sites. Since an accurate simulation should conserve mass, the difference between Eqs. (5.1) and (5.2), defined as the absolute error  $\varepsilon_a$  (Šimůnek et al., 1998), should be small.  $Q_{in}^j$  and  $Q_{out}^j$  were calculated using information from the *soluteN.out* output files generated by HYDRUS1D, while  $M_t^j - M_0^j$  were calculated using values from the output file from PHREEQC defined by the keyword **SELECTED\_OUTPUT** every 15 days. Figure 5.2 compares Eqs. (5.1) and (5.2) for Cl, Na, Ca and Cd for the 10-year simulation. Since differences between values obtained with Eqs. (5.1) and (5.2) are very small, absolute errors are small as well and no mass balance errors are expected.

The accuracy of the numerical solution can be evaluated also by using the relative mass balance error,  $\varepsilon_r$  (Eq. 6.52 in Šimůnek et al., 1998):

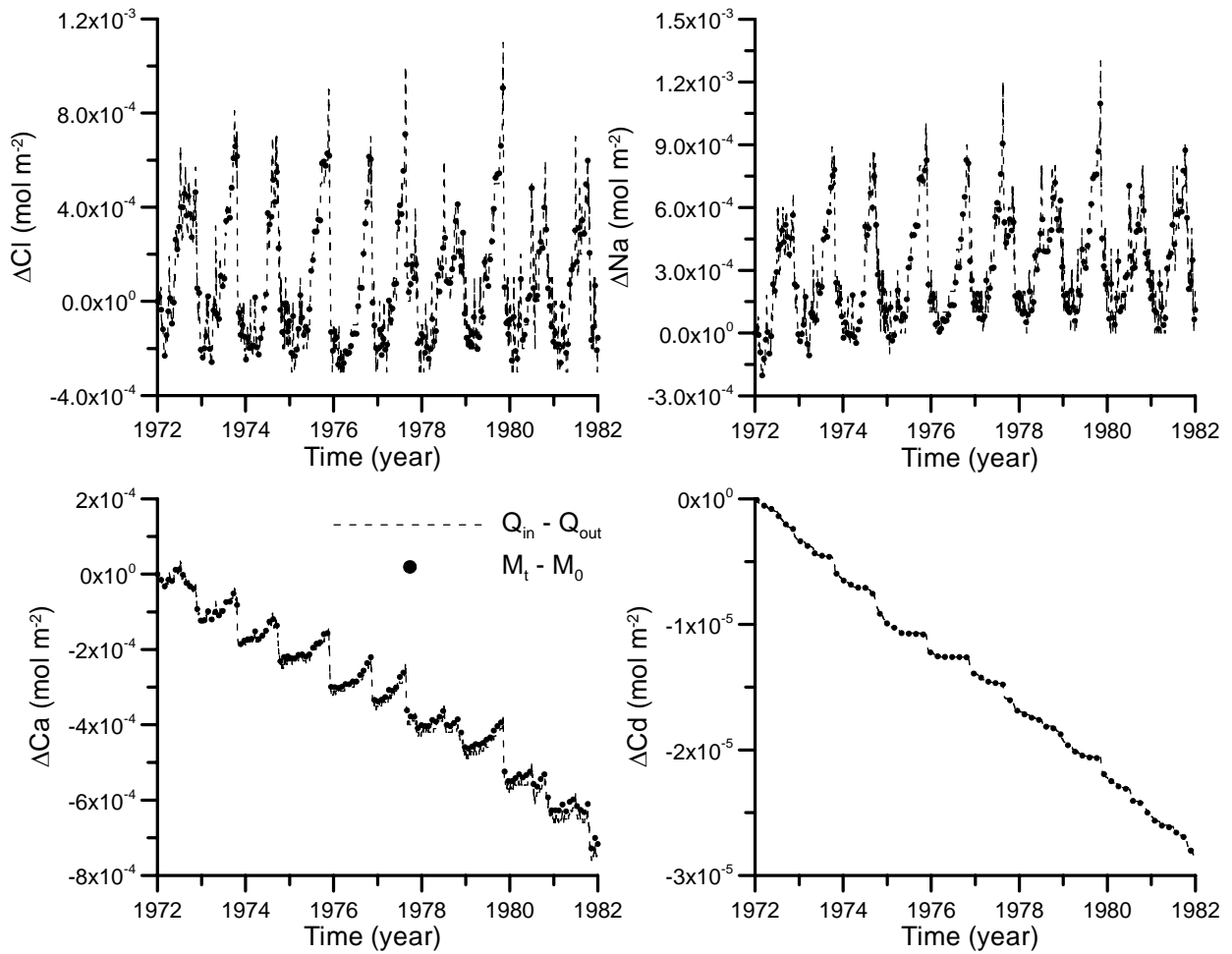


**Figure 5.2** Time series of inflow minus outflow (dashed line) and change in the total amount present in the soil profile (dots) for Cl, Na, Ca, and Cd.

$$\varepsilon_r^j = \frac{100 \varepsilon_a}{\max \left( \sum_{i=1}^{N_{\text{cells}}} |M_{t,i}^j - M_{0,i}^j|, |M_0^j| + \int_0^t (|q_{s0}^j| + |q_{sN}^j|) dt \right)} \quad (5.3)$$

where  $M_{t,i}^j$  and  $M_{0,i}^j$  are the total amount of the  $j$ th master species in the  $i$ th cell at time  $t$  and at the beginning of the simulation, respectively. Figure 5.3 shows relative mass balance errors for Na, Ca, and Cd. The errors were consistently smaller than 1%, indicating that mass balance errors were small in this HP1 simulation using the non-iterative sequential approach for solving the coupled transport-reaction equations.

### 5.1.2.2 Simulation results

As an illustration, two-dimensional time-depth plots are shown in Figure 5.4 for the top 7 cm (the A horizon) for the water content, pH, mass of Cl (mmol / 1000 cm<sup>3</sup> soil), and mass of aqueous Cd (mmol / 1000 cm<sup>3</sup> soil). The alternation between precipitation (wet conditions) and evaporation (dry conditions) as dictated by the atmospheric boundary conditions clearly affected the dynamics of the water content (Figure 5.4a), including upward flow of water during the dry periods (not shown). The flow dynamics in turn significantly influenced the

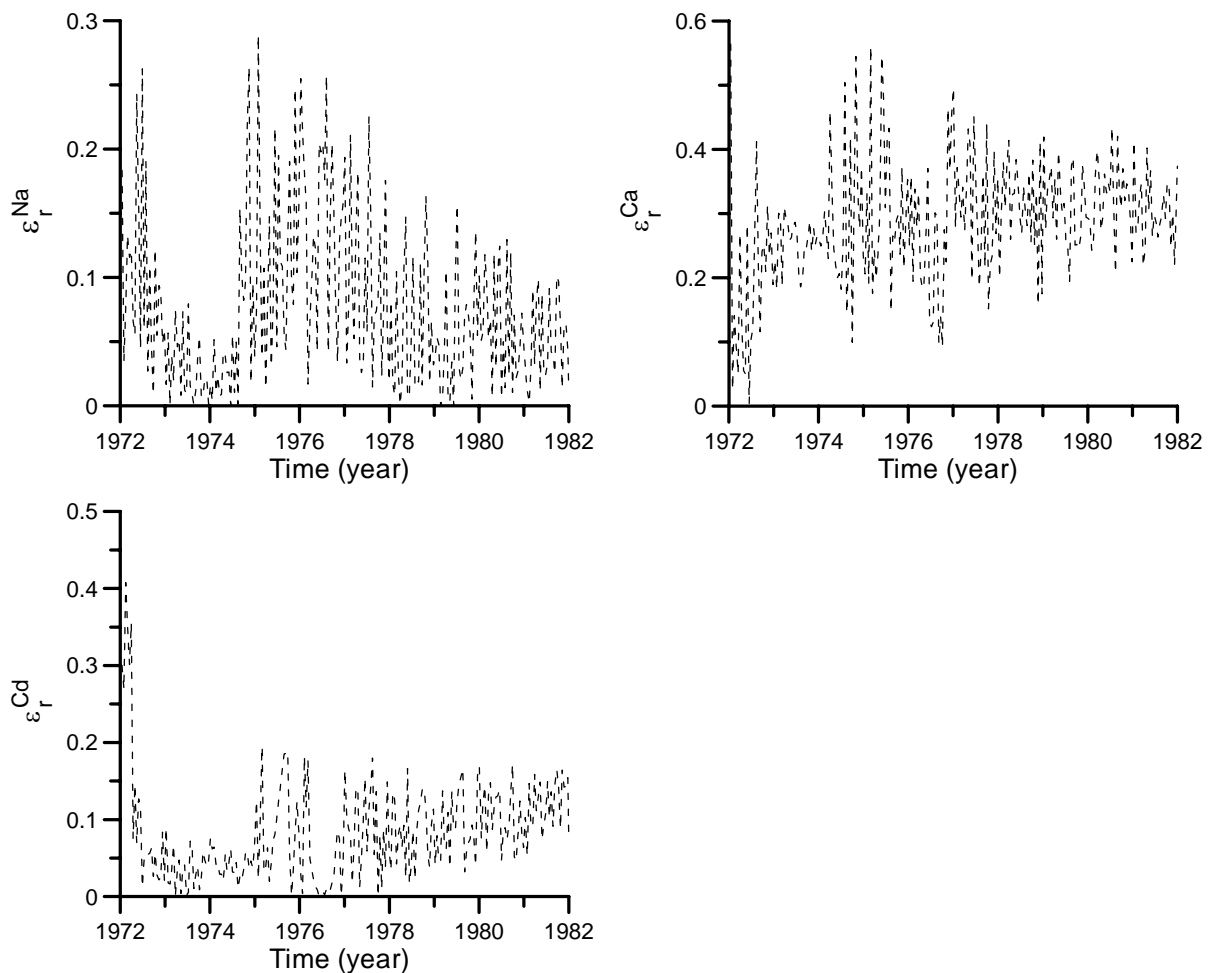


**Figure 5.3** Relative mass balance errors,  $\epsilon_r$ , as a function of time for Na, Ca, and Cd.

geochemistry near the soil surface. The most mobile elements, such as Cl and the monovalent cations ( $H^+$ ,  $Na^+$ ) moved upwards during the evaporation periods, leading to higher concentrations near the soil surface (e.g., Cl in Figure 5.4b). The increased proton concentration (induced by the lower water content and the supply from deeper horizons in the soil profile) produced lower pH values near the soil surface during the summer periods with their lower water contents (Figure 5.4c). The pH in actuality may have been affected also by soil carbon dioxide concentrations, which usually change in response to the biological activity and moisture status of the soil (Šimůnek and Suarez, 1993). This process, however, was not considered in our simulations here. Although upward flow during the summer had almost no effect on the total amount of heavy metals near the soil surface (results not shown) due to the low mobility of these elements, the concentrations of these elements did vary significantly during the various seasons.

Because of lower water contents, concentrations of all aqueous species and elements increased significantly during the summer periods. The changing aqueous concentrations in turn also caused changes in the cation exchange equilibrium by promoting monovalent cations to sorb on the cation exchange complex. The lower cation exchange capacity (defined here as the amount of deprotonated sites) during summer (lower pH) implied the presence of fewer

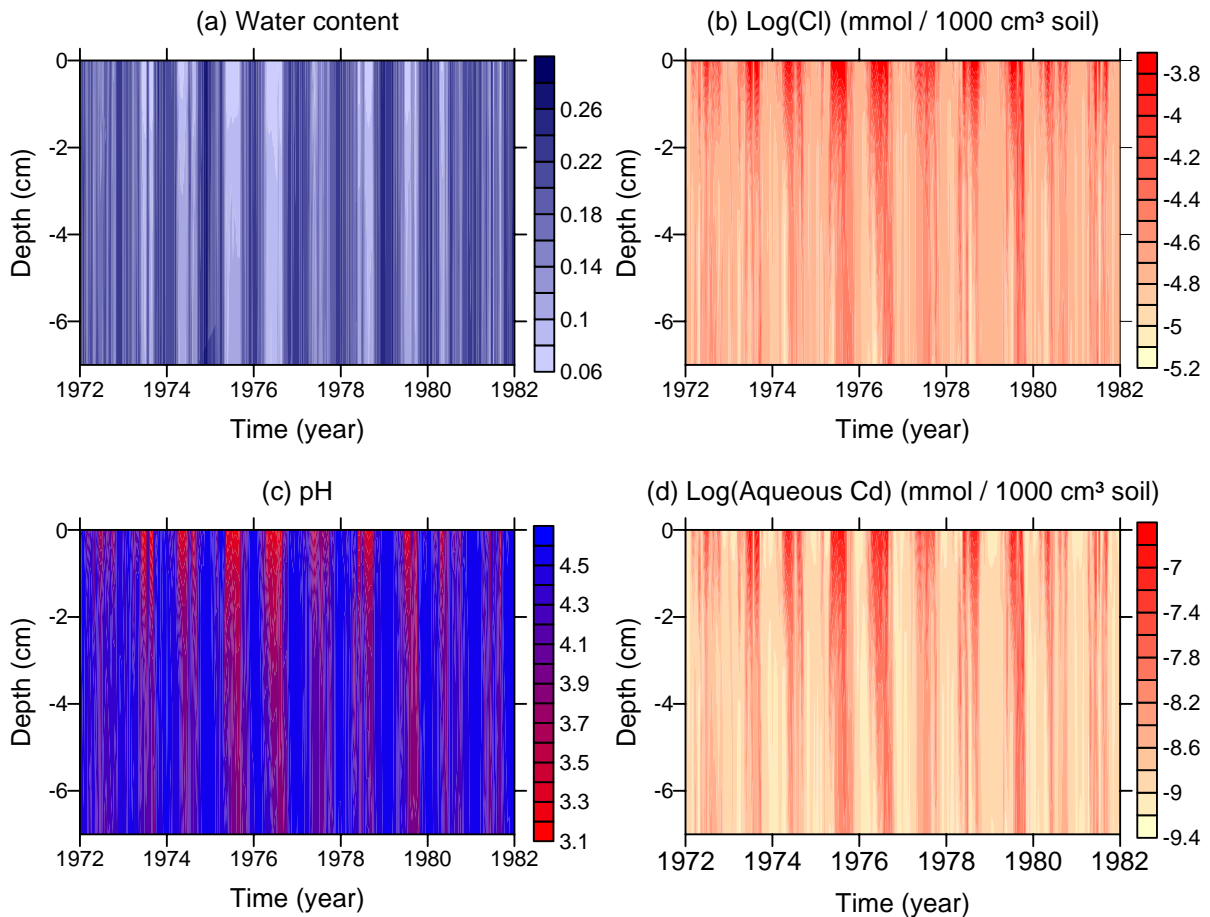


**Figure 5.4** Space-time plots of (a) water content, (b) amount of Cl (mmol / 1000 cm<sup>3</sup> soil), (c) pH, and (d) amount of aqueous Cd (mmol / 1000 cm<sup>3</sup> soil) in the A-horizon (0 – 7 cm depth).

sorption sites for the other cations. The increased supply of monovalent cations due to upward water flow during summer further increased competition for the sorption sites, leading to relatively more sorption of the monovalent cations and higher concentrations of divalent cations and heavy metals in the soil solution. Another important process is the complexation of the heavy metals with Cl. Because of the presence of relative stable aqueous complexes (e.g., CdCl<sup>+</sup>), the amounts of Cd, Pb, and Zn will increase when Cl concentrations are high (i.e., during summer periods). Figure 5.4d shows the amount of Cd in the aqueous phase. Differences in the amount of aqueous Cd between the summer and winter periods are more than two orders of magnitude. Since water contents are lower during summer, the differences in the concentrations will be even larger. Similar, but less distinct, patterns can be observed also deeper in the soil profile (Figure 5.5).

This example shows that atmospheric boundary conditions can have a significant effect on the amounts of Cd and other heavy metals in the solution, and hence also on their bioavailability, since uptake processes by plants and soil micro-organisms are often concentration dependent (i.e., passive uptake of solutes together with uptake of water by roots, as well as active uptake which can be simulated with HP1 using Monod or Michealis-Menten kinetics). Moreover, the high concentrations of the heavy metals occur during periods with the highest

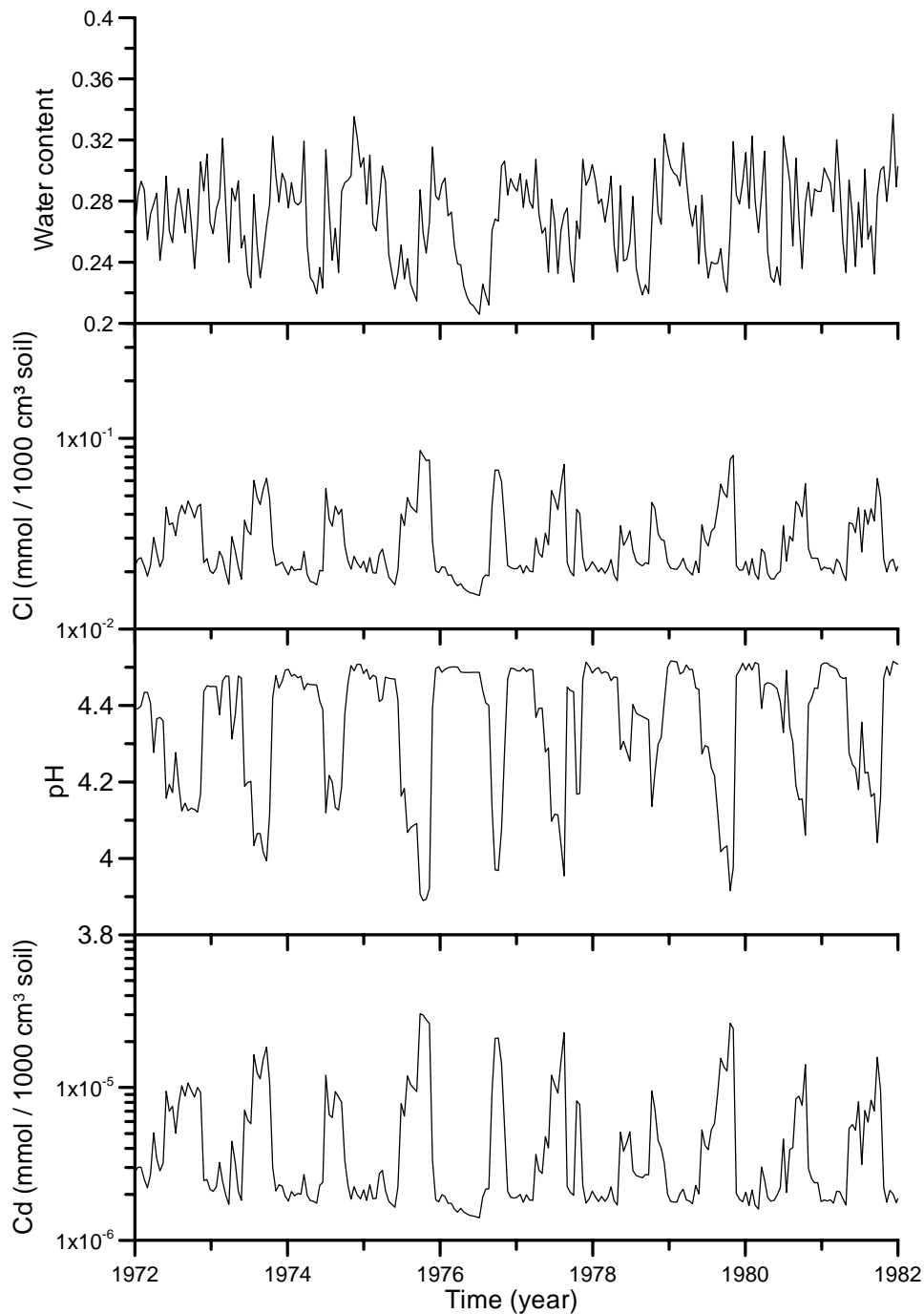


**Figure 5.5** Time series of water content, Cl concentration (mmol / 1000 cm<sup>3</sup> soil), pH, and Cd concentration (mmol / 1000 cm<sup>3</sup> soil) in the third horizon (Bh1-horizon) at 22 cm depth.

(micro)biological activity during the year (the summer months). HP1 hence seems to be a very attractive tool for evaluating the effects of atmospheric boundary conditions on the long-term mobility and leaching of the heavy metals in and from soils. While not further addressed here, such evaluations possibly could also account for the transport of colloids such as microorganisms, humics or fulvics.



## 6 Concluding Remarks

The HP1-code, presented in this report, couples HYDRUS-1D (a one-dimensional variably-saturated water flow and solute transport model) with PHREEQC (a general biogeochemical code). The new code is able to handle (1) transient water flow in variably-saturated media, (2) transport of multiple components, (3) heat flow, and (4) mixed equilibrium (aqueous speciation, mineral dissolution / precipitation, cation exchange) and kinetic geochemical reactions.

The non-iterative sequential approach used to solve the coupled transport-reaction equations generally worked very well. The accuracy of the coupling approach was tested using nine verification examples with different degrees of complexity. Overall, compared to other models / codes, HP1 was found to be accurate when time steps were not too large. The easiest and most efficient way to control the time step is by defining a relatively small maximum time step and/or a small performance index (both in HYDRUS-1D). Our analyses indicate that the performance index should be about five times smaller than the value previously suggested for HYDRUS-1D simulations (i.e., 0.4 rather than 2).

The nine verification problems and the application example serve as guidelines to create the input files using the graphical user interfaces of HYDRUS-1D and PHREEQC. The user interfaces also display the output created with the HP1 simulations.



## **ACKNOWLEDGEMENTS**

The work of Dr. J. Šimůnek was supported in part by SAHRA (Sustainability of semi-Arid Hydrology and Riparian Areas) under the STC Program of the National Science Foundation, Agreement No. EAR-9876800 and the Terrestrial Sciences Program of the Army Research Office (Terrestrial Processes and Landscape Dynamics And Terrestrial System Modeling and Model Integration). Additional support was obtained through the bilateral agreement project “Development and evaluation of a coupled geochemical transport model” (Agreement No. 58-5310-0-F105) between SCK•CEN – USDA, ARS and (Agreement No. C0-90001412.01) between SCK•CEN – University of California, Riverside.

The work of Dr. D. Jacques was supported by SCK•CEN R&D program on “Environmental Remediation” (project E022031 and CO91002).

The project coordinator at SCK•CEN was Dr. D. Mallants.



## References

- Aagaard, P., and H. C. Helgeson, 1982. Thermodynamic and kinetic constraints on reaction rates among minerals and aqueous solutions, I. Theoretical considerations. *Amer. J. Sci.*, 282:237-285.
- Adler, M., 2001. Interaction of claystone and hyperalkaline solutions at 30°C: A combined experimental and modeling study. Ph. Dissertation, Universität Bern, 120 p.
- Appelo, C.A.J., and D. Postma, 1993. *Geochemistry, groundwater and pollution*. A.A. Balkema, Rotterdam, 536 p.
- Appelo, C.A.J., E. Verweij, and H. Schäfer, 1998. A hydrogeochemical transport model for an oxidation experiment with pyrite/calcite/exchangers/organic matter containing sand. *Applied geochemistry*, 13:257-268.
- Appelo, C.A.J., M.J.J. Van der Weiden, C. Tournassat, and L. Charlet, 2002. Surface complexation of ferrous iron and carbonate on ferrihydrite, and the mobilisation of arsenic. *Environ. Sci. Technol.* 36:3096-3103.
- Brooks, R.H., and A.T. Corey, 1966. Properties of porous media affecting fluid flow. *J. Irrig. Drainage Div., ASCE Proc.* 72(IR2), 61-88.
- Carsel, R.F., and R.S. Parish, 1988. Developing joint probability distributions of soil water retention characteristics. *Water Res. Res.*, 24:755-769.
- Casey, F., and J. Šimůnek, 2001. Inverse analyses of transport of chlorinated hydrocarbons subject to sequential transformation reactions. *J. Envir. Qual.*, 30:1354-1360.
- Casey, F. X. M., G. L. Larsen, H. Hakk, and J. Šimůnek, 2003. Fate and transport of 17 $\beta$ -Estradiol in soil-water systems. *Environmental Science and Technology*, 37(11):2400-2409.
- Casey, F.X.M., G. L. Larsen, H. Hakk, and J. Šimůnek, 2004. Fate and transport of testosterone in agriculturally significant soils. *Environ. Sci. Technol.*, 38(3):790-798.
- Chung, S.-O., and R. Horton, 1987. Soil heat and water flow with a partial surface mulch. *Water Resour. Res.*, 23:2175-2186.
- Dane, J.H. and G.C. Topp, 2002. *Methods of soil analysis, Part 4 Physical systems*. SSSA Book Series no. 5, SSSA, Inc. Madison, Wisconsin, USA, 1692 pp.
- de Marsily, G., 1986. *Quantitative Hydrogeology*. Academic Press, London.
- de Vries, D.A.. The thermal properties of soils. In '*Physics of plant environment*' (Ed. R.W. van Wijk), North Holland, Amsterdam, pp. 210-235.
- Gaines, G.L., and H.C. Thomas, 1953. Adsorption studies on clay minerals. II. A formulation of the thermodynamics of exchange adsorption. *J. Chem. Phys.*, 21:714-718.
- Hopmans, J.W., J. Šimůnek, N. Romano, and W. Durner, 2002. Inverse methods. In '*Methods of soil analysis, Part 4*', (Co-eds. Dane and Topp), Book Series no. 5, SSSA, Inc. Madison, Wisconsin, USA, 693-1008.
- Jacques, D., J. Šimůnek, D. Mallants, M. Th. van Genuchten, 2002. Multicomponent transport model for variably-saturated porous media: Application to the transport of heavy metals in

- soils, In: *Computational Methods in Water Resources* (Eds. Hassanizadeh, S.M., R.J. Schotting, W.G. Gray, and G.F. Pinder), XIVth International Conference on Computational Methods in Water Resources, June 23-28, 2002, Delft, The Netherlands. Elsevier, *Developments in Water Science*, 47, 555-562.
- Jacques, D., J. Šimůnek, D. Mallants, and M. Th. van Genuchten, 2003. The HYDRUS-PHREEQC multicomponent transport model for variably-saturated porous media: Code verification and application, MODFLOW and More 2003: Understanding through Modeling, Conference Proceedings, ed. E. Poeter, Ch. Zheng, M. Hill, and J. Doherty, International Ground Water Modeling Center, Colorado School of Mines, 23-27.
- Jaynes, D.B., A.S. Rogowski, and H.B. Pionke, 1984. Acid mine drainage from reclaimed coal strip mines. 1. Model description. *Water Resources Research*, 20: 233-242.
- Källvenius, G., and C. Ekberg, 2003. TACK – a program coupling chemical kinetics with a two-dimensional transport model in geochemical systems. *Comp. and Geosci.*, 29:511-521.
- Kirkham, D., and W.L. Powers, 1972. *Advanced Soil Physics*. John Wiley&Sons, New York, NY.
- Lichtner, P.C., 1996. Continuum formulation of multicomponent-multiphase reactive transport. In '*Reactive transport in porous media*' (Eds. P.C. Lichtner, C.I. Steefel and E.H. Oelkers), *Reviews in Mineralogy*, no. 34, Mineralogical Society of America, Washington, DC, p. 1-81.
- Mallants, D., D. Jacques, and T. Zeevaert, 2003. Modelling  $^{226}\text{Ra}$ ,  $^{222}\text{Rn}$ , and  $^{210}\text{Pb}$  in a proposed surface repository of very low-level long-lived radioactive waste. ICEM'03 Conference, Oxford, 21-25 Sept. 2003. ASME, Proc. On CD-ROM, session 25, paper 6.
- Mayer, U., 1999. A numerical model for multicomponent reactive transport in variably saturated porous media. Ph.D. thesis, Department of Earth Sciences, University of Waterloo, 285p.
- Millington, R.J., and J.M. Quirk, 1961. Permeability of porous solids. *Trans. Faraday Soc.*, 57:1200-1207.
- Morel, F., and J. Hering, 1993. *Principles and applications of aquatic chemistry*. New York, John Wiley & Sons Inc.
- Parkhurst, D.L., and C.A.J. Appelo, 1999. User's guide to PHREEQC (Version 2) – A computer program for speciation, batch-reaction, one-dimensional transport, and inverse geochemical calculations. *Water-Resources Investigations*, Rept 99-4259, Denver, Co, USA, 312 pp.
- Perrochet, P., and D. Berod, 1993. Stability and the standard Crank-Nicolson-Galerkin scheme applied to the diffusion-convection equation: some new insights. *Water Resour. Res.*, 29:3291-3297.
- Postma, D. and C.A.J. Appelo, 2000. Reduction of Mn-oxides by ferrous iron in a flow system: column experiments and reactive transport modeling. *Geochim. Cosmochim. Acta*, 64:1237-1247.

- Prommer, H., 2002. A reactive multicomponent transport model for saturated porous media. User's Manual Version 1.0. Contaminated Land Assessment and Remediation Research Centre, University of Edinburgh, UK, 132 p.
- Schaerlaekens, J., D. Mallants, J. Šimůnek, M.Th. van Genuchten, and J. Feyen, 1999. Numerical simulation of transport and sequential biodegradation of chlorinated aliphatic hydrocarbons using CHAIN\_2D. *Hydrol. Process.*, 13:2847-2859.
- Šimůnek, J., and D. L. Suarez, 1993. Modeling of carbon dioxide transport and production in soil: 1. Model development. *Water Resour. Res.*, 29: 487-497.
- Šimůnek, J., and D.L. Suarez, 1994. Two-dimensional transport model for variably saturated porous media with major ion chemistry. *Water Resour. Res.*, 30:1115-1133.
- Šimůnek, J., and D. L. Suarez, 1997. Sodic soil reclamation using multicomponent transport modelling. *ASCE J. Irrig. and Drain. Engineering*, 123(5):367-376.
- Šimůnek, J. and A. J. Valocchi, 2002. Geochemical Transport, In: *Methods of Soil Analysis, Part 1, Physical Methods, Chapter 6.9*, Eds. J. H. Dane and G. C. Topp, Third edition, SSSA, Madison, WI, 1511-1536.
- Šimůnek, J., M. Šejna, and M.Th. van Genuchten, 1998. The HYDRUS-1D software package for simulating the one-dimensional movement of water, heat, and multiple solutes in variably-saturated media. Version 2.0, IGWMC-TPS-70, International Ground Water Modeling Center, Colorado School of Mines, Golden, CO, 202 p.
- Šimůnek, J., D. L. Suarez, and M. Šejna, 1996. The UNSATCHEM software package for simulating one-dimensional variably saturated water flow, heat transport, carbon dioxide production and transport, and multicomponent solute transport with major ion equilibrium and kinetic chemistry, Version 2.0, Research Report No. 141, U.S. Salinity Laboratory, USDA, ARS, Riverside, California, 186pp.
- Šimůnek, J., T. Vogel, and M.Th. van Genuchten, 1992. The SWMS-2D code for simulating water flow and solute transport in two-dimensional variably saturated media, Version 1.1, Res. Rep. 126, U.S. Salinity Lab., Agric. Res. Serv., U.S. Dept. of Agric., Riverside, Ca.
- Singer, P.C., and W. Stumm, 1970. Acid mine drainage: the rate-determining step. *Science*, 167:1121-1123.
- Steefel, C.I., 2000. New directions in hydrogeochemical transport modeling: Incorporating multiple kinetic and equilibrium reaction pathways. In 'Computational Methods in Water Resources XIII' (Eds. L.R. Bentley, J.F. Sykes, C.A. Brebbia, W.G. Gray, and G.F. Pinder), A.A. Balkema, Rotterdam, 331-338.
- Steefel, C.I., and K.T.B. MacQuarrie, 1996. Approaches to modeling of reactive transport in porous media. In '*Reactive transport in porous media*' (Eds. P.C. Lichtner, C.I. Steefel and E.H. Oelkers), *Reviews in Mineralogy*, no. 34, Mineralogical Society of America, Washington, DC, p. 83-129.
- Steefel, C.I., and S.B. Yabusaki, 1996. OS3D/GIMRT, Software for multicomponent-multidimensional reactive transport, user manual and programmer's guide. PNL-11166, Pacific North west Laboratory, Richland, Washington.

- Stolk, A.P., 2001. Landelijk Meetnet Regenwatersamenstelling, Meetresultaten 1999. RIVM, The Netherlands, RIVM Rapport 723101 056, 61 p.
- Suarez, D.L., and J. Šimůnek, 1997. UNSATCHEM: Unsaturated water and solute transport model with equilibrium and kinetic chemistry. *Soil Sci. Soc. Am. J.*, 61:1633-1646.
- Tipping, E., 2002. Cation binding by humic substances. Cambridge University Press, Cambridge, UK, 434 p.
- Truesdell, A.H., and B.F. Jones, 1974. WATEQ, A computer program for calculating chemical equilibria of natural waters. *J. Res. U.S. Geol. Surv.*, 2:233-274.
- Thury, M., and Bossart, P., 1999. The Mont Terri rock laboratory, a new international research project in a Mesozoic shale formation, in Switzerland. *Eng. Geol.*, 52:347-359.
- van Genuchten, M.Th., 1980. A closed-form equation for predicting the hydraulic conductivity of unsaturated soils. *Soil Sci. Soc. Am. J.*, 44:892-898.
- van Genuchten, M.Th., 1985. Convective-dispersive transport of solutes involved in sequential first-order decay reactions. *Comp. Geosci.*, 11:159-147.
- van Genuchten, M.Th., and P.J. Wierenga, 1976. Mass transfer studies in sorbing porous media I. Analytical solutions. *Soil Sci. Soc. Am. J.*, 40:473-480.
- Vogel, T., and M. Cislerova, 1988. On the reliability of unsaturated hydraulic conductivity calculated from the moisture retention curve. *Transport in Porous Media*, 3:1-15.
- Wagenet R. J., and J. L. Hutson. 1987. LEACHM: Leaching Estimation And CHemistry Model, A process-based model of water and solute movement, transformations, plant uptake and chemical reactions in the unsaturated zone, Continuum 2, Dept. of Agronomy, Cornell University, Ithaca, New York, NY.
- Walter, A.L., E.O. Frind, D.W. Blowes, C.J. Ptacek, and J.W. Molson, 1994. Modeling of multicomponent reactive transport in groundwater. 1. Model development and evaluation. *Water Res. Res.*, 30:3137-3148.
- Xu, T., 1996. Modeling nonisothermal multi-component reactive solute transport through variably saturated porous media. Civil Engineering School, University of La Coruña, Coruña, Spain, 310 p.
- Yeh, G.-T., and H.-P. Cheng, 1999. 3DHYDROGEOCHEM: A 3-dimensional model of density-dependent subsurface flow and thermal multispecies-multicomponent HYDROGEOCHEMical transport. EPA/600/R-98/159, 150p.
- Zheng, C., 1990. A modular three-dimensional transport model for simulation of advection, dispersion and chemical reaction of contaminants in groundwater systems. Technical report, U.S. Environmental Protection Agency.
- Zheng, C., and P.P. Wang, 1998. MT3DMS, A modular three-dimensional transport model. Technical report, U.S. Army Corps of Engineers Waterways Experiment Station, Vicksburg, Miss.

## APPENDIX A – LISTING OF NOTATION

$a_{i_e}$	activity of $i_e$ th secondary exchange species	[M L <sup>-3</sup> ]
$A$	amplitude of temperature sine wave at soil surface	[K]
$A_i$	chemical formula of $i$ th secondary species	[-]
$A_i$	chemical formula of $i$ th secondary species	[-]
$A_{m,0}$	initial reactive surface area of a mineral	[L <sup>2</sup> ]
$A_{i_e}^e$	chemical formula of $i_e$ th secondary exchange species	[-]
$A_i^l$	chemical formula of $i$ th aqueous secondary species	[-]
$A_i^m$	chemical formula of $i$ th mineral	[-]
$A_j^m$	chemical formula of $j$ th master species	[-]
$b$	normalized water uptake distribution	[L <sup>-1</sup> ]
$b_i$	parameters to calculate soil thermal conductivity ( $i=1,2,3$ )	[ML <sup>-1</sup> T <sup>-2</sup> K <sup>-1</sup> ]
$b_{i_e j_e}$	number of equivalents of the $i_e$ th secondary exchange species on the $j_e$ th master exchanger	[equivalents]
$c_i$	aqueous concentration of $i$ th species	[M L <sup>-3</sup> ]
$c_{i,im}$	aqueous concentration of $i$ th species in the immobile region	[M L <sup>-3</sup> ]
$c_{i,m}$	aqueous concentration of $i$ th species in the mobile region	[M L <sup>-3</sup> ]
$c_i^l$	aqueous concentration of $i$ th aqueous secondary species	[M L <sup>-3</sup> ]
$c_j^m$	aqueous concentration of $j$ th master species	[M L <sup>-3</sup> ]
$c_r$	concentration of the sink term	[M L <sup>-3</sup> ]
$c_{ri}^l$	concentration of $i$ th secondary species in the sink term	[M L <sup>-3</sup> ]
$c_{rj}^m$	concentration of $j$ th master species in the sink term	[M L <sup>-3</sup> ]
$C$	aqueous concentration	[L L <sup>-3</sup> ]
$C_a$	volumetric heat capacity of the gas phase	[MLT <sup>-3</sup> K <sup>-1</sup> ]
$C_j$	total concentration of $j$ th master species	[M L <sup>-3</sup> ]
$C_r$	Courant number	[-]
$C_{rj}$	total concentration of $j$ th master species in the sink term	[M L <sup>-3</sup> ]
$C_n$	volumetric heat capacity of solid phase	[MLT <sup>-3</sup> K <sup>-1</sup> ]
$C_o$	volumetric heat capacity of organic matter	[MLT <sup>-3</sup> K <sup>-1</sup> ]
$C_p$	volumetric heat capacity of porous medium	[MLT <sup>-3</sup> K <sup>-1</sup> ]
$C_w$	volumetric heat capacity of liquid phase	[MLT <sup>-3</sup> K <sup>-1</sup> ]
$D_i^v$	dispersion coefficient of $i$ th species in liquid phase	[L <sup>2</sup> T <sup>-1</sup> ]
$D_{i,w}$	dispersion coefficient of $i$ th species in free water	[L <sup>2</sup> T <sup>-1</sup> ]
$D_L$	longitudinal dispersivity	[L]
$E$	evaporation	[L]
$H$	soil water pressure head	[L]
$h_\phi$	osmotic head	[L]
$i$	index number of secondary species	[-]
$i_e$	index number of secondary exchange species	[-]
$j$	index number of master species	[-]
$j_e$	index number of master exchanger	[-]
$k$	index number of solute in a decay chain	[-]
$k_{0,m}$	intrinsic rate constant of mineral m	[M L <sup>-2</sup> T <sup>-1</sup> ]
$K$	unsaturated hydraulic conductivity	[L T <sup>-1</sup> ]
$K_d$	empirical adsorption coefficient	[M <sub>a</sub> <sup>(1-n)</sup> L <sup>3n</sup> Ms <sup>-1</sup> ]

$K_d^w$	adsorption coefficient in mass per unit of volume water	$[M^{(1-n)}L^{3n}L^{-3}]$
$K_{i_e}^e$	equilibrium constant of reaction for $i_e$ th secondary exchange species	[-]
$K_i^j$	equilibrium constant of reaction for $i$ th aqueous secondary species	[-]
$K_i^p$	equilibrium constant of reaction for $i$ th mineral	[-]
$K_s$	saturated hydraulic conductivity	$[L T^{-1}]$
$m$	parameter in the water retention curve	[-]
$m$	index number of a mineral	[-]
$M_t^j$	amount of the $j$ th master species in the flow region at time $t$	$[M L^{-2}]$
$M_{t,i}^j$	amount of the $j$ th master species in element $i$ at time $t$	$[M L^{-2}]$
$M_0^j$	amount of the $j$ th master species in the flow region at the beginning of the simulation	$[M L^{-2}]$
$M_{0,i}^j$	amount of the $j$ th master species in element $i$ at the beginning of the simulation	$[M L^{-2}]$
$t$		
$l$	pore connectivity parameter	[-]
$n$	parameter in the water retention curve	[-]
$n$	reaction order of the $OH^-$ dependence of the reaction rate	[-]
$n_F$	empirical Freundlich exponent	[-]
$n_{i_e j_e}$	moles of $i_e$ th secondary exchange species on $j_e$ th master exchanger	[moles]
$n_m$	number of moles of mineral $m$	[moles]
$n_{m,0}$	initial number of moles of mineral $m$	[moles]
$N_{lk}$	number of kinetically-controlled homogeneous reactions	[-]
$N_m$	number of master species	[-]
$N_p$	number of minerals	[-]
$N_s$	number of secondary species	[-]
$N_{sa}$	number of secondary aqueous species	[-]
$N_{se}$	number of secondary exchange species	[-]
$N_X$	number of master exchange sites	[-]
$P$	precipitation	[L]
$P_e$	Peclet number	[-]
$P_t$	period of time necessary to complete one temperature cycle (one day)	[T]
$q$	volumetric flux density	$[L T^{-1}]$
$q_{s0}^j$	solute flux at the bottom of the soil profile of the $j$ th master species	$[M L^{-2} T^{-1}]$
$q_{sN}^j$	solute flux at soil surface of the $j$ th master species	$[M L^{-2} T^{-1}]$
$Q_{in}^j$	cumulative inflow of the $j$ th master species	$[M L^{-2}]$
$Q_{out}^j$	cumulative outflow of the $j$ th master species	$[M L^{-2}]$
$Q_m^p$	ion activity product of mineral $m$	[-]
$R$	decay rate	$[M L^{-3} T^{-1}]$
$R_i$	source/sink term due to geochemical reactions for $i$ th species	$[M L^{-3} T^{-1}]$
$R_{i,im}$	source/sink term due to geochemical reactions for $i$ th species in immobile region	$[M L^{-3} T^{-1}]$
$R_{i,m}$	source/sink term due to geochemical reactions for $i$ th species in mobile region	$[M L^{-3} T^{-1}]$
$R_m$	dissolution rate of a mineral	$[M T^{-1}]$
$R^{eq,hom}$	homogeneous equilibrium reactions of source/sink term	$[M L^{-3} T^{-1}]$
$R^{eq,het}$	heterogeneous equilibrium reactions of source/sink term	$[M L^{-3} T^{-1}]$
$R^{kin,hom}$	homogeneous kinetic reactions of source/sink term	$[M L^{-3} T^{-1}]$
$R^{kin,het}$	heterogeneous kinetic reactions of source/sink term	$[M L^{-3} T^{-1}]$
$S$	water sink term	$[L^3 L^{-3} T^{-1}]$
$S_e$	effective saturation	[-]
$S_p$	potential root water uptake	$[T^{-1}]$

$S^s$	adsorbed concentration	$[M_a M_s^{-1}]$
$S^w$	adsorbed concentration per unit volume of water	$[M_a L^{-3}]$
$t$	time	[T]
$T$	temperature	[T]
$T_{avg}$	average temperature at soil surface	[K]
$T_{j_e}$	total number of exchange sites for $j_e$ th master exchanger	[equivalents]
$T_p$	potential transpiration	$[L T^{-1}]$
$v$	average pore water velocity	$[L T^{-1}]$
$V_m$	volume of mineral $m$	$[L^3]$
$V_{m,0}$	initial volume of mineral $m$	$[L^3]$
$x$	spatial coordinate	[L]
$X_{j_e}^m$	chemical formula of $j_e$ th master exchanger	[-]
$\alpha$	dimensionless water stress response function	[-]
$\alpha$	parameter in the water retention curve	$[L^{-1}]$
$\alpha$	angle between flow direction and the vertical axis	[-]
$\beta_{i_e j_e}$	equivalent fraction of $i_e$ th exchange species on $j_e$ th exchanger	
$\beta_t$	thermal dispersivity	[L]
$\varepsilon_a$	absolute error in the solute mass balance	$[M L^{-2}]$
$\varepsilon_r^j$	relative error in the solute mass balance of the $j$ th master species	[%]
$\gamma_{i_e}^e$	activity coefficient of $i_e$ th secondary exchange species	[-]
$\gamma_i^l$	activity coefficient of $i$ th aqueous secondary species	[-]
$\gamma_{j_e}^e$	activity coefficient of $j_e$ th master exchanger	[-]
$\gamma_j^m$	activity coefficient of $j$ th master species	[-]
$\theta$	volumetric water content	$[L^3 L^{-3}]$
$\theta_{im}$	immobile water content	$[L^3 L^{-3}]$
$\theta_m$	mobile water content	$[L^3 L^{-3}]$
$\theta_n$	volumetric fraction of the solid phase	$[L^3 L^{-3}]$
$\theta_o$	volumetric fraction of the organic matter	$[L^3 L^{-3}]$
$\theta_r$	residual water content	$[L^3 L^{-3}]$
$\theta_s$	saturated water content	$[L^3 L^{-3}]$
$\theta_v$	volumetric fraction of the air phase	$[L^3 L^{-3}]$
$\lambda$	apparent thermal conductivity of the soil	$[MLT^{-3}K^{-1}]$
$\lambda_0$	thermal conductivity of the soil	$[MLT^{-3}K^{-1}]$
$\mu_w$	first-order rate constant for solutes in the liquid phase	$[T^{-1}]$
$\mu_w'$	first-order rate constants for decay chain solutes in the liquid phase	$[T^{-1}]$
$\nu_{ji}$	stoichiometric coefficient of $j$ th master species in $i$ th secondary species	[-]
$\nu_{j_e i_e}^e$	stoichiometric coefficient of $j$ th master species in $i_e$ th secondary exchange species	[-]
$\nu_{j_e i_e}^e$	stoichiometric coefficient of $j_e$ th master exchanger in $i_e$ th secondary exchange species	[-]
$\nu_{ji}^l$	stoichiometric coefficient of $j$ th master species in $i$ th aqueous secondary species	[-]
$\nu_{ji}^k$	stoichiometric coefficient of $j$ th master species in $i$ th homogeneous kinetic reaction	[-]
$\nu_{ji}^p$	stoichiometric coefficient of $j$ th master species in $i$ th mineral	[-]
$\rho$	bulk density	$[M_s L^{-3}]$
$\tau_w$	tortuosity factor in liquid phase	[-]
$\omega_i$	mass transfer coefficient for $i$ th species	$[T^{-1}]$

$\omega_s$  performance index

[-]

## APPENDIX B – RELEASED VERSIONS AND BENCHMARKING

### B.1 Version 1.0

*Released date:* November 2004

*Status:* beta version – controlled distribution

*Versions used of the original codes:*

- HYDRUS-1D, Version (Version 2.0, July 1998)
- PHREEQC (Version 2.4)
- *Manual:* Jacques, D., and J. Šimůnek, 2005. User manual of the Multicomponent variably-saturated transport model HP1 (Version 1.0): Description, Verification and Examples. SCK•CEN, Mol, Belgium, BLG-998, 79.

*Overview of verification problems*

- Steady-state physical (non)equilibrium transport of chloride (Verification Problem 1 - HYDRUS-1D – EQCL and NEQCL)
- Transient physical nonequilibrium transport of chloride (Verification Problem 2 - HYDRUS-1D – TRANSCL)
- Steady-state transport of a nonlinearly adsorbing contaminant (Verification Problem 3 - HYDRUS-1D / PHREEQC – STADS)
- Steady-state transport of a nonlinearly adsorbing contaminant subject to first-order decay (Verification Problem 4 - HYDRUS-1D, PHREEQC – STDECAY)
- Transport of first-order decay chain of nonlinearly adsorbing contaminants during unsteady flow (Verification Problem 5 - HYDRUS-1D – SEASONCHAIN)
- Transport of heavy metals subject to multiple cation exchange (Verification Problem 6 – PHREEQC – CATEXCH)
- Transport with mineral dissolution (Verification Problem 7 – PHREEQC - MINDIS)
- Heavy metal transport with a pH-dependent cation exchange complex (Verification Problem 8 – CRUNCH – MCATEXCH)
- Infiltration of a hyperalkaline solution in a clay sample (Verification Problem 9 – CRUNCH – ALKALINE)

*Overview of examples*

- Long term transient flow and transport of major cations and heavy metals in a soil profile (HEAVMET)